



universität  
wien

# MASTERARBEIT / MASTER'S THESIS

Titel der Masterarbeit / Title of the Master's Thesis

Structural and functional studies of *Trypanosoma brucei*  
flagellar pocket collar protein BILBO421 and  
*Saccharomyces cerevisiae* SNARE-associated proteins  
Sso1/2 and Sec3

verfasst von / submitted by

Maximilian Alexander Peer, BSc

angestrebter akademischer Grad / in partial fulfilment of the requirements for the degree of  
Master of Science (MSc)

Wien, 2022 / Vienna, 2022

Studienkennzahl lt. Studienblatt /  
degree programme code as it appears on  
the student record sheet:

UA 066 834

Studienrichtung lt. Studienblatt /  
degree programme as it appears on  
the student record sheet:

Masterstudium Molekulare Biologie

Betreut von / Supervisor:

Assoc. Prof. Dr. Gang Dong



# Acknowledgements

I would like to express my gratitude towards my supervisor Dr. Gang Dong for making this project possible, being a remarkable mentor and providing excellent support – thank you very much, it has been a great pleasure!

Special thanks go to Katharina Korbula, Alexander Stadler, Arda Kara, Beidong Zheng, Harald Hornegger, Tamara Groffics and so many more – without you this wouldn't have been possible!

And of course, I would like to thank my friends and family for their unconditional and devoted support.

# Table of Contents

Abstract

Zusammenfassung

<b>1. Introduction</b>	<b>- 9 -</b>
<b>1.1. Trypanosoma brucei</b>	<b>- 9 -</b>
1.1.1. Human African trypanosomiasis	- 9 -
1.1.2. <i>Trypanosoma brucei</i> – Life Cycle	- 10 -
1.1.3. <i>Trypanosoma brucei</i> – Morphology	- 11 -
1.1.4. <i>Trypanosoma brucei</i> – The Flagellar Pocket Collar	- 11 -
<b>1.2. Exocytosis in Yeast</b>	<b>- 13 -</b>
<b>2. Aim</b>	<b>- 16 -</b>
<b>3. Materials and Methods</b>	<b>- 17 -</b>
<b>3.1. Buffers and Solutions</b>	<b>- 17 -</b>
<b>3.2. DNA Methods</b>	<b>- 18 -</b>
3.2.1. Competent Cells	- 18 -
3.2.2. Vectors	- 19 -
3.2.2.1. General Information	- 19 -
3.2.2.2. Vector Preparation	- 22 -
3.2.3. Insert Preparation	- 23 -
3.2.3.1. Insert Amplification via Polymerase Chain Reaction	- 23 -
3.2.3.2. Insert Digestion and Cleanup	- 24 -
3.2.4. Ligation of Inserts and Vectors	- 25 -
3.2.5. Transformation	- 25 -
3.2.6. DNA Miniprep of Constructs	- 25 -
<b>3.3. Protein Methods</b>	<b>- 26 -</b>
3.3.1. Transformation of Constructs into BL21(DE3) Competent Cells	- 26 -
3.3.2. Protein Expression	- 26 -
3.3.3. Cell Lysis	- 27 -
3.3.4. HisTrap Affinity Chromatography (HisTrap)	- 27 -
3.3.5. Nickle-Bead Gravity-Column Purification	- 27 -
3.3.6. PEI Nucleic Acid Precipitation	- 28 -
3.3.7. Tag-Removal	- 28 -
3.3.8. Anion-Exchange Chromatography (AEX)	- 29 -
3.3.9. Cation-Exchange Chromatography (CEX)	- 29 -
3.3.10. Size-Exclusion Chromatography (SEC)	- 30 -
3.3.11. MBP-Tag Affinity Chromatography (MBP-Trap)	- 30 -
3.3.12. SDS-PAGE	- 31 -
3.3.13. Electrophoretic Shift Assay	- 31 -
3.3.14. Isothermal Titration Chromatography (ITC)	- 32 -
3.3.15. Rotary Shadowing Electron Microscopy (rsEM)	- 33 -
<b>3.4. Crystallography Methods</b>	<b>- 33 -</b>
3.4.1. Sec3(aa75-260) Sso2(aa1-270) Complex	- 33 -
3.4.2. Sec3(aa75-260) Sso1(aa1-224) Complex	- 34 -
3.4.2.1. Crystallization Set-up and Screening	- 34 -
3.4.2.2. Crystal Harvesting	- 34 -
3.4.2.3. Data Acquisition and Processing	- 35 -
3.4.2.4. Model Build and Refinement	- 35 -
<b>3.5. In Vivo Methods</b>	<b>- 36 -</b>
3.5.1. Growth Test	- 36 -
3.5.2. Bgl2 and Invertase Secretion Assay	- 37 -
3.5.3. Screening for Accumulation of Secretory Vesicles	- 37 -
3.5.4. Screening for Snc1 Recycling	- 38 -
3.5.5. Screening for Effects on Actin-independent Localization of Sec3	- 38 -



<b>4. Results</b>	<b>- 39 -</b>
<b>4.1. Cloning</b>	<b>- 39 -</b>
<b>4.2. Protein expression</b>	<b>- 40 -</b>
<b>4.3. TbBILBO421-NTD – Purification and Results</b>	<b>- 41 -</b>
4.3.1. TbBILBO421-NTD – HisTrap (1)	- 41 -
4.3.2. TbBILBO421-NTD – Tag-Removal	- 42 -
4.3.3. TbBILBO421-NTD – HisTrap (2)	- 43 -
4.3.4. TbBILBO421-NTD – AEX	- 44 -
4.3.5. TbBILBO421-NTD – SEC	- 45 -
4.3.6. TbBILBO421-NTD FPC4-CTD – Electrophoretic Shift Assay	- 47 -
<b>4.4. TbBILBO421-EFh – Purification and Results</b>	<b>- 48 -</b>
4.4.1. TbBILBO421-EFh – HisTrap	- 48 -
4.4.2. TbBILBO421-EFh – MBP-Trap	- 49 -
4.4.3. TbBILBO421-EFh – Tag-Removal	- 50 -
4.4.4. TbBILBO421-EFh – SEC	- 51 -
<b>4.5. TbBILBO421-EFh-CCD – Purification and Results</b>	<b>- 55 -</b>
4.5.1. TbBILBO421-EFh-CCD – Ni-Bead Purification	- 55 -
4.5.2. TbBILBO421-EFh-CCD – SEC	- 56 -
<b>4.6. TbBILBO421-EFh-CCD-ct – Purification and Results</b>	<b>- 60 -</b>
4.6.1. TbBILBO421-EFh-CCD-ct – HisTrap	- 60 -
4.6.2. TbBILBO421-EFh-CCD-ct – SEC	- 61 -
4.6.3. TbBILBO421-EFh-CCD-ct – rsEM	- 65 -
<b>4.7. TbBILBO421-CCD-ct – Purification and Results</b>	<b>- 66 -</b>
4.7.1. TbBILBO421-CCD-ct – HisTrap	- 66 -
4.7.2. TbBILBO421-CCD-ct – SEC (1)	- 67 -
4.7.3. TbBILBO421-CCD-ct – rsEM	- 69 -
4.7.4. TbBILBO421-CCD-ct – Tag-Removal	- 70 -
4.7.5. TbBILBO421-CCD-ct – SEC (2)	- 70 -
<b>4.8. TbBILBO421-CCD – Purification and Results</b>	<b>- 72 -</b>
4.8.1. TbBILBO421-CCD (HM15b)	- 72 -
4.8.1.1. TbBILBO421-CCD – HisTrap	- 72 -
4.8.1.2. TbBILBO421-CCD – SEC (1)	- 73 -
4.8.1.3. TbBILBO421-CCD – rsEM	- 75 -
4.8.1.4. TbBILBO421-CCD – Tag-Removal	- 76 -
4.8.1.5. TbBILBO421-CCD – SEC (2)	- 76 -
4.8.2. TbBILBO421-CCD (Sumo15b)	- 78 -
4.8.2.1. TbBILBO421-CCD – HisTrap (1)	- 78 -
4.8.2.2. TbBILBO421-CCD – Tag-Removal	- 79 -
4.8.2.3. TbBILBO421-CCD – HisTrap (2)	- 80 -
4.8.2.4. TbBILBO421-CCD – SEC	- 81 -
<b>4.9. Sec3(aa75-260) Sso2(aa1-270) Complex</b>	<b>- 83 -</b>
<b>4.10. Sec3-PH – Purification and Results</b>	<b>- 84 -</b>
4.10.1. Sec3-PH – HisTrap (1)	- 84 -
4.10.2. Sec3-PH – PEI Nucleic Acid Precipitation	- 85 -
4.10.3. Sec3-PH – HisTrap (2)	- 85 -
4.10.4. Sec3-PH – Tag-Removal	- 86 -
4.10.5. Sec3-PH – CEX	- 87 -
<b>4.11. Sec3-PH – ITC</b>	<b>- 88 -</b>
<b>4.12. SSO1Δ Sso2<sup>mut</sup> – In Vivo Results</b>	<b>- 91 -</b>
4.12.1. SSO1Δ Sso2 <sup>mut</sup> – Growth Test	- 91 -
4.12.2. SSO1Δ Sso2 <sup>mut</sup> – Bgl2 Secretion Assay	- 92 -
4.12.3. SSO1Δ Sso2 <sup>mut</sup> – Invertase Secretion	- 93 -
4.12.4. SSO1Δ Sso2 <sup>mut</sup> – Accumulation of Secretory Vesicles	- 94 -
4.12.5. SSO1Δ Sso2 <sup>mut</sup> – Snc1 Recycling	- 95 -
4.12.6. SSO1Δ Sso2 <sup>mut</sup> – Sec3 Actin Independent Localization	- 96 -
<b>4.13. Sso1(aa1-224) – Purification and Results</b>	<b>- 98 -</b>
4.13.1. Sso1(aa1-224) – HisTrap	- 98 -
4.13.2. Sso1(aa1-224) – Tag-Removal	- 99 -
4.13.3. Sso1(aa1-224) – AEX	- 100 -

<b>4.14. Sec3-PH/Sso1(aa1-224) – Complex .....</b>	<b>- 101 -</b>
4.14.1. Sec3-PH/Sso1(aa1-224) Complex – SEC .....	- 101 -
4.14.2. Sec3-PH/Sso1(aa1-224) Complex – Crystallization Results .....	- 103 -
<b>5. Discussion.....</b>	<b>- 106 -</b>
<b>6. References .....</b>	<b>- 110 -</b>
<b>7. List of Figures .....</b>	<b>- 113 -</b>
<b>8. List of Tables .....</b>	<b>- 115 -</b>
<b>9. Appendix .....</b>	<b>- 116 -</b>
<b>9.1. Protein Sequences .....</b>	<b>- 116 -</b>
9.1.1. TbBILBO421 [ <i>Trypanosoma brucei</i> TREU927] – DNA Sequence .....	- 116 -
9.1.2. TbBILBO421 [ <i>Trypanosoma brucei</i> TREU927] – Protein sequence .....	- 116 -
9.1.3. Sec3 [ <i>Saccharomyces cerevisiae</i> S288C] – Protein Sequence .....	- 117 -
9.1.4. Sso1 [ <i>Saccharomyces cerevisiae</i> S288C] – Protein Sequence .....	- 117 -
9.1.5. Sso2 [ <i>Saccharomyces cerevisiae</i> S288C] – Protein Sequence .....	- 117 -
<b>9.2. Sequencing Results .....</b>	<b>- 118 -</b>
<b>9.3. Hampton Research Crystal Screen HT Formulation .....</b>	<b>- 119 -</b>
<b>9.4. Data Collection and Refinement Statistics .....</b>	<b>- 122 -</b>

## Abstract

This study focuses on two topics. The first part focuses on the structure and function of *Trypanosoma brucei* flagellar pocket collar protein BILBO421. *Trypanosoma brucei* is a unicellular protozoan parasite of the Trypanosomatidae family and cause of the vector-borne disease Human African trypanosomiasis. The cell features a distinctive flagellum, which emerges from a bulb-like invagination at the posterior end of the cell, the flagellar pocket (FP). The FP is formed by invagination of the cells membrane and is held in place by a horseshoe-like structure, the flagellar pocket collar (FPC). The FP is the sole site of endo- and exocytosis. Protein BILBO1 was the first component of the FPC to be identified. BILBO1 is a multi-domain cytoskeletal protein proposed to form a belt-like solenoid structure circling the flagellar pocket neck. This solenoid structure is achieved by assembly into antiparallel homodimers, via its coiled-coil domain, which themselves are linked to long filamentous structures, via their C-terminal leucine-zipper domain, forming a filament of potentially indefinite length. Another confirmed FPC component, besides BILBO1, is FPC4. FPC4 is a microtubule-binding protein. FPC4 has been found to interact with BILBO1 via its C-terminal region. Computational studies have shown that four BILBO1-like proteins share a similar NTD. One of these BILBO1-like proteins, FPC3/BILBO2, was found to also bind the C-terminal region of FPC4 via its NTD. In this study BILBO421, being one those four identified proteins, has been found to shares the ability of BILBO1 and FPC3/BILBO2 to interact with the C-terminal domain of FPC4. Further, rotary shadowing electron microscopy imaging unveiled that BILBO421 forms antiparallel dimers, as previously observed in BILBO1. The ability of the BILBO421 EFh-motifs to alter the proteins conformation, as seen in BILBO1, could be verified as well.

The second part of the study focuses on the interaction of *Saccharomyces cerevisiae* SNARE-associated proteins Sso1/2 and Sec3. For exocytosis in yeast, the vesicle docking site is marked by an octameric complex called the exocyst. This tethering factor captures and brings secretory vesicles to the site of exocytosis. To facilitate exocytosis, two t-SNARE proteins of the target membrane, Sso1/2 and Sec9, must interact with the v-SNARE protein Snc1/2 of the vesicle. Sso1/2 consists of four helices (H<sub>abc</sub> & H3), with the first three (H<sub>abc</sub>) forming an inhibitory domain and H3 as the SNARE motif to interact with Sec9 and Snc1/2 during membrane fusion. Sec3, part of

the exocyst complex consists of a N-terminal pleckstrin homology domain (PH), a central putative coiled-coil, and a C-terminal helical domain. The Sec3 PH domain promotes conformational change in the four-helix-bundle of Sso2, releasing H3 from the inhibitory domain, allowing the formation of an initial binary complex between H3 of Sso2 and the two helices of Sec9. Thus, allowing this newly formed complex to interact with the v-SNARE Snc1/2 to facilitate membrane fusion. A new crystal structure, of the Sec3/Sso2 complex revealed an additional binding site for Sec3 on Sso2, located at the N-terminal end of Sso2, comprised of two highly conserved Asn-Pro-Tyr (NPY) motifs. These two NPY motives are connected to the helical core of Sso2 via a long flexible linker. The data suggests that the NPY motifs act like a fishing hook, enhancing recruitment of the Sso2 t-SNARE protein to the vesicle targeting site. The crystal structure revealed two distinct heterodimeric complexes, each showing one of the two NPY motifs to be bound to a conserved hydrophobic pocket on Sec3 respectively. Via an isothermal titration calorimetry assay this study was not only able to show, that either of the NPY-motifs are able to bind Sec3, but also that the NPY-motifs bind Sec3 synergistically. The results obtained by the isothermal titration calorimetry assay could be largely confirmed by extensive in vivo assays.

# Zusammenfassung

Die folgende Arbeit beleuchtet zwei Themen. Der erste Teil nimmt sich der Struktur und Funktion des *Trypanosoma brucei* „Flagellar Pocket Collar“ (FPC, dt. Geißeltaschenkragen) Proteins BILBO421 an. *Trypanosoma brucei*, ein unizellulärer, protozoischer Parasit der Trypanosomatidae Familie, ist der Erreger der Afrikanischen Trypanosomiasis. Seine Zelle besitzt ein charakteristisches Flagellum, welches aus einer birnenförmigen Einstülpung am posterioren Ende, der Geißeltasche, hervorragt. Die Geißeltasche, der einzige Ort der Endo- und Exozytose, wird durch eine Einstülpung der Zellmembran geformt und durch eine hufeisenartige Struktur, dem FPC, zusammengehalten. Das Protein BILBO1 war die erste identifizierte Komponente des FPCs. Es ist Teil des Zytoskeletts und formt eine gürtelartige Struktur, welche den Hals des FPCs umringt. Diese gürtelartige Struktur wird durch den Zusammenbau von einzelnen BILBO1 Molekülen über ihre „Coiled-Coil“-Domäne zu antiparallelen Dimeren erreicht, wobei diese Dimere sich wiederum über eine C-terminale „Leucine-Zipper“-Domäne des Proteins zu theoretisch unbegrenzt langen, filamentösen Strukturen zusammenschließen. Eine weitere bestätigte Komponente des FPCs, nebst BILBO1, ist das Protein FPC4. Dem Protein, welches die Fähigkeit besitzt Mikrotubuli zu binden, wurde nachgewiesen mit der N-terminalen Domäne (NTD) BILBO1s über seine C-terminalen Domäne (CTD) zu interagieren. Computergestützte Untersuchungen haben vier weitere Proteine identifiziert, welche eine BILBO1 homologe NTD besitzen. Einem dieser Proteine, FPC3/BILBO2, konnte ebenfalls eine Interaktion mittels seiner NTD mit der CTD FPC4s nachgewiesen werden. In dieser Arbeit konnte dem Protein BILBO421, einem dieser vier identifizierten Proteine, nachgewiesen werden, dass es die Fähigkeit BILBO1s und FPC3/BILBO2s teilt, mit der CTD FPC4s zu interagieren. Zusätzlich konnte die Anwendung von Rotationsschatten-Elektronenmikroskopie (rsEM) nachweisen, dass BILBO421, ähnlich zu BILBO1, antiparallele Dimere ausbildet. Ebenso konnte nachgewiesen werden, dass die EF-Hand Motive BILBO421s, in Gegenwart von  $\text{Ca}^{2+}$ -Ionen, die Struktur des Proteins beeinflussen können, so wie es schon bei BILBO1 beobachtet wurde.

Der zweite Teil der Arbeit widmet sich der Interaktion der *Saccharomyces cerevisiae* SNARE-assoziierten Proteine Sso1/2 und Sec3. Zum Zwecke der Exozytose in Hefen ist die Vesikel-Andockstelle durch einen oktameren „Exocyst“-Komplex markiert. Dieser Bindungs-Faktor fängt sekretorische Vesikel ein und bringt diese zum Ort der Exozytose. Um die Exozytose zu vollziehen, müssen die zwei „t-SNARE“ Proteine Sso1/2 und Sec9 der Ziellmembran mit den „v-SNARE“ Proteinen des Vesikels interagieren. Sso1/2 besteht aus vier Helices, den ersten drei ( $H_{abc}$ ), welche die inhibitorische Domäne bilden, und H3, dem SNARE-Motiv, welches mit den SNARE Proteinen Sec9 und Snc1/2 während der Membranfusion interagiert. Sec3, Teil des Exocyst-Komplexes besteht aus einer N-terminalen „Pleckstrin Homology“-Domäne (PH), einer zentralen Coiled-Coil-Domäne und einer C-terminalen helikalen Domäne. Die Sec3 PH Domäne regt Konformationsänderungen innerhalb des aus vier Helices bestehenden Bündels von Sso2 an, was zur Abspaltung der H3-Domäne von der inhibitorischen Domäne führt. Dies erlaubt wiederum die Bildung eines initialen binären Komplexes zwischen H3 Sso2s und den zwei Helices Sec9s, was diesem neugebildeten Komplex wiederum ermöglicht, mit dem v-SNARE Protein Snc1/2 zu interagieren und so die Membranfusion anzustoßen. Eine neue Proteinstruktur des Sec3/Sso2 Komplexes deckt nun eine weitere Bindungsstelle für Sec3 auf Sso2 auf. Diese Bindungsstelle ist am N-terminalen Ende Sso2s lokalisiert und bestehend aus zwei hoch-konservierten Asn-Pro-Tyr (NPY) Motiven. Diese neuen NPY-Motive sind mit dem helikalen Kern Sso2s mittels einem langen und flexiblen „Linker“ verbunden. Die Kristallographischen Daten legen nahe, dass diese NPY-Motive ähnlich einem Angelhaken agieren und somit die Rekrutierung des Sso2 t-SNARE Proteins zur Vesikel-Andockstelle steigern. Die Proteinstruktur dieser neuen noch unveröffentlichten kristallographischen Daten, besteht aus zwei heterodimeren Komplexen, welche jeweils zeigen, wie eines der NPY-Motive in einer konservierten hydrophoben Tasche auf der Oberfläche Sec3s bindet. Mittels isothermer Titrationskalorimetrie konnte in dieser Arbeit nicht nur nachgewiesen werden, dass beide NPY-Motive die Fähigkeit besitzen Sec3 zu binden, sondern, dass dieses auch synergetisch geschieht. Die Ergebnisse der isothermen Titrationskalorimetrie konnten weitreichend durch mehrere in vivo Experimente gestützt werden.

# 1. Introduction

The following master's thesis focuses on two topics. Structure and function of *Trypanosoma brucei* flagellar pocket collar protein BILBO421 and the interaction of *Saccharomyces cerevisiae* SNARE-associated proteins Sso1/2 and Sec3.

## 1.1. *Trypanosoma brucei*

*Trypanosoma brucei* is a unicellular protozoan parasite of the Trypanosomatidae family and cause of the vector-borne disease Human African trypanosomiasis (HAT), also known as *sleeping sickness* and the animal form of the disease *Nagana*. *T. brucei* is transmitted between mammalian hosts via the blood-feeding tsetse fly (*Glossina*), limiting the spread of HAT and Nagana to the Sub-Saharan African area. The main subspecies responsible for HAT are *Trypanosoma brucei gambiense*, the predominant subspecies in Central and West Africa, and *Trypanosoma brucei rhodesiense*, prevalent in East and South Africa. While both subspecies can infect humans and animals alike, making livestock a reservoir for zoonosis, a third subspecies, *Trypanosoma brucei brucei*, only infects livestock and wildlife. (Brun *et al.*, 2009; Franco *et al.*, 2014; Gibson, 2007).

### 1.1.1. Human African trypanosomiasis

The course of HAT can be divided into two main stages. A hemolytic stage, in which the parasite is restricted to the blood and lymph system, with febrile episodes, and a meningo-encephalitic stage, after the parasite crosses the blood-brain barrier, reaching the brain parenchyma and cerebrospinal fluid, with various neurological symptoms, such as general motor weakness and akinesia. The meningo-encephalitic stage is also accompanied by severe sleep disorder, giving rise to the name *sleeping sickness*. The duration and severity of both stages varies strongly between patients infected with *T. b. gambiense* and those infected with *T. b. rhodesiense*. While *T. b. gambiense*, cause for 98% of all annually reported cases, causes a chronic progressive form of HAT, *T. b. rhodesiense* causes an acute form of HAT, reducing the progression of the disease from an average of 3 years to merely a couple of weeks or months. Both infections inevitably lead to coma and death if left untreated. (Blum *et al.*, 2005; Brun *et al.*, 2009).

### 1.1.2. *Trypanosoma brucei* – Life Cycle

The predominant form of *T. brucei* in the human bloodstream is a morphologically slender, proliferative form. In this form *T. brucei* is coated by variable surface glycoproteins (VSGs), which provide protection against lytic factors in the human plasma. As these VSGs are recognized by the immune system, *T. brucei* evades immune response by constantly switching to new variants of the surface glycoproteins, using its vast array of VSG genes present in its genome (~200 genes), achieving a high degree of antigenic variation. (Brun *et al.*, 2009; Marcello *et al.*, 2017; Matthews, 2005).

As the population of *T. brucei*'s increases in the hosts bloodstream, the parasite differentiates to a morphologically stumpy, division-arrested form, preadapted to tsetse fly transmission (Matthews, 2005).

As the tsetse fly feasts on the mammalian hosts blood, the parasite is taken up by the tsetse fly and differentiates to a procyclic form, losing the VSG coating. In this proliferative stage *T. brucei* establishes in the fly's midgut. After the parasite established itself in the midgut, division arrest is followed by migration to the salivary gland. *T. brucei* attaches to the salivary gland in its proliferative epimastigote form. The epimastigotes generate non-proliferative metacyclic forms. These non-proliferative metacyclic forms reestablish the VSG coating in preparation of host transmission. As the tsetse fly feasts on the mammalian hosts blood once again, the parasite is transmitted and the complex lifecycle switching between vector and mammalian host is complete. It is to be noted that newly hatched flies have never been observed to be infected. (Brun *et al.*, 2009; Matthews, 2005).



### **1.1.3. *Trypanosoma brucei* – Morphology**

*Trypanosoma brucei* is a unicellular organism with a distinct elongated morphology. The cell's shape is defined by a highly polarized microtubule cytoskeleton, of uniform polarity in the direction of the anterior- posterior-axis. The cell features a distinctive flagellum, which emerges from a bulb-like invagination at the posterior end of the cell, the flagellar pocket (FP). The FP is formed by invagination of the cells membrane and is held in place by a horseshoe-like structure, the flagellar pocket collar (FPC). The FP is the sole site of endo- and exocytosis, as the bloodstream form of *T. brucei* features an exterior densely packed with VSGs. The flagellum is tethered alongside the exterior of the cell, defining the anterior- posterior-axis. The flagellum plays a key role in cellular development and pathogenesis of the parasite by enabling motility, cell division, morphogenesis, mediating host-cell attachment and providing a scaffold for assembly of signaling proteins and virulent factors. The flagellum is structurally comprised of a canonical 9x2 axoneme arrangement, symmetrically surrounding a central pair of singlet microtubules. The flagellum is anchored in the cytoplasm at the posterior end of the cell, via the basal body, a cylindrical structure comprised of 9 sets of microtubule triplets. Lateral attachment of the flagellum to the parasite's body is facilitated via the flagellum attachment zone (FAZ). The FAZ is comprised of a central subpellicular FAZ filament flanked by a microtubule quartet on each side, extending from the basal body to the anterior end. (Langousis *et al.*, 2014; Matthews, 2005).

### **1.1.4. *Trypanosoma brucei* – The Flagellar Pocket Collar**

The neck of the FP is characterized by an electron-dense cytoskeletal structure, the FPC. Protein BILBO1 was the first component of the FPC to be identified. BILBO1 is a multi-domain cytoskeletal protein proposed to form a belt-like solenoid structure circling the flagellar pocket neck. (Vidilaseris *et al.*, 2014a).

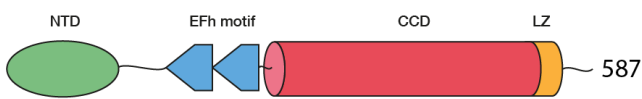
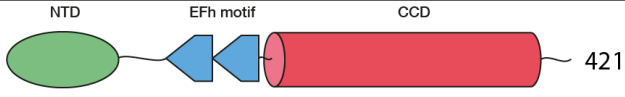
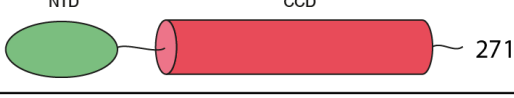
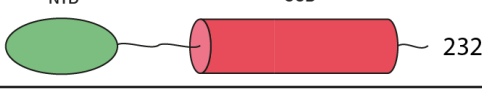

BILBO1 has been found contain four putative functional domains. On the N-terminal side a ubiquitin-like motif (NTD), followed by two EFh-motifs, a long coiled-coil domain (CCD) and a leucine-zipper domain (LZ) at the C-terminal end. The EFh-motifs seemingly play a key role in the structural integrity of the whole protein, as structural changes in the protein in the absence of calcium have been observed. The protein has been found to assemble into antiparallel homodimers via their CCD which are

themselves linked to long filamentous structures via their C-terminal LZ, forming a filament of potentially indefinite length. (Vidilaseris *et al.*, 2014c).

Another confirmed FPC component, besides BILBO1, is FPC4. FPC4 is a microtubule-binding protein. Microtubule binding is facilitated by the proteins N-terminal domain. FPC4 has also been found to interact with BILBO1 via its C-terminal region. (Albisetti *et al.*, 2017).

A novel crystal structure of the BILBO1 NTD has revealed a conserved hydrophobic pocket formed by a long loop structure. This hydrophobic pocket has been found to interact with three conserved aromatic residues (Trp-71, Tyr-87, Phe-89) of the FPC4 C-terminal region. (Vidilaseris *et al.*, 2014b; Vidilaseris *et al.*, 2019).

Computational studies have shown that four BILBO1-like proteins share a similar NTD (Figure 1). One of these BILBO1-like proteins, FPC3, alternatively named BILBO2, was found to also bind the C-terminal region of FPC4 via its NTD. This was verified via a crystal structure of a FPC3-NTD/FPC4 complex. The crystal structure revealed that FPC4 docks to the conserved hydrophobic cleft of FPC3 via residues <sup>432</sup>VLTSVPV<sup>438</sup>. (Isch *et al.*, 2021).

BILBO1		BILBO1-NTD vs. homolog NTD Sequence identity / similarity [%] (aligned length)
BILBO421		35.7 / 50.0 (98aa)
BILBO2/FPC3		32.6 / 46.5 (86aa)
BILBO232		40.8 / 60.2 (103aa)
BILBO159		28.6 / 48.4 (91aa)

**Figure 1: BILBO1-Like Proteins**

NTD comparison between BILBO1 and its homologs BILBO421, BILBO2/FPC3, BILBO232, BILBO159, including a schematic illustration of their putative domains.

## 1.2. Exocytosis in Yeast

Membrane trafficking, in eukaryotes, and the associated membrane fusion of transport vesicles and target organelles is largely driven by soluble N-ethylmaleimide-sensitive factor-attachment protein receptors (SNAREs). SNARE proteins are a group of typically C-terminally anchored membrane proteins. There are several types of SNARE proteins, v-SNAREs, which are attached to the vesicle membrane, and t-SNAREs, which are part of the target membrane. Interaction via the formation of parallel dimers of SNARE proteins of opposing membranes mediates the fusion of those compartments. (Pelham, 1999). This formation of parallel SNARE protein dimers is regulated by SNARE chaperones of the Sec1/Munc18 (SM) protein family, which are capable of inhibition and catalyzation of the SNARE complex assembly. (Eisemann *et al.*, 2020).

For exocytosis in yeast, the vesicle docking site is marked by an octameric complex called the exocyst. This tethering factor captures and brings secretory vesicles to the site of exocytosis. (Wu *et al.*, 2015).

To facilitate exocytosis, two t-SNARE proteins of the target membrane, Sso1/2 and Sec9, must interact with the v-SNARE protein Snc1/2 of the vesicle. Sso1/2 consists of four helices ( $H_{abc}$  &  $H_3$ ), with the first three ( $H_{abc}$ ) forming an inhibitory domain and  $H_3$  as the SNARE motif to interact with Sec9 and Snc1/2 during membrane fusion (Fiebig *et al.*, 1999).

Sec3, part of the exocyst complex consists of a N-terminal pleckstrin homology domain (PH), a central putative coiled-coil, and a C-terminal helical domain. The Sec3 PH domain promotes conformational change in the four-helix-bundle of Sso2, releasing  $H_3$  from the inhibitory domain, allowing the formation of an initial binary complex between  $H_3$  of Sso2 and the two helices of Sec9. Thus, allowing this newly formed complex to interact with the v-SNARE Snc1/2 to facilitate membrane fusion (Figure 2). (Yue *et al.*, 2019).

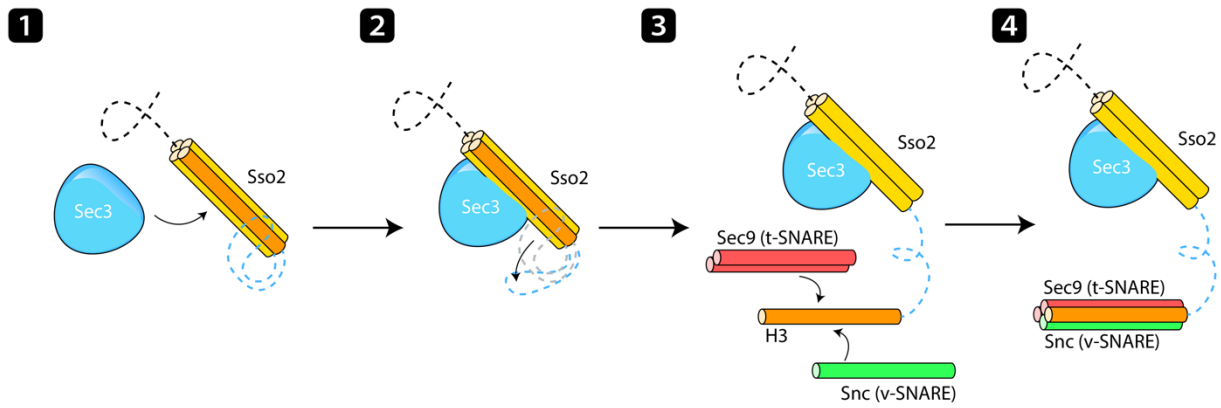


**Figure 2: Illustration of Sec3/Sso2 Interaction**

Step-by-step illustration of the recruitment of Sso2 to the site of exocytosis by Sec3 and subsequent SNARE complex assembly. **1:** Recruitment of Sso2 to the vesicle targeting site by Sec3. **2:** Sec3 PH domain promoting conformational change in the four-helix bundle of Sso2. **3:** Release of H3 from the inhibitory domain and formation of an initial binary complex between H3 of Sso2 and the two helices of Sec9 with subsequent interaction of this new complex with v-SNARE Snc. **4:** SNARE complex assembly complete.

This interaction between the Sec3 PH domain and the four-helix-bundle of Sso2 has previously been verified via a crystal structure of a complex between Sec3(aa75-249) and Sso2(aa33-223) by Yue *et al.*, 2019, as seen in Figure 3, A. It is reminiscent of the interaction of SM proteins Munc18, Vps45 and their respective SNARE partners syntaxin-1 (Stx) and Tlg2 (Figure 3, B, C). Both aforementioned SM proteins contain three domains, which are folded into a “horseshoe”-like conformation, engulfing the helical bundles of their SNARE partners, establishing a strong interaction between both proteins, which is further reinforced by a small helical C-terminal extension of the corresponding SNARE protein, which is additionally inserted into a hydrophobic pocket deep inside the “horseshoe”-like conformation. (Burkhardt *et al.*, 2008; Eisemann *et al.*, 2020). In contrast, the Sec3 PH domain is a much smaller, single globular domain, presenting a comparatively small Sec3/Sso2 interaction interface, suggesting significantly weaker interaction between the two proteins (Figure 3).

Additionally, Munc18, Vsp45 and their respective partners Stx and Tlg2 feature a second interaction interface consisting of a short N-terminal helical motif of Stx/Tlg2 called the “N-peptide”, which binds distally to the opposite to the aforementioned interaction-site (Figure 3, B, C). The presence of dual interaction interfaces is shared among multiple SM proteins and their corresponding SNARE interaction partners. (Burkhardt *et al.*, 2008; Eisemann *et al.*, 2020).

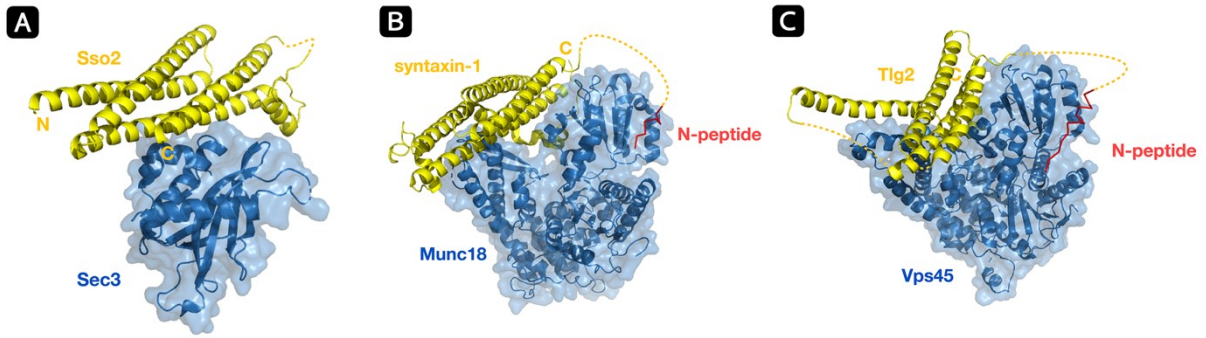


**Figure 3: Structural Information Sec3/Sso2 and Homologues**

**A:** Structure of Sec3(aa75-249) Sso2(aa33-223) complex (PDB: 5M4Y). **B:** Structure of Munc18/syntaxin-1 complex with N-peptide of syntaxin-1 highlighted in red (PDB: 3C98). **C:** Structure of Vps45/Tlg2 complex with N-peptide of Tlg2 highlighted in red (PDB: 6XM1).

As the crystal structure of the Sec3/Sso2 complex (Figure 3, A) did not cover the N-terminal region of Sso2, the presence of a N-peptide homolog structure has not been verified yet. Computational studies have shown though, that a highly conserved double NPY-motif is present among multiple species, potentially mimicking the function of the previously described N-peptides of other t-SNARE species (Figure 4).

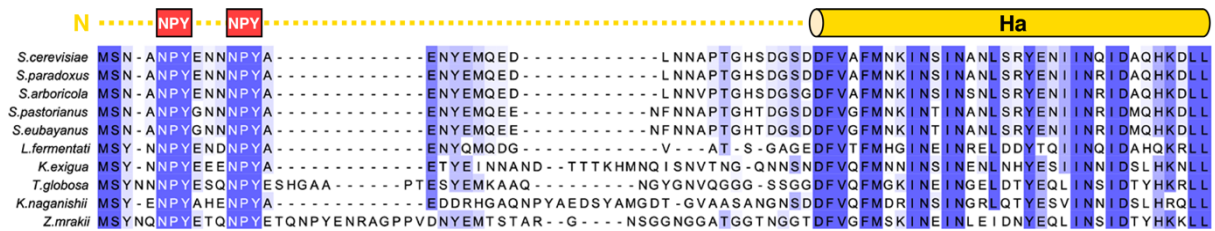


**Figure 4: Sso2 N-terminal Region Multiple Sequence Alignment of Multiple Species**  
Multiple sequence alignment of the Sso2 N-terminal protein sequence among multiple species, covering helical domain  $H_a$  to the N-terminus. Highly conserved double NPY-motif highlighted in red.

## 2. Aim

The main aim of the study, concerning *Trypanosoma brucei* flagellar pocket collar protein BILBO421, was to compare the, among all BILBO1 homologues, strongly conserved NTD to the ones of BILBO1 and FPC3/BILBO2, trying to reproduce a possible interaction of the proteins NTD with FPC4, as previously observed in the before mentioned BILBO421 homologues.

With BILBO421 being the most similar one of the four identified homologues, to BILBO1, regarding its size and functional domains, this study also focuses on its EFh-motifs and CCD, which it shares with BILBO1. By trying to replicate the ability of BILBO1 to form antiparallel dimers via its CCD in BILBO421 and investigating if its EFh-motifs also alter the proteins conformation in dependence of  $\text{Ca}^{2+}$ -ions, as observed with BILBO1, hopefully more information on the proteins function in the FPC can be unveiled.

The main aim of the study, regarding *Saccharomyces cerevisiae* SNARE-associated proteins Sso1/2 and Sec3, was to further investigate a possible interaction of the newly identified N-terminal NPY-motifs of Sso2 with Sec3. For this purpose, X-ray Crystallography of a new Sec3/Sso2 complex containing the whole N-terminal region of Sso2, isothermal titration calorimetry and various in vivo assays were carried out. To gain further insights into this possible novel form of interaction between Sec3 and Sso2 crystal screening for a complex of the Sec3 pleckstrin homology domain together with Sso2 homolog Sso1 was performed.

## 3. Materials and Methods

### 3.1. Buffers and Solutions

#### **(Selective) LB-Medium**

25 g/l of Luria Broth Base  
For selectivity add:  
50 µg/ml Ampicillin or  
30 µg/ml Kanamycin

#### **(Selective) Agarose Plates**

25 g/l of Luria Broth Base,  
15 g/l Agarose  
For selectivity add:  
50 µg/ml Ampicillin or  
30 µg/ml Kanamycin

#### **6x DNA Loading Dye**

0.25% (w/v) Bromphenol blue,  
30% (v/v) Glycerol

#### **50x TAE Buffer**

2M Tris-HCL (pH 8.0),  
5.71% (v/v) Acetic acid,  
50 mM EDTA

#### **4x Tris-HCl/SDS, pH 6.8**

0.4% (w/v) SDS,  
0.5 M Tris Base, pH 6.8

#### **4x Tris-HCl/SDS, pH 8.8**

0.4% (w/v) SDS,  
1.5 M Tris Base, pH 8.8

#### **SDS-Running Buffer**

100 mM Tris base, 100 mM Tricine,  
0.1% (w/v) SDS

#### **6x SDS Loading Dye**

0.35 M Tris-HCl, 10% (w/v) SDS,  
30% (v/v) Glycerol, 0.6 M DTT,  
0.06% (w/v) Bromphenol blue, pH 6.8

#### **Staining solution**

40% (v/v) EtOH,  
10% (v/v) Acetic acid,  
0.025% (w/v) Coomassie brilliant blue  
R250

#### **Destaining solution**

50% (v/v) MeOH,  
10% (v/v) Acetic acid

#### **HisTrap Buffer A**

100 mM NaCl, 20 mM Imidazol,  
10 mM β-MeOH, 20 mM HEPES,  
pH 7.5

#### **HisTrap Buffer B**

100 mM NaCl, 1 M Imidazol,  
10 mM β-MeOH, 20 mM HEPES,  
pH 7.5

#### **IEX Buffer A**

50 mM NaCl, 1 mM DTT,  
20 mM HEPES, pH 7.5

#### **IEX Buffer B**

1M/2M NaCl, 1 mM DTT,  
20 mM HEPES, pH 7.5

#### **SEC Buffer**

100 mM NaCl, 1 mM DTT,  
20 mM HEPES, pH 7.5

#### **MBP-Trap Buffer A**

100 mM NaCl, 10 mM β-MeOH,  
20 mM HEPES, pH 7.5

#### **MBP-Trap Buffer B**

10 mM Maltose, 100 mM NaCl,  
10 mM β-MeOH, 20 mM HEPES,  
pH 7.5

## 3.2. DNA Methods

### 3.2.1. Competent Cells

5 ml of LB-Medium were inoculated with 3-4 drops of the respective *E. coli* strain (BL21(DE3) or DH5 $\alpha$ ) and incubated overnight at 37 °C, 140 rpm. The next day 100 ml of LB-Medium were inoculated with 3 ml of the overnight-culture. The cultures were incubated at 37 °C, 140 rpm until an OD<sub>600</sub> of 0.35-0.40 was reached. The cultures were subsequently divided into 2x50 ml fractions and incubated on ice for 15 min before they were spun down at 4 °C, 2,500 rpm using an Eppendorf 5804R centrifuge. The following steps were all carried out at 4 °C. The supernatants were discarded, and the pellets were gently resuspended using 10 ml of RF1-solution (Table 1) each. After resuspension an additional 23 ml of RF1-solution were added to each fraction. The fractions were again spun down at 4 °C, 2,500 rpm, the supernatant discarded, and the pellets gently resuspended in 4 ml of RF2-solution (Table 1). The final cell suspensions were aliquoted, flash-frozen using LN<sub>2</sub> and stored at -80 °C before use.

RF1-solution	
KCl	100 mM
MnCl <sub>2</sub>	50 mM
Potassium acetate	30 mM
CaCl <sub>2</sub>	10 mM
Glycerol	15% (v/v)
pH adjusted to 5.8 (HCl)	
RF2-solution	
MOPS	10 mM
KCl	10 mM
CaCl <sub>2</sub>	75 mM
Glycerol	15% (v/v)
pH adjusted to 7.0 (KOH)	

Table 1: Competent Cells – RF1/2-Solutions



### 3.2.2. Vectors

#### 3.2.2.1. General Information

For cloning a variety of vectors were used (pET15b, SUMO15b, HM15b, MalpET, HT15b). Each vector features a unique set of different tags and cleavage sites, as listed below.

pET15b:
MGSSHHHHHHSSGLVPR  GSHMLEDP
<ul style="list-style-type: none"><li>• <u>His<sub>6</sub>-tag</u>; <u>Thrombin cutting-site</u></li><li>• MCS: NdeI, BamHI</li><li>• Expression induced by Isopropyl-β-D-thiogalactopyranosid (IPTG) (lac-operon)</li><li>• Ampicillin resistance cassette</li></ul>

Table 2: Vector pET15b

pET15b is a standard vector featuring a His<sub>6</sub> polyhistidine affinity tag for metal affinity purification. The His<sub>6</sub>-tag is followed by a cutting site for the serine protease Thrombin. The multiple cloning site features NdeI and BamHI cutting sites. Protein expression is induced by Isopropyl-β-D-thiogalactopyranosid (IPTG) as the insert is under control of the lac operon. The vector contains an Ampicillin resistance cassette.

SUMO15b:
MGSSHHHHHHSSGLVPR  GSHNSDSEVNQEAKPEVKPEVKPETHINLKVSD GSSEIFFKIKKTTPLRRLMEAFKRQ GKEMDSL RFLYDGISIQADQTPEDLD MEDNDIIEAHREQIGG  HMAAAGS
<ul style="list-style-type: none"><li>• <u>His<sub>6</sub>-tag</u>; <u>Thrombin cleavage-site</u>; <u>SUMO-tag</u>; <u>SenP2 cutting-site</u></li><li>• MCS: NdeI, BamHI</li><li>• Expression induced by Isopropyl-β-D-thiogalactopyranosid (IPTG) (lac-operon)</li><li>• Ampicillin resistance cassette</li></ul>

Table 3: Vector SUMO15b

SUMO15b is a custom vector based on pET15b introducing an additional SUMO-tag and SenP2 cleavage-site. SUMO is a small ubiquitin-related protein that is covalently conjugated to the protein of interest during expression. SUMO enhances expression and solubility of the recombinant protein. (Panavas *et al.*, 2009). SenP2 catalyzes the

deconjugation of SUMO from the recombinant protein. The vector contains an Ampicillin resistance cassette.

HM15b:
MSSHHHHHHSSGLVPR  GSMGKLVIWINGDKGYNGLAEVGKKFEKDTGIKV TVEHPDKLEEKFPQVAATGDGPDIIFWAHDRFGGYAQSGLLAEITPDKAFQD KLYPFTWDAVRYNGKLIAYPIAVEALSLIYNKDLLPNPPKTWEEIPALDKEL KAKGKSALMFNLQEPYFTWPLIAADGGYAFKYENGKYDIKDVGVDNAGAKAG LTFLVDLIKNKHMNADTDYSIAEAAFNKGETAMTINGPWAWSNIDTSKVNYG VTVLPTFKGQPSKPFVGVLSAGINAASPNKELAKEFLENYLLTDEGLEAVNK DKPLGAVALKSYYYEELAKDPRIAATMENAQKGEIMPNI PQMSAFWYAVRTAV INAASGRQTVDEALKDAQTNAAHMAAAGS
<ul style="list-style-type: none"> <li>• <u>His<sub>6</sub>-tag</u>; <u>Thrombin cleavage-site</u>; <u>MBP-tag</u>; <u>NAAH-linker</u></li> <li>• MCS: <b>NdeI</b>, <b>BamHI</b></li> <li>• Expression induced by Isopropyl-β-D-thiogalactopyranosid (IPTG) (lac-operon)</li> <li>• Ampicillin resistance cassette</li> </ul>

Table 4: Vector HM15b

HM15b is a custom vector based on pET15b. In addition to the His<sub>6</sub>-tag and Thrombin cleavage-site it features an MBP-tag (Maltose-binding protein) which is conjugated to the recombinant protein via a flexible linker. The MBP-tag enhances solubility and allows for purification of the recombinant protein as it binds to amylose columns. HM15b features no cleavage-site between the MBP-tag and the recombinant protein, the MBP-tag can therefore not be removed. The vector contains an Ampicillin resistance cassette.

MalpET:
MEIKTGARILALSALTMMFSASALAKIEEGKLVIWINGDKGYNGLAEVGKK FEKDTGIKVTVEHPDKLEEKFPQVAATGDGPDIIFWAHDRFGGYAQSGLLAE ITPDKAFQDKLYPFTWDAVRYNGKLIAYPIAVEALSLIYNKDLLPNPPKTWE EIPALDKELKAKGKSALMFNLQEPYFTWPLIAADGGYAFKYENGKYDIKDVG VDNAGAKAGLTFLVDLIKKNKHMNADTDYSIAEAAFNKGETAMTINGPWAWSN IDTSKVNYGVTVLPTFKGQPSKPFVGVLSAGINAASPNKELAKEFLENYLLT DEGLEAVNKDKPLGAVALKSYYYEELAKDPRIAATMENAQKGEIMPNI PQMSA FWYAVRTAVINAASGRQTVDEALKDAQTNSSSSNNNNNNNNNNNLGHHHHHHHH HHENLYFO    GHMASMTGGQQMGRGS
<ul style="list-style-type: none"> <li>• <u>MBP-tag</u>; <u>His<sub>10</sub>-tag</u>; <u>TEV cleavage-site</u></li> <li>• MCS: <b>NdeI</b>, <b>BamHI</b></li> <li>• Expression induced by Isopropyl-β-D-thiogalactopyranosid (IPTG) (lac-operon)</li> <li>• Kanamycin resistance cassette</li> </ul>

Table 5: Vector MalpET

MalpET features an MBP-tag, His<sub>10</sub>-tag and tobacco etch virus (TEV) protease cleavage-site. Unlike HM15b the MBP-tag is not attached to the recombinant protein via a flexible linker. The TEV cleavage-site allows for removal of the MBP-tag though. The vector contains a Kanamycin resistance cassette.

HT15b:
MNLGHHHHHHHENLYFO    GHMLEDP
<ul style="list-style-type: none"> <li>• <u>His<sub>6</sub>-tag</u>; <u>TEV cutting-site</u></li> <li>• MCS: <b>NdeI</b>, <b>BamHI</b></li> <li>• Expression induced by Isopropyl-β-D-thiogalactopyranosid (IPTG) (lac-operon)</li> <li>• Ampicillin resistance cassette</li> </ul>

Table 6: Vector HT15b

HT15b features a His<sub>6</sub>-tag followed by a tobacco etch virus (TEV) protease cleavage-site. The tag can be removed completely. The vector contains an Ampicillin resistance cassette.

### 3.2.2.2. Vector Preparation

1 µl of the respective plasmid was added to 50 µl of competent DH5α *E. coli* cells. The solution was incubated for 20 min on ice followed by heat-shocking for 45 sec at 42 °C. The reactions were incubated on ice for 5 min before 200 µl of ice-cold LB-medium was added. The culture was incubated at 37°C, 140 rpm for 1 h. After incubation 2-3 drops of the respective culture were used to inoculate 25 ml of LB-medium. The remaining culture was plated onto a LB-plate as a backup. Both plate and liquid culture were incubated overnight at 37 °C, while the liquid culture was constantly agitated at 140 rpm.

20 ml of the overnight liquid culture were used for purification using the Promega Wizard® *Plus* SV Minipreps DNA Purification System following the supplied protocol (Promega, 2009a). The concentration was determined via microvolume measurement using the DeNovix DS-11+ Spectrophotometer.

To prepare the circular plasmid for ligation with an insert 55 µl of the miniprep eluate were used for the following double-digestion reaction:

Vector Digestion Reaction			
Plasmid	55 µl		
3x rCutsmart Buffer (NEB)	7 µl		
NdeI Restriction Enzyme	3 µl	37 °C	30 min
BamHI-HF Restriction Enzyme	3 µl	37 °C	30 min
Quick CIP (NEB)	2 µl	37 °C	30 min
TOTAL	70 µl		

*Table 7: Vector Digestion Reaction*

The Enzymes were added subsequently in 30 min intervals to minimize the risk of them interfering with one another.

After digestion the reaction was mixed with 6x DNA loading dye and loaded onto a 1% (w/v) agarose, 1x TAE, 1x SYBR™ Safe DNA Gel Stain gel and run at 120 V for 40 min. The band of according size was cut, and the vector was extracted from the gel using the Promega Wizard® SV Gel and PCR Clean-Up system according to the provided protocol (Promega, 2009b). The concentration was determined via microvolume measurement using the DeNovix DS-11+ Spectrophotometer. To ensure the digest was successful, an uncut sample of the plasmid was loaded onto the same gel for comparison.

### 3.2.3. Insert Preparation

#### 3.2.3.1. Insert Amplification via Polymerase Chain Reaction

To generate and amplify the inserts PCR reactions (Table 9 and Table 10) were carried out. All TbBILBO421 inserts were generated using a full length TbBILBO421 construct as the DNA template. The primers (Table 8) were designed so that the coding sequence is always flanked by NdeI (5'-end) and BamHI (3'-end), or BamHI compatible (BglII, SpeI) restriction sites to match the multiple cloning sites of the vectors.

It is to be noted that the constructs of TbBILBO421-NTD (aa1-124)/Sumo15b, Sec3-PH(aa75-260)/pET15b and Sso1(aa1-224)/HT15b were already pre-prepared, ready for expression and therefore not subject to the cloning procedure.

Primer for Insert Amplification	
BILBO421-EFh-CCD-ct (aa210-421)	
TbBil421F2- <b>NdeI</b>	5' -GACACTG <b>CATATG</b> GCTGATAAAGTGGTGAGGAAGC-3'
TbBil421R1- <b>SpeI</b>	5' -CGAC <b>ACTAGT</b> CAGTCATGAATGTCGTACCC-3'
BILBO421-EFh-CCD (aa210-404)	
TbBil421F2- <b>NdeI</b>	5' -GACACTG <b>CATATG</b> GCTGATAAAGTGGTGAGGAAGC-3'
TbBil421R5- <b>BglII</b>	5' -GCA <b>AGATCT</b> TCAACCCATTACAGCCGCCGAC-3'
BILBO421-EFh (aa210-295)	
TbBil421F2- <b>NdeI</b>	5' -GACACTG <b>CATATG</b> GCTGATAAAGTGGTGAGGAAGC-3'
TbBil421R6- <b>BamHI</b>	5' -GCAG <b>GATCCT</b> CAGCTGAAGCGCGCATAAGCAA-3'
BILBO421-CCD-ct (aa296-421)	
TbBil421F3- <b>NdeI</b>	5' -GACACTG <b>CATATG</b> AACGAAAGGAGACAGCAAGTTG-3'
TbBil421R1- <b>SpeI</b>	5' -CGAC <b>ACTAGT</b> CAGTCATGAATGTCGTACCC-3'
BILBO421-CCD (aa296-404)	
TbBil421F3- <b>NdeI</b>	5' -GACACTG <b>CATATG</b> AACGAAAGGAGACAGCAAGTTG-3'
TbBil421R5- <b>BglII</b>	5' -GCA <b>AGATCT</b> TCAACCCATTACAGCCGCCGAC-3'
Restriction Sites	

Table 8: Primer for Insert Amplification

PCR Reaction Mix	
5x Q5 Reaction Buffer	10 µl
10 mM dNTPs	1 µl
20 µM Forward Primer	1.5 µl
20 µM Reverse Primer	1.5 µl
Template DNA	1 µl
Q5 Hight-Fidelity DNA Polymerase	0.5 µl
5x Q5 High GC Enhancer	10 µl
Nuclease-Free Water	24.5 µl
TOTAL	50 µl

Table 9: PCR Reaction Mix

PCR Program			
1x	30 s	98 °C	Initial Denaturation
35x	10 s	98 °C	Denaturation
	30 s	58 °C	Annealing
	20-30 s/kb	72 °C	Extension
1x	120 s	72 °C	Final Extension
1x	∞	10 °C	Hold

*Table 10: PCR Program*

After PCR the reactions were loaded onto a 1% (w/v) agarose, 1x TAE, 1x SYBR™ Safe DNA Gel Stain gel and run at 120 V for 40 min. The bands of according size were cut, and the inserts were extracted from the gel using the Promega Wizard® SV Gel and PCR Clean-Up system according to the provided protocol (Promega, 2009b). Inserts were eluted in 55 µl of nuclease free water. Concentrations were determined via microvolume measurement using the DeNovix DS-11+ Spectrophotometer.

### 3.2.3.2. Insert Digestion and Cleanup

After gel-extraction the eluted inserts were cut using their respective restriction enzymes (Table 8). The double-digest reactions were set up as follows:

Double digest of Insert DNA	
Insert	44 µl
Restriction Enzyme 1	2 µl
Restriction Enzyme 2	2 µl
Restriction Buffer	6 µl
TOTAL	54 µl
Incubate for 1 h at 37°C	

*Table 11: Double Digest of Insert DNA*

To ensure compatibility and maximal efficiency for digests with restriction enzymes NdeI/BglII restriction buffer NEBuffer™ 3.1 was chosen, for NdeI/BamHI NEB CutSmart®.

After digestion the inserts were purified using the Promega Wizard® SV Gel and PCR Clean-Up system according to the provided protocol (Promega, 2009b). Inserts were eluted in 55 µl of nuclease free water.

### 3.2.4. Ligation of Inserts and Vectors

The following insert/vector-combinations were set up for ligation:

Constructs	
Insert	Vector
BILBO421-EFh-CCD-ct (aa210-421)	HM15b
BILBO421-EFh-CCD (aa210-404)	MalpET
BILBO421-EFh (aa210-295)	MalpET
BILBO421-CCD-ct (aa296-421)	HM15b
BILBO421-CCD (aa296-404)	HM15b
BILBO421-CCD (aa296-404)	Sumo15b

Table 12: Constructs

The ligation mixes were set up using 2.2 µl insert, 2.0 µl of the respective vector, 0.5 µl T4 ligase buffer and 0.3 µl of T4 ligase. The reactions were incubated for approx. 72 h at 10-14 °C.

### 3.2.5. Transformation

The ligation mixes (5 µl) were each added to 50 µl of competent DH5α *E. coli* cells respectively and subsequently incubated on ice for 20 min. The reactions were heat-shocked for 45 sec at 42 °C followed by 5 min on ice. 200 µl of cooled down LB-medium were added. The cultures were incubated for 1 h at 37 °C, 140 rpm. After incubation the cells were plated onto appropriate selective LB-plates and incubated overnight at 37 °C.

### 3.2.6. DNA Miniprep of Constructs

5 ml of appropriate selective LB-medium were inoculated using single colonies of the overnight cultures. The cultures were incubated overnight at 37 °C, 140 rpm.

After incubation the constructs were purified using the Promega Wizard® *Plus* SV Minipreps DNA Purification System following the supplied protocol (Promega, 2009a). The plasmids were eluted using 55 µl of nuclease free water. Concentrations were determined via microvolume measurement using the DeNovix DS-11+ Spectrophotometer. The correct insertion of the inserts into the vector was checked using the Microsynth Sanger Sequencing service.

### **3.3. Protein Methods**

#### **3.3.1. Transformation of Constructs into BL21(DE3) Competent Cells**

Transformation reactions for large-scale expression were set up by adding 1  $\mu$ l of the respective constructs to 50  $\mu$ l of competent BL21(DE3) *E. coli* cells. The reactions were subsequently incubated on ice for 20 min and heat-shocked for 45 sec at 42 °C followed by another 5 min on ice. 200  $\mu$ l of cooled down LB-medium were added. The cultures were incubated for 1 h at 37 °C, 140 rpm. After incubation the cells were plated onto appropriate selective LB-plates and incubated overnight at 37 °C as a backup. Approx. 4 drops of the incubated culture were used to inoculate an over-night starter-culture with selective LB-media for large-scale expression. The size of the starter-culture varied as for every liter of expression culture 10 ml starter-culture were used for inoculation.

#### **3.3.2. Protein Expression**

Expression cultures consisted of selective LB-medium inoculated with 10 ml of starter-culture per 1 l of LB-medium. The cultures were inoculated at 37 °C, 180 rpm until they reached an OD<sub>600</sub> of 0.600-0.800. As the cultures reached the desired optical density, they were incubated on ice for 20 min to stop further growth, and subsequently further incubated at 18 °C, 180 rpm for 40 min. IPTG was added to a concentration of 0.5 mM to induce the over-night expression of the recombinant protein.

The cells were harvested the following day by centrifugation using a Beckman Coulter Avanti J-26 XP Series (Rotor: J-LITE JLA-8.1000) at 4200 rpm, 4 °C for 2x 12 min. The supernatant was discarded, and the remaining pellets were either flash-frozen in LN<sub>2</sub> for longtime storage at -80 °C or directly resuspended in 10 ml HisTrap Buffer A, per 1 l of harvested culture.



### **3.3.3. Cell Lysis**

If still pending, the cell pellets were resuspended in 10 ml of HisTrap Buffer A per 1 l of original culture. Protease inhibitor phenylmethanesulphonyl fluoride (PMSF) was added to a concentration of 1 mM and 10 µl per 10 ml resuspension of a 2 mg/ml DNase stock solution.

The cells were ruptured using the Avestin EmulsiFlex-C3 homogenizer at 10,000-14,000 psi, 4 °C for 5 cycles/sample.

After cell lysis the samples were centrifuged at 4 °C, 1,500 rpm for 40 min using a Himac CR22N (Rotor: R20A2) centrifuge. The supernatant was filtered through a 0.45 µm membrane and subsequently stored at 4 °C.

### **3.3.4. HisTrap Affinity Chromatography (HisTrap)**

Histidine-tagged samples were loaded onto a Ni Sepharose packed Cytiva Life Sciences™ HisTrap™ HP 5 ml column. Before sample application the column was equilibrated using 25 ml of HisTrap Buffer A. After sample loading the column was washed with 25 ml HisTrap Buffer A. During sample application and column washing the flow-through was collected in 20 ml fractions. The columns were eluted in three consecutive steps. First with 5% of HisTrap Buffer B mixed to HisTrap Buffer A over 25 ml. Second with a linear gradient of HisTrap Buffer B ranging from 5% to 40% over 100 ml. Third with 100% of HisTrap Buffer B for 25 ml. During elution the eluate was fractionated in 1.5 ml fractions and subsequently stored at 4 °C.

### **3.3.5. Nickle-Bead Gravity-Column Purification**

As viscous samples cannot be loaded onto a HisTrap affinity column 3 ml of Nickel-coated Agarose beads were added to the corresponding sample. The sample was agitated overnight on a tumbler at 4 °C. The next day the sample was loaded onto a gravity column and the beads were washed with 9 ml HisTrap Buffer A, collecting the flow-through of both steps separately. The beads were subsequently eluted using 9 ml of HisTrap Buffer B collecting 1.5 ml fractions. The eluate was stored at 4 °C.

### **3.3.6. PEI Nucleic Acid Precipitation**

To eliminate nucleic acids which are non-specifically bound to the target protein PEI precipitation was performed in samples exhibiting a high 254 nm signal during purification.

The sample was transferred to a beaker and kept on ice during the whole process. A stirring rod was added and polyethyleneimine (PEI) was added drop by drop to a final concentration of 0.5%. After all required PEI was added, the sample was left to stir on ice for 20 min. The sample was spun down at 4 °C, 1,500 rpm for 20 min using a Himac CR22N (Rotor R20A2) centrifuge. After palletization the pellet was discarded, and the supernatant was placed back into a beaker on ice. Ammonium sulfate was gradually added under constant stirring to obtain a 70% (at 4 °C) ammonium sulfate saturation. After all ammonium sulfate was added, the sample was set to stir for 60 min. The sample was again centrifuged under the same conditions as before. The supernatant was discarded, and the sample was resuspended in HisTrap Buffer A to the original volume. An overnight dialysis at 4 °C was set up against HisTrap Buffer A using Thermo Scientific™ SnakeSkin™ Dialysis Tubing of adequate molecular weight cut-off. After dialysis the sample was stored at 4 °C.

### **3.3.7. Tag-Removal**

In order to cleave of the tags partially or completely, the SENP2, Thrombin and TEV cutting sites depicted in section 3.2.2.1. were utilized. Depending on the use case 1-2% (v/v) of SENP2, TEV or a small spatula tip of pure Thrombin protease was added to the samples. The samples were subsequently dialyzed against the original buffer at 4 °C, overnight using Thermo Scientific™ SnakeSkin™ Dialysis Tubing of adequate molecular weight cut-off. To validate the successful cleavage of the tag, SDS-PAGE of a previously set-aside uncut sample against the processed sample was performed.

### **3.3.8. Anion-Exchange Chromatography (AEX)**

Samples were loaded onto a Cytiva Life Sciences™ Quaternary ammonium cation packed RESOURCE Q anion exchange chromatography 5 ml column. Before sample application the column was equilibrated using 25 ml of IEX Buffer A. After sample loading the column was washed with 25 ml IEX Buffer A. During sample application and column washing the flow-through was collected in 20 ml fractions. The columns were eluted in two consecutive steps:

TbBILBO421-NTD (aa1-124):

First with a linear gradient of IEX Buffer B (2 M NaCl) ranging from 0% to 100% over 100 ml. Second with 100% of IEX Buffer B (2 M NaCl) for 25 ml.

Sso1(aa1-224):

First with a linear gradient of IEX Buffer B (1 M NaCl) ranging from 0% to 30% over 100 ml. Second with 100% of IEX Buffer B (1 M NaCl) for 25 ml.

During elution the eluate was fractionated in 1.5 ml fractions and subsequently stored at 4 °C.

### **3.3.9. Cation-Exchange Chromatography (CEX)**

The Sec3-PH sample was loaded onto a Cytiva Life Sciences™ Sulfoethyl packed RESOURCE S cation exchange chromatography 5 ml column. Before sample application the column was equilibrated using 25 ml of IEX Buffer A. After sample loading the column was washed with 25 ml IEX Buffer A. During sample application and column washing the flow-through was collected in 20 ml fractions. The column was eluted in two consecutive steps:

First, with a linear gradient of IEX Buffer B (1 M NaCl) ranging from 0% to 30% over 100 ml, second, with 100% of IEX Buffer B (1 M NaCl) for 25 ml.

During elution the eluate was fractionated in 1.5 ml fractions and subsequently stored at 4 °C.

### **3.3.10. Size-Exclusion Chromatography (SEC)**

In preparation of sample loading samples larger than 4 ml were concentrated to a smaller volume to increase sharpness and decrease peak broadening. For this purpose, Merck Amicon™ Ultra-15 Centrifugal filter units with an appropriate molecular weight cut-off were used.

Samples were loaded onto a Cytiva Life Sciences™ HiLoad Superdex 200pg 16/600 preparative SEC column. Before Sample application the column was equilibrated using 1.5 CV (column volume) of SEC Buffer. After sample application the column was eluted using 1.5 CV SEC Buffer. Fractioning of the eluate in 1.5 ml fractions began after 0.2 CV were eluted. The eluate was stored at 4 °C.

### **3.3.11. MBP-Tag Affinity Chromatography (MBP-Trap)**

The MBP-tagged sample was loaded onto a Dextrin Sepharose packed Cytiva Life Sciences™ MBPTrap HP 5 ml column. Before sample application the column was equilibrated using 25 ml of MBPTrap Buffer A. After sample loading the column was washed with 100 ml MBPTrap Buffer A. During sample application and column washing the flow-through was collected in 20 ml fractions. The columns were eluted with 100% of MBPTrap Buffer B for 25 ml. During elution the eluate was fractionated in 1.5 ml fractions and subsequently stored at 4 °C.

### 3.3.12. SDS-PAGE

To check for identity, quantity, purity and state of the proteins, SDS-PAGE was performed after each purification step. The gels were casted according to Table 13 using the Bio-Rad Mini-PROTEAN® Tetra Cell system. Samples were mixed with 6x SDS loading dye and incubated at 96 °C for 10 min before loading. Gels were run for approx. 40 min at 240 V before they were stained in Coomassie brilliant blue staining solution for a minimum of 20 min under constant agitation. After staining the gels were rinsed with water and set to destain in destaining solution until the individual bands were clearly visible.

SDS-PAGE Gel Composition			
Stacking Gel 4% (1 Gel; 2 ml)		Resolving Gel 17.5% (1 Gel; 4 ml)	
ddH <sub>2</sub> O	1.23 ml	ddH <sub>2</sub> O	0.67 ml
4x Tris-HCl/SDS, pH 6.8	0.5 ml	4x Tris-HCl/SDS, pH 8.8	1.0 ml
30% (w/v) Acrylamide	0.27 ml	30% (w/v) Acrylamide	2.33 ml
10% (w/v) APS	16 µl	10% (w/v) APS	25 µl
TEMED	2.55 µl	TEMED	3 µl

Table 13: SDS-PAGE Gel Composition

### 3.3.13. Electrophoretic Shift Assay

To check if the purified TbBILBO421-NTD (aa1-124) and synthetic FPC4-CTD peptides of variable length (Table 14) interact, native electrophoresis was performed. Previous to electrophoresis the synthetic FPC4-CTD peptides, which were stored in powdered state, were resuspended in SEC buffer. Samples were loaded onto the gel in a 1:2 molar ratio (TbBILBO421-NTD (aa1-124) 0.65 nmol, peptides 1.3 nmol per sample).

Gels were casted using the Bio-Rad Mini-PROTEAN® Tetra Cell system.

Gel composition (5% acrylamide; 1 Gel; 6 ml):

4.25 ml ddH<sub>2</sub>O, 120 µl 50x TAE, 0.6 ml 50% (v/v) glycerol,

1 ml 30% (w/v) acrylamide, 30 µl 10% (w/v) APS and 10 µl TEMED.

Gels were run in pre-cooled 1x TAE buffer at 4 °C. Before sample loading the gels were run for 30 min at 120 V. To ensure samples flow to the bottom of the wells, glycerol was added to the sample to a final concentration of 10%. Once the samples were loaded, actual electrophoresis took place for 2.5 h at 120 V.

Peptide	MW [kDa]	pI	Sequence
FPC4- <b>394C</b> (aa394-444)	5.61	5.09	SLSPRLRYLPDVS <del>GG</del> EW <del>DK</del> PDVGDVLCFQAKE <b><u>PQRRRVLTSPVPDELLIK</u></b>
FPC4- <b>N426</b> (aa394-426)	3.51	4.23	SLSPRLRYLPDVS <del>GG</del> EW <del>DK</del> PDVGDVLCFQAKE
FPC4- <b>427C</b> (aa427-444)	2.12	10.74	<b><u>PQRRRVLTSPVPDELLIK</u></b>
FPC4- <b>432C</b> (aa432-444)	1.42	4.37	<b><u>VLTSPVPDELLIK</u></b>

Table 14: Synthetic FPC4 Peptides

### 3.3.14. Isothermal Titration Chromatography (ITC)

ITC measurements were conducted using a MicroCal PEAQ-ITC microcalorimeter (Malvern Panalytical). Purified Sec3-PH protein was dialyzed overnight against SEC Buffer. Sso2 polypeptides (Table 15) were dissolved in the very same buffer and their concentrations were determined using the DS-11+ Spectrophotometer (DeNovix). Concentration of Sec3-PH after dialysis was determined to be 2.14 mg/ml (MW 22,193.21 Da,  $\epsilon$  26930<sup>-1</sup>cm<sup>-1</sup>) using the same method. For each ITC measurement the cell held 250  $\mu$ l of 59  $\mu$ M Sec3-PH, while the injection syringe contained 45  $\mu$ l of the 590  $\mu$ M respective titrants. To match these values, the protein and peptides were diluted using the left-over dialysis buffer, to ensure buffers match throughout all samples and measurements reducing buffer related artefacts during measurements. The experiments consisted of one initial 0.4  $\mu$ l injection followed by 18 consecutive 2  $\mu$ l injections with a duration of 4 sec each at an interval of 120 sec. The resulting data was analyzed using the MicroCal PEAQ-ITC Analysis Software (Malvern Panalytical, Version 1.22) using the one-set-of-site fitting model. Non-linear least square fitting using one binding site model was used to calculate the association constant ( $K_a$ ). Dissociation ( $K_d$ ) were calculated according to the formula  $K_d = 1/K_a$ .

Synthetic Sso2 Polypeptides	
Peptide	Sequence
Sso2-N15	<sup>1</sup> MSNAN <b>NPY</b> ENNN <b>NPY</b> AE <sup>15</sup>
Sso2-N9	<sup>1</sup> MSNAN <b>NPY</b> EN <sup>9</sup>
Sso2-1015	<sup>10</sup> NN <b>NPY</b> AE <sup>15</sup>
Sso2-N15-m1	<sup>1</sup> MSNAAAAANN <b>NPY</b> AE <sup>15</sup>
Sso2-N15-m2	<sup>1</sup> MSNAN <b>NPY</b> ENNNAAAAE <sup>15</sup>
Sso2-N15-m1m2	<sup>1</sup> MSNAAAAANNAAAAE <sup>15</sup>

Table 15: Synthetic Sso2 Polypeptides

### **3.3.15. Rotary Shadowing Electron Microscopy (rsEM)**

The concentration of all samples was determined via microvolume measurement using the DeNovix DS-11+ Spectrophotometer. Concentrations were cross-verified by SDS-PAGE. If samples exhibited a concentration higher than 1 mg/ml they were diluted to reach this value using SEC Buffer. Rotary shadowing electron microscopy itself was carried out by the Vienna Biocenter Core Facilities.

## **3.4. Crystallography Methods**

### **3.4.1. Sec3(aa75-260) Sso2(aa1-270) Complex**

To further analyze the interaction of the two newly discovered NPY motifs of Sso2 with the pleckstrin homology domain of Sec3, a complex of Sec3s PH domain (aa75-260) and a longer version of Sso2(aa1-270), covering all of Sso2s sequence except the C-terminal transmembrane part, has been crystallized for X-ray Crystallography analysis. Both proteins were purified individually, mixed and a stable complex was obtained via size-exclusion chromatography. The crystal was obtained via hanging drop vapor diffusion crystal screening. Diffraction data was obtained at the European Synchrotron Radiation Facility (ESRF) to a maximum resolution of 2.19 Å. The crystal belonged to space group *P1* ( $a = 50.961$  Å,  $b = 58.402$  Å,  $c = 83.286$  Å;  $\alpha = 104.284^\circ$ ,  $\beta = 98.494^\circ$ ,  $\gamma = 113.198^\circ$ ). Further Data collection and refinement statistics are presented in Table 22. The structure was determined via maximum-likelihood molecular replacement utilizing the Phaser crystallographic software (McCoy *et al.*, 2007).

Protein purification, crystallization and crystallographic analysis has been completed prior to this master's thesis and a more detailed overview of all methods can be obtained in the corresponding paper (Peer *et al.*, 2022).

### 3.4.2. Sec3(aa75-260) Sso1(aa1-224) Complex

#### 3.4.2.1. Crystallization Set-up and Screening

Before crystallization set-up the sample was concentrated to 100  $\mu$ l using a Merck Amicon™ Ultra-15 Centrifugal filter units with a molecular weight cut-off of 10 kDa. The protein complex was screened in 96 unique conditions of the Hampton Research Crystal Screen HT (Table 21). For screening MRC 2 lens 96 well crystallization plates were set up to contain 50  $\mu$ l of the respective screening condition in each reservoir, 100 nl sample, 100 nl condition in drop-well 1 and 200 nl sample, 100 nl condition in drop-well 2. Conditions and sample were pipetted using SPT Labtech's Mosquito® crystal. After pipetting crystal plates were covered using sealing film and set for crystallization at 4 °C and RT. Each drop was checked periodically for crystal formation.

#### 3.4.2.2. Crystal Harvesting

The crystal (Table 16) was harvested using a cryo-loop and transferred into a fresh drop (approx. 1 $\mu$ l) of the appropriate Hampton Research Crystal Screen HT crystallization condition (Table 21), to dispose of any precipitant or residues. To protect the crystal and assist vitrification, cryoprotectant buffer was repeatedly added to and removed from the drop by carefully pipetting without interfering with the crystal, to gradually exchange buffers. Cryoprotectant buffer consisted of the respective crystallization buffer mixed with a percentage of cryoprotectant glycerol as recommended by Hampton Research. After buffer exchange the crystal was picked up again using a cryo-loop to be flash-frozen and secured in a LN<sub>2</sub> submerged UniPuck. For transport and storage, crystal-loaded UniPucks were transferred to a LN<sub>2</sub>-filled Dewar flask.


Crystal	Well	Condition	Cryo-protectant	Crystal Image
Sec3-PH / Sso1(aa1-224) Complex	F1 Drop 2	0.095 M Sodium citrate tribasic dihydrate pH 5.6, 2.375 M 1,6- Hexanediol, 4 °C	5% v/v Glycerol	

Table 16: Sec3-PH/Sso1(aa1-224) Complex - Crystal



### 3.4.2.3. Data Acquisition and Processing

X-ray diffraction patterns were acquired at beamline ID23-1 of the European Synchrotron Radiation Facility (ESRF) using a fixed wavelength of 7.999 KeV (0.6888 Å) and a Dectris Pilatus 6M detector. Data was acquired using 3600 images over 360°, at an exposure time of 0.01 s and a transmission of 4.2%. The crystal diffracted X-rays to a maximal resolution of 1.4 Å and belonged to the space group *P*1 ( $a = 45.509$  Å,  $b = 45.972$  Å,  $c = 46.092$  Å;  $\alpha = 93.23^\circ$ ,  $\beta = 91.53^\circ$ ,  $\gamma = 113.645^\circ$ ). Data collection and refinement statistics are presented in Table 23. The Matthews coefficient of  $2.00 \text{ Å}^3 \text{ Da}^{-1}$  and the solvent content of 38.38% (Data resolution: 1.4 Å, Sec3-PH: MW 22060 Da) suggested that there are probably two molecules present in the unit, as determined using MATTPROB (Kantardjieff *et al.*, 2003; Matthews, 1968; Weichenberger *et al.*, 2014).

### 3.4.2.4. Model Build and Refinement

The structure was determined via maximum-likelihood molecular replacement utilizing the Phaser crystallographic software (McCoy *et al.*, 2007) and a previously solved structure.

The resulting model was carefully checked and extra electron densities that were clearly visible were manually built using the Coot software toolkit (Emsley *et al.*, 2010). Refinement was carried out using the Phenix.refine crystallographic structure refinement program (Adams *et al.*, 2010).

Figure generation and all further analysis were carried out using PyMOL (Schrödinger, LLC). Data collection and refinement statistics are shown in Table 23.

### 3.5. In Vivo Methods

Our collaborators at the Department of Cellular and Molecular Medicine at the University of California, San Diego have conducted extensive in vivo assays based on various alanine substitution mutations of the Sso2 NPY-motifs (Table 17) in a yeast integrating vector introduced in a SSO2 paralog SSO1 deleted yeast strain.

A more detailed overview of all methods concerning the in vivo data can be obtained in the corresponding paper (Peer *et al.*, 2022).

Sso2 Mutations	
Mutation	Sequence
Sso2	<sup>1</sup> MSNANPYENNNPYAE <sup>15</sup>
Sso2M1	<sup>1</sup> MSNANPY <b>A</b> NNNPYAE <sup>15</sup>
Sso2M2	<sup>1</sup> MSNANP <b>A</b> ENNNPYAE <sup>15</sup>
Sso2M3	<sup>1</sup> MSNA <b>AA</b> YENNNPYAE <sup>15</sup>
Sso2M4	<sup>1</sup> MSNA <b>AAA</b> ENNNPYAE <sup>15</sup>
Sso2M5	<sup>1</sup> MSNA <b>AAAA</b> NNNPYAE <sup>15</sup>
Sso2M6	<sup>1</sup> MSNANPYENN <b>AAAA</b> E <sup>15</sup>
Sso2M7	<sup>1</sup> MSNA <b>AAAA</b> NN <b>AAAA</b> E <sup>15</sup>

Table 17: Sso2 Mutations Introduced in SSO1Δ Yeast Strain

#### 3.5.1. Growth Test

To investigate the effect of Sso2 NPY-motif mutations (Table 17) on cell growth, SSO1Δ Sso2<sup>mut</sup> cells were spotted on YPD plates, grown at 25 °C and 37 °C for 2 days and compared to a SSO1Δ Sso2 control.

### 3.5.2. Bgl2 and Invertase Secretion Assay

Bgl2, a constitutively synthesized and secreted protein involved in cell wall maintenance, is kept at the cell surface by the cell walls glucan. Its external pool can be released by treating the cell wall with exogenous glucanase. The internal pool will remain in the remaining spheroplasts. (Yuan *et al.*, 2017).

The treatment of cells with exogenous glucanase therefore allows to investigate the effect of Sso2 NPY-motif mutations (Table 17) on Bgl2 secretion, by quantifying the internal and external pools of Bgl2 via western blot analysis. The secretory efficiency of the various SSO1Δ Sso2<sup>mut</sup> cells was tested at 37 °C and compared to a SSO1Δ Sso2 control.

Like Bgl2 invertase is trapped on the cell surface by cell wall glucan and can be released by treating the cell wall with exogenous glucanase. (Yuan *et al.*, 2017). As the synthesis of invertase is under hexose repression, cells were grown in 5% (w/v) glucose at 25 °C, repressing synthesis, before being shifted to 0.1% (w/v) glucose at 37 °C, inducing expression, for western blot analysis of the internal and external pools of invertase. Again, the secretory efficiency of the various SSO1Δ Sso2<sup>mut</sup> cells was compared to a SSO1Δ Sso2 control.

### 3.5.3. Screening for Accumulation of Secretory Vesicles

In yeast the exocyst captures and localizes secretory vesicles to the sites of active cell surface expansion, such as the bud tip of the daughter cell or the mother daughter cell junction. Mutant cells deficient of certain exocyst members accumulate secretory vesicles at the site of cell surface expansion. (Lipschutz & Mostov, 2002).

Likewise spores devoid of combined Sso1 and Sso2 activity, fail to germinate and accumulate secretory vesicles within the bud. (Aalto *et al.*, 1993).

To investigate the effect of Sso2 NPY-motif mutations (Table 17) on the accumulation of secretory vesicles, thin section electron microscopy was used.

#### **3.5.4. Screening for Snc1 Recycling**

The Snc1 v-SNARE protein has previously been shown to undergo rapid cycling from secretory vesicles to the plasma membrane, back from the cell surface to endocytic vesicles with subsequent recycling via the Golgi apparatus to a new set of secretory vesicles (Lewis *et al.*, 2000).

To monitor the effect of Sso2 NPY-motif mutations (Table 17) on Snc1 recycling SSO1Δ Sso2<sup>mut</sup> cells expressing GFP-Snc1 were analyzed using fluorescence microscopy and quantitative localization analysis.

#### **3.5.5. Screening for Effects on Actin-independent Localization of Sec3**

Previous studies have shown that the transport of secretory vesicles to sites of cell surface growth is facilitated by the movement of Myo2, a class V myosin, along polarized actin cables (Pruyne *et al.*, 2004). Loss of function of either Myo2 or actin results in rapid depolarization of the vesicle markers such as GTP binding protein Sec4 (Salminen & Novick, 1989). Polarization of Sec3 has been shown to be unaffected by disruption of actin polymerization via the addition of Latrunculin A (LatA), leaving Sec3 associated with sites of cell surface growth (Finger *et al.*, 1998).

As the localization of Sec3 seems to be actin independent, the interaction between Sec3 and the NPY-motifs of Sso2 might play a crucial role in Sec3 recruitment to the sites of cell surface growth.

To see if the interaction of Sec3 with the NPY-motifs of Sso2 is required for localization we investigated the effect of Sso2 NPY-motif mutations M5 and M7 (Table 17) on Sec3 localization. GFP-Sec4 and Sec3-3xGFP expressing SSO1Δ Sso2, SSO1Δ Sso2M5 and SSO1Δ Sso2M7 cells were evaluated via fluorescence microscopy and quantitative localization analysis after treatment with either LatA or DMSO.

## 4. Results

### 4.1. Cloning

To prepare the inserts for the newly prepared constructs (Table 12) PCR was carried out as described in section 3.2.3.1. The PCR products were loaded onto a 1% agarose gel to verify the successful amplification.

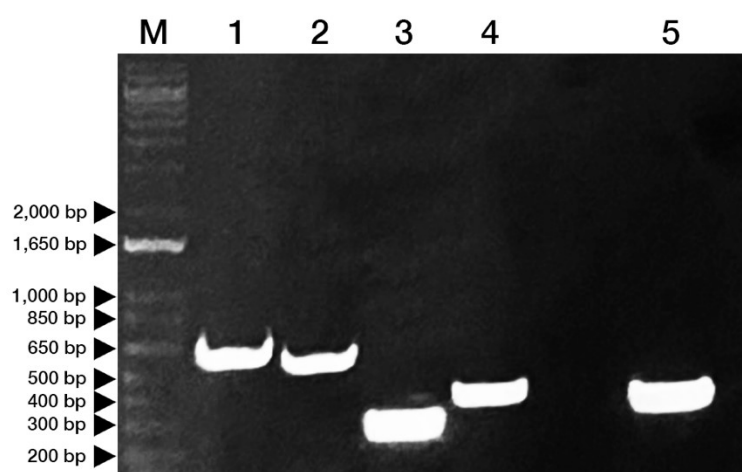


**Figure 5: PCR Insert Amplification Gel**

1% Agarose gel showing PCR products of insert amplification. M: 10 kb DNA Ladder; 1: TbBILBO421-EFh-CCD-ct (aa210-421, 636 bp); 2: TbBILBO421-EFh-CCD (aa210-404, 585 bp); 3: TbBILBO421-EFh (aa210-295, 258 bp); 4: TbBILBO421-CCD-ct (aa296-421, 378 bp); 5: TbBILBO421-CCD (aa296-404, 342 bp).

Following insert concentrations were observed after gel extraction:

TbBILBO421 EFh-CCD-ct (aa210-421)	48,1 ng/μl
TbBILBO421 EFh-CCD (aa210-404)	64.7 ng/μl
TbBILBO421 EFh (aa210-295)	47.1 ng/μl
TbBILBO421 CCD-ct (aa296-421)	52.2 ng/μl
TbBILBO421 CCD (aa296-404)	64.5 ng/μl

**Table 18: Insert Concentrations**

After gel extraction the inserts were digested as described in section 3.2.3.2.

Ligation mixes were set up with the corresponding vectors (Table 12) as described in section 3.2.4. After ligation the constructs were transformed into competent DH5 $\alpha$  *E. coli* cells (3.2.5.). All selective LB-plates contained colonies. Single colonies were used for inoculation of 5 ml of selective LB media. Colonies were grown overnight and miniprep was performed as described in section 3.2.6. Construct concentrations as determined via microvolume measurement:

TbBILBO421 EFh-CCD-ct (aa210-421)/HM15b	87.1 ng/ $\mu$ l
TbBILBO421 EFh-CCD (aa210-404)/MalpET	218.9 ng/ $\mu$ l
TbBILBO421 EFh (aa210-295)/MalpET	125.5 ng/ $\mu$ l
TbBILBO421 CCD-ct (aa296-421)/HM15b	82.2 ng/ $\mu$ l
TbBILBO421 CCD (aa296-404)/HM15b	86.1 ng/ $\mu$ l
TbBILBO421 CCD (aa296-404)/Sumo15b	134.5 ng/ $\mu$ l

*Table 19: Construct Concentrations*

The purified constructs were sent for sequencing to verify identity, integrity and correct insertion of the inserts into the vector. Sequencing results can be obtained in section 9.2. (Table 20).

## 4.2. Protein expression

For protein expression the constructs were transformed into competent BL21(D3) *E. coli* cells according to section 3.3.1. After transformation starter cultures were used to inoculate the large-scale expression cultures (Section 3.3.2). For TbBILBO421-EFh-CCD (aa210-404)/MalpET, TbBILBO421-EFh (aa210-295)/MalpET and TbBILBO421-CCD (aa296-404)/Sumo15b 2 l of LB-medium were used for expression. For TbBILBL421-NTD (aa1-124)/Sumo15b, TbBILBO421-EFh-CCD-ct (aa210-421)/HM15b, TbBILBO421-CCD-ct (aa296-421)/HM15b, TbBILBO421-CCD (aa296-404)/HM15b and Sso1(aa1-224)/HT15b 4 l were used. For Sec3-PH(aa75-260)/pET15b 6 l.

After expression the cells were harvested, lysed and the samples were prepared for purification according to section 3.3.3.

### 4.3. TbBILBO421-NTD – Purification and Results

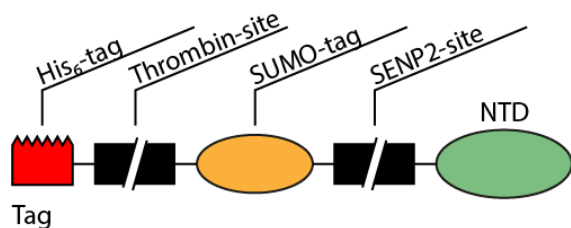


**Figure 6: Construct TbBILBO421-NTD – Illustration**

*Illustration of TbBILBO421-NTD construct features relevant for purification.*

*Depicted is the N-terminal conjugated Sumo15b tag and the proteins NTD (aa1-124).*

#### 4.3.1. TbBILBO421-NTD – HisTrap (1)

In a first step the histidine-tagged protein was purified via HisTrap affinity chromatography (Figure 7) as described in section 3.3.4. The flow-through and fractions spanning the resulting peaks were analyzed via SDS-PAGE (Figure 8). The protein eluted between approx. 80-153 ml in two peaks and can be clearly identified via SDS-PAGE. Fractions between 80-153 ml were pooled.

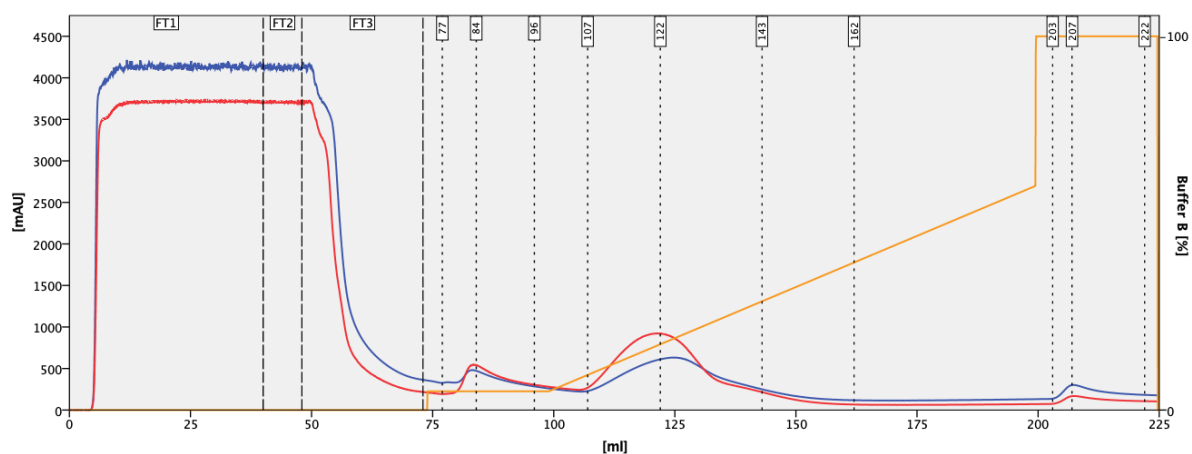


**Figure 7: Elution Profile TbBILBO421-NTD HisTrap (1)**

*Elution profile of HisTrap affinity chromatography (1) of TbBILBO421-NTD (aa1-124) uncut (28 kDa).*

*Elution between 77-162 ml, 5-35% Buffer B. Red line: A<sub>280</sub>; Blue line: A<sub>254</sub>; Orange line: Buffer B;*

*FT1/2: Sample loading; FT3: Column wash.*

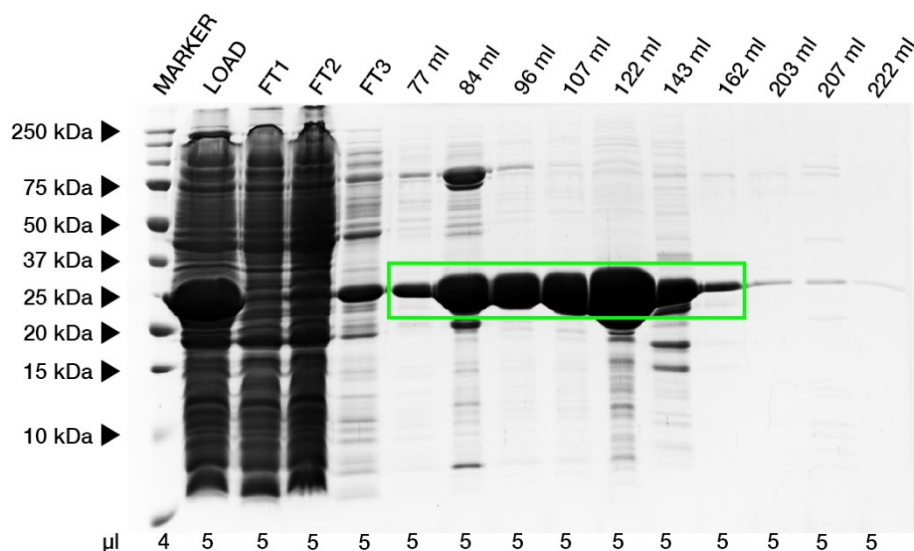


**Figure 8: SDS-PAGE TbBILBO421-NTD HisTrap (1)**

17.5% SDS-PAGE of TbBILBO421-NTD HisTrap (1) affinity purification fractions. Protein size: 28 kDa; Elution between 77-162 ml (green box). Fractions between 81-144.5 ml were pooled.

#### 4.3.2. TbBILBO421-NTD – Tag-Removal

As TbBILBO421-NTD was expressed using the Sumo15b vector it is conjugated to a combined His<sub>6</sub>-Sumo-tag as described in section 3.2.2.1. To cut off both tags utilizing the SENP2 cutting site of the Sumo15b vector, the sample was processed as described in section 3.3.7. The tag was successfully cleaved (Figure 9).

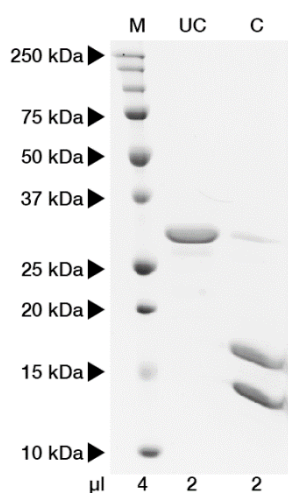


**Figure 9: TbBILBO421-NTD Uncut/Cut**

17.5% SDS-PAGE of TbBILBO421-NTD HisTrap (1) affinity purification fractions 80-153 ml before (UC) and after (C) SENP2 treatment. UC: uncut protein (28 kDa); C: cut protein and tag (Protein: 14.6 kDa; Tag: 13.4 kDa).



#### 4.3.3. TbBILBO421-NTD – HisTrap (2)

To eliminate impurities caused by proteins that are inherently able to bind to the HisTrap column, a second HisTrap affinity chromatography (Figure 10) was performed. In this case the His<sub>6</sub>-tag deprived TbBILBO421-NTD is not expected to bind to the column, unlike the impurities.

The SDS-PAGE analysis of the second HisTrap affinity purification (Figure 11) fractions showed strong bands of approx. 15 kDa in FT1-3 resembling TbBILBO421-NTD (14.6 kDa). Fractions FT1-3 were combined. The fractions show stark contamination with a protein of approx. 17 kDa.

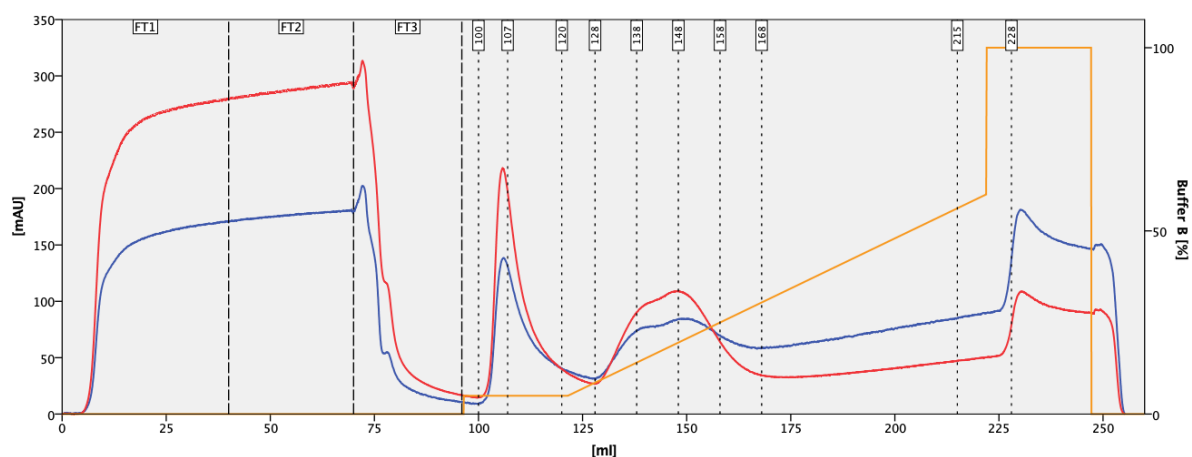


**Figure 10: Elution Profile TbBILBO421-NTD HisTrap (2)**

Elution profile of HisTrap affinity chromatography (2) of TbBILBO421-NTD (aa1-124) cut (14.6 kDa). Peak 1: 100-128 ml, 5-9% Buffer B; Peak 2: 128-168 ml, 9-30% Buffer B; Red line: A<sub>280</sub>; Blue line: A<sub>254</sub>; Orange line: Buffer B; FT1/2: Sample loading; FT3: Column wash.

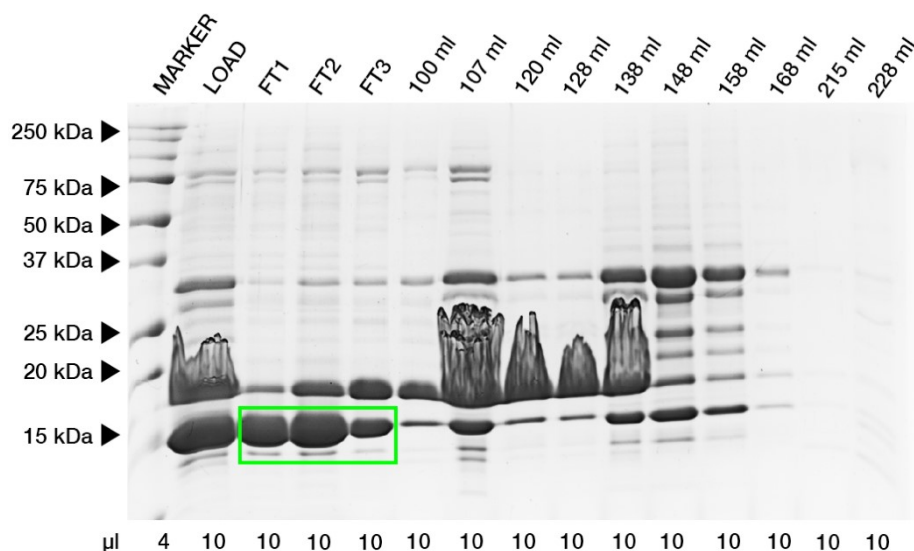


**Figure 11: SDS-PAGE TbBILBO421-NTD HisTrap (2)**  
 17.5% SDS-PAGE of TbBILBO421-NTD (cut) HisTrap (2) affinity purification fractions.  
 Protein size: 14.6 kDa; Tag size: 13.4 kDa; Elution of protein in FT1-3 (green box). Fractions FT1-3 were pooled.

#### 4.3.4. TbBILBO421-NTD – AEX

To further eliminate contamination anion-exchange chromatography was performed as described in section 3.3.8. (Figure 12). TbBILBO421-NTD eluted in fractions 163-213 ml and FT1-7. Not all protein was binding to the column, yet most of the impurities did. Resulting in FT1-7 fractions being of high purity (Figure 13). Fractions FT1-7 were pooled and concentrated down to 4 ml using a Merck Amicon™ Ultra-15 Centrifugal filter unit with a molecular weight cut-off of 10 kDa.

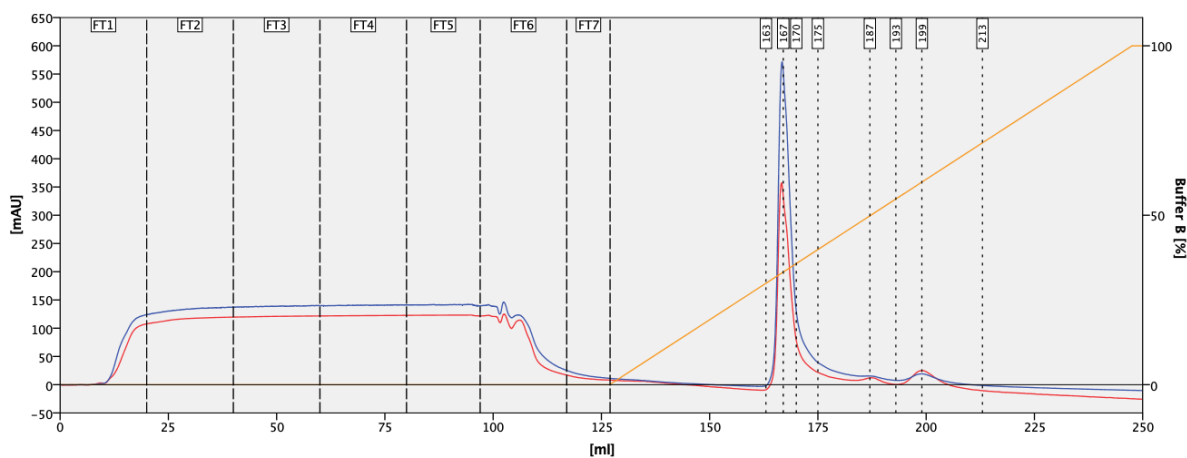


**Figure 12: Elution Profile TbBILBO421-NTD AEX**  
 Elution profile of anion-exchange chromatography of TbBILBO421-NTD (aa1-124) cut (14.6 kDa, pI 5.3). Peak: 167 ml, 660 mM NaCl (33% Buffer B); Red line:  $A_{280}$ ; Blue line:  $A_{254}$ ; Orange line: Buffer B; FT1-5: Sample loading; FT6-7: Column wash.

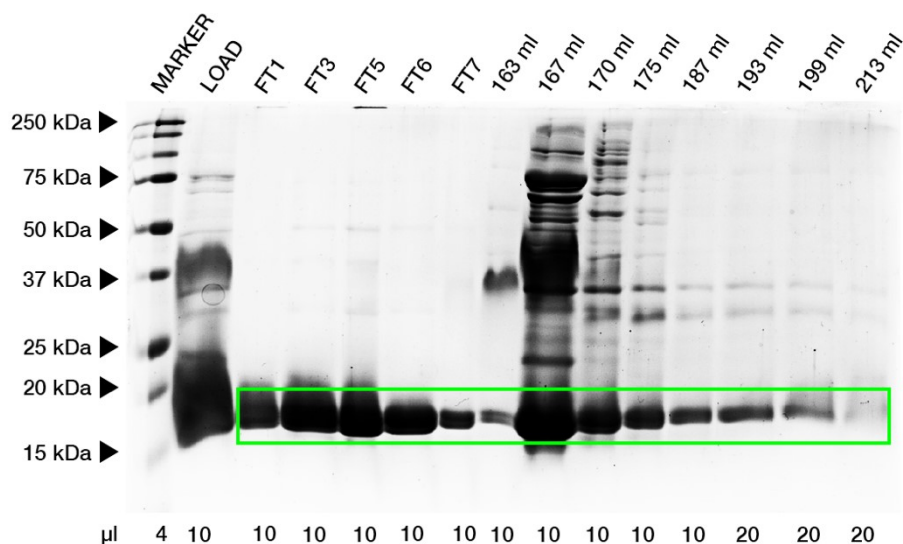


**Figure 13: SDS-PAGE TbBILBO421-NTD AEX**

17.5% SDS-PAGE of TbBILBO421-NTD anion-exchange chromatography fractions. Protein size: 16.4 kDa; Elution between FT1-7 and 163-213 ml (green box). Fractions FT1-7 were pooled due to their high purity.

#### 4.3.5. TbBILBO421-NTD – SEC

As a final purification step size-exclusion chromatography using a Cytiva Life Sciences™ HiLoad Superdex 200pg 16/600 preparative SEC column was performed (Figure 14) as described in chapter 3.3.10.

Elution resulted in two peaks, with the first peak (48.5 ml) being close to the void volume of the column (~ 36 ml). The protein of interest eluted in both peaks as verified by SDS-PAGE (Figure 15). When compared to a HiLoad Superdex 200pg 16/600 SEC column protein standard supplied by the manufacturer (Cytiva, 2020), the elution volume of the first peak corresponds to a protein size of >440 kDa, indicating oligomerization of the protein. Therefore, only fractions 90-102 ml of the second peak (94.5 ml) were combined and concentrated down to 1.5 ml using a Merck Amicon™ Ultra-15 Centrifugal filter unit with a molecular weight cut-off of 10 kDa. The final concentration was 18.84 mg/ml (MW 14,587.46 Da,  $\epsilon$  11585 M<sup>-1</sup>cm<sup>-1</sup>) as determined by microvolume measurement.

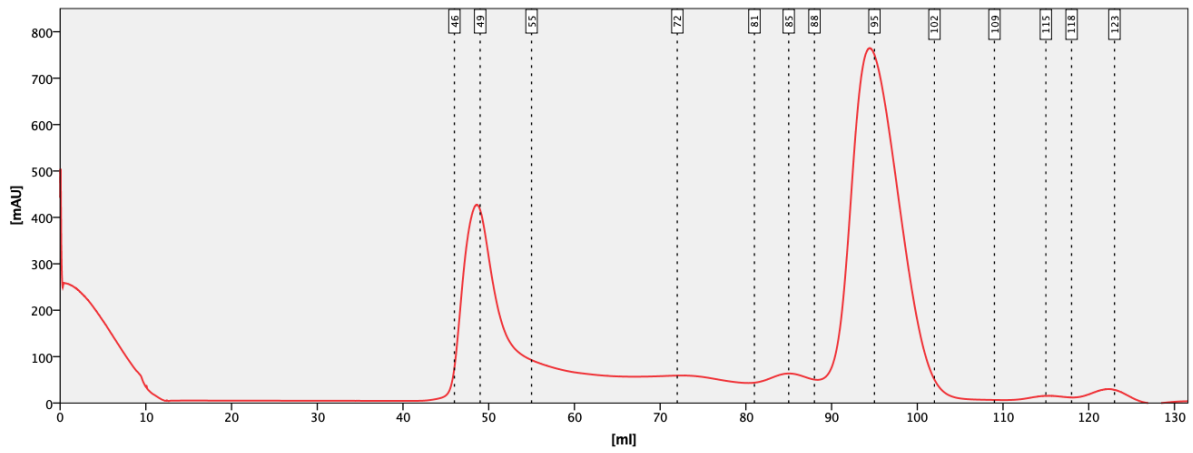


**Figure 14: Elution Profile TbBILBO421-NTD SEC**

Elution profile of size-exclusion chromatography of TbBILBO421-NTD (aa1-124) cut (14.6 kDa).

Peak 1: 48.6 ml, Peak 2: 94.5 ml; Red line:  $A_{280}$ .

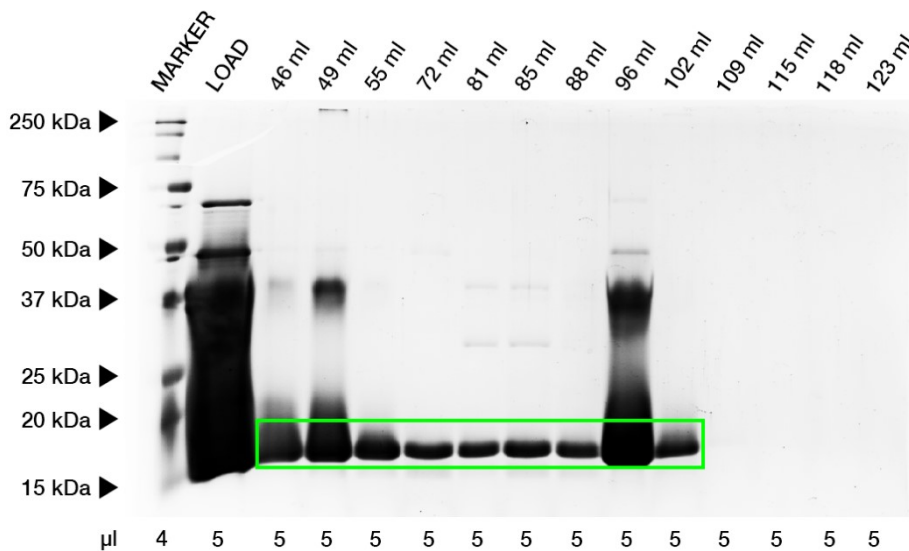


**Figure 15: SDS-PAGE TbBILBO421-NTD SEC**

17.5% SDS-PAGE of TbBILBO421-NTD size-exclusion chromatography fractions. Protein size: 14.6 kDa; Elution between 46-102 ml (green box), Peak 1: 48.6 ml, Peak 2: 94.5 ml. Fractions 90-102 ml were pooled.

#### 4.3.6. TbBILBO421-NTD FPC4-CTD – Electrophoretic Shift Assay

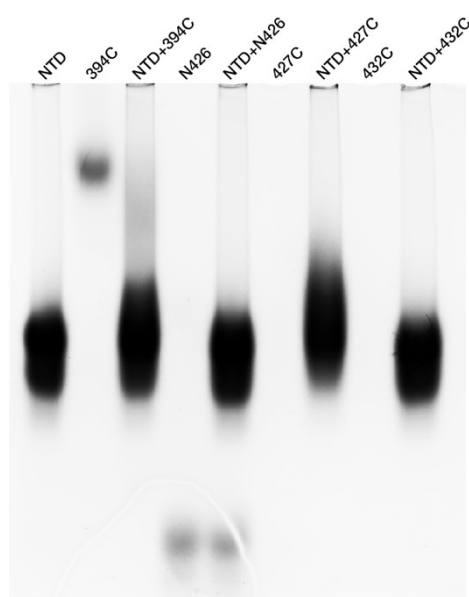
To check if the purified TbBILBO421-NTD (aa1-124) and synthetic FPC4-CTD peptides of variable length (Table 14) interact, native electrophoresis was performed, as described in section 3.3.13.

As depicted in Figure 16 interaction between the TbBILBO421-NTD and the full length FPC4-CTD (FPC4-394C, aa1-124) resulted in an upwards shift of the TbBILBO421-NTD band and in the disappearance of the distinct FPC4-394C band.

An interaction between the TbBILBO421-NTD and FPC4-N426 cannot be observed as there is no visible shift of the TbBILBO421-NTD and FPC4-N426 bands in the combined sample.

FPC4-427C did not enter the gel due to its high pI of 10.74, yet the combined sample of FPC4-427C and TbBILBO421-NTD shows a distinct upwards shift of the NTD related band, therefore implying a possible interaction.

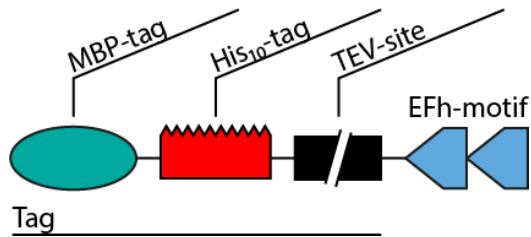
For sample FPC4-432C no band can be observed, which is probably due to the relatively small size of the peptide (1.42 kDa), causing it to run out of the gel. As there is no clear shift of the NTD related band in the combined sample, an interaction is unlikely, yet not to be ruled out, as the shift might be minor due to the small size of the peptide and a comparison to a peptide-only band is not possible.



**Figure 16: TbBILBO421-NTD FPC4-CTD Electrophoretic Shift Assay**

5% Acrylamide gel; **NTD**: TbBILBO421-NTD (aa1-124), 0.65 nmol; **394C**: FPC4-394C (aa394-444), 1.3 nmol; **NTD+394C**: TbBILBO421-NTD (aa1-124), 0.65 nmol + FPC4-394C (aa394-444), 1.3 nmol; **N426**: FPC4-N426 (aa394-426), 1.3 nmol; **NTD+N426**: TbBILBO421-NTD (aa1-124), 0.65 nmol + FPC4-N426 (aa394-426), 1.3 nmol; **427C**: FPC4-472C (aa427-444), 1.3 nmol; **NTD+427C**: TbBILBO421-NTD (aa1-124), 0.65 nmol + FPC4-472C (aa427-444), 1.3 nmol; **432C**: FPC4-432C (aa432-444), 1.3 nmol; **NTD+432C**: TbBILBO421-NTD (aa1-124), 0.65 nmol + FPC4-432C (aa432-444), 1.3 nmol.

## 4.4. TbBILBO421-EFh – Purification and Results



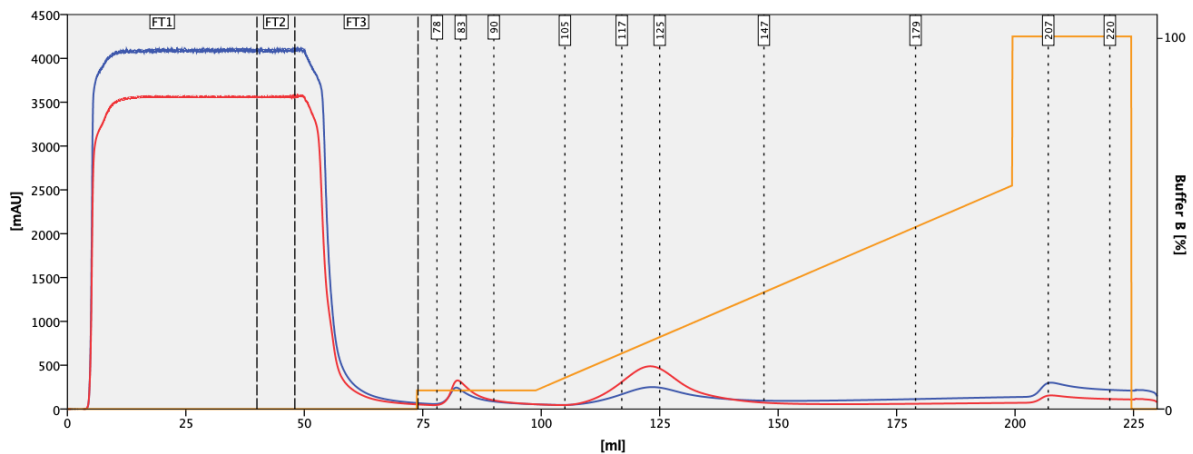
**Figure 17: Construct TbBILBO421-EFh – Illustration**

Illustration of TbBILBO421-EFh construct features relevant for purification.

Depicted is the N-terminal conjugated MalpET tag and the proteins EFh-motif (aa210-295).

### 4.4.1. TbBILBO421-EFh – HisTrap

In a first step the histidine- and MBP-tagged protein was purified via HisTrap affinity chromatography (Figure 18) as described in section 3.3.4. The flow-through and fractions spanning the resulting peaks were analyzed via SDS-PAGE (Figure 19). The protein of interest eluted in fractions FT1-3 and 109.5-129 ml. Unlike fraction FT1-3, fraction 109.5-129 ml shows contamination in form of a second band of similar size. Fractions FT1-3 and 109.5-129 ml were pooled respectively.



**Figure 18: Elution Profile TbBILBO421-EFh HisTrap**

Elution profile of HisTrap affinity chromatography of TbBILBO421-EFh (aa210-295, 56.9 kDa). Peak:

105-147 ml, 8-30% Buffer B; Red line: A<sub>280</sub>; Blue line: A<sub>254</sub>; Orange line: Buffer B; FT1/2:

Sample loading, FT3: Column Wash.

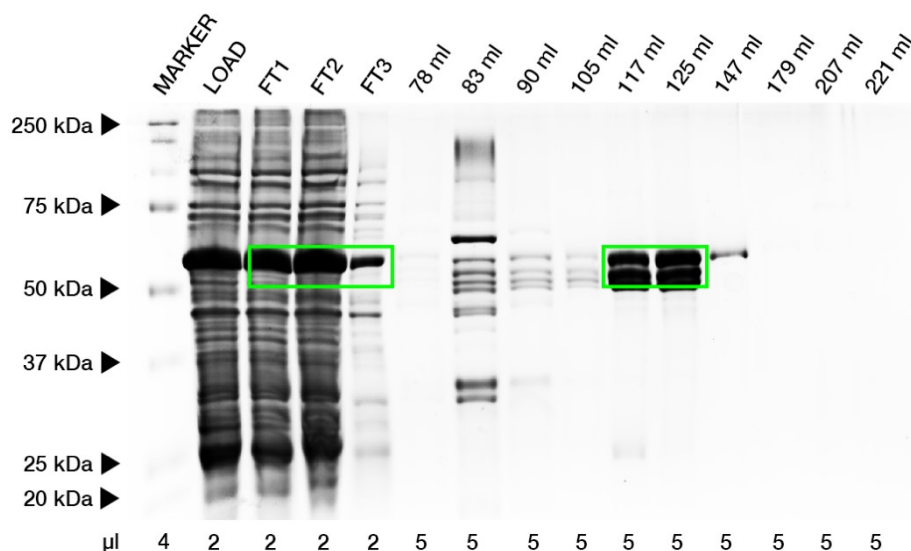


**Figure 19: SDS-PAGE TbBILBO421-EFh HisTrap**

17.5% SDS-PAGE of TbBILBO421-EFh HisTrap affinity purification fractions. Protein size: 56.9 kDa; Elution between FT1-3 and 109.5-129 ml (green box). Fractions FT1-3 and 109.5-129 ml were pooled respectively.

#### 4.4.2. TbBILBO421-EFh – MBP-Trap

To further purify fractions FT1-3 MBP-tag affinity chromatography (Figure 20) was performed, as described in section 3.3.11. The flow-through and fractions spanning the resulting peak were analyzed via SDS-PAGE (Figure 21). The protein of interest eluted between 137-146 ml. Fractions 137-143 ml and 143-146 ml were pooled respectively.

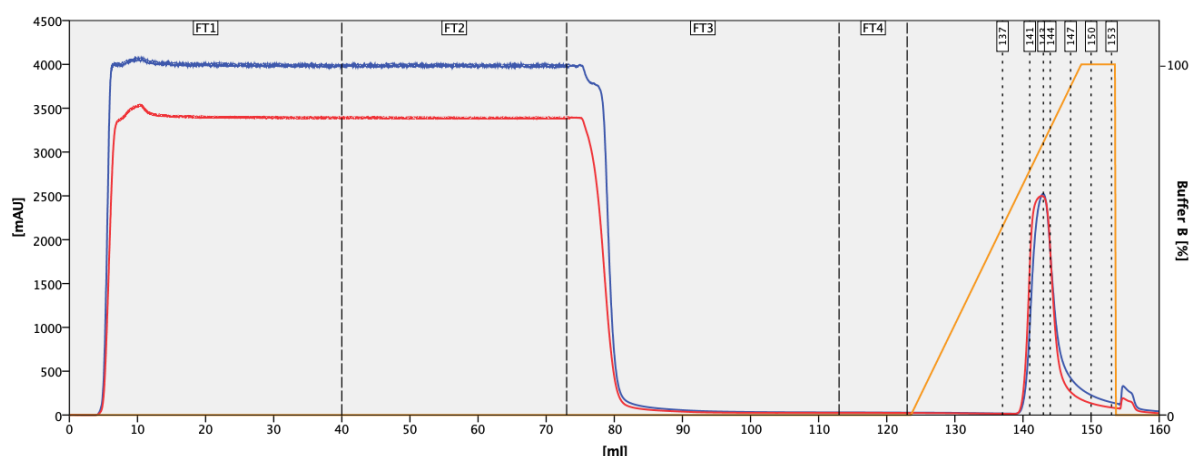


**Figure 20: Elution Profile TbBILBO421-EFh MBP-Trap**

Elution profile of MBP-tag affinity chromatography of TbBILBO421-EFh (aa210-295, 56.9 kDa). Peak: 143 ml (78% Buffer B); Red line:  $A_{280}$ ; Blue line:  $A_{254}$ ; Orange line: Buffer B; FT1/2: Sample loading, FT3: Column Wash.

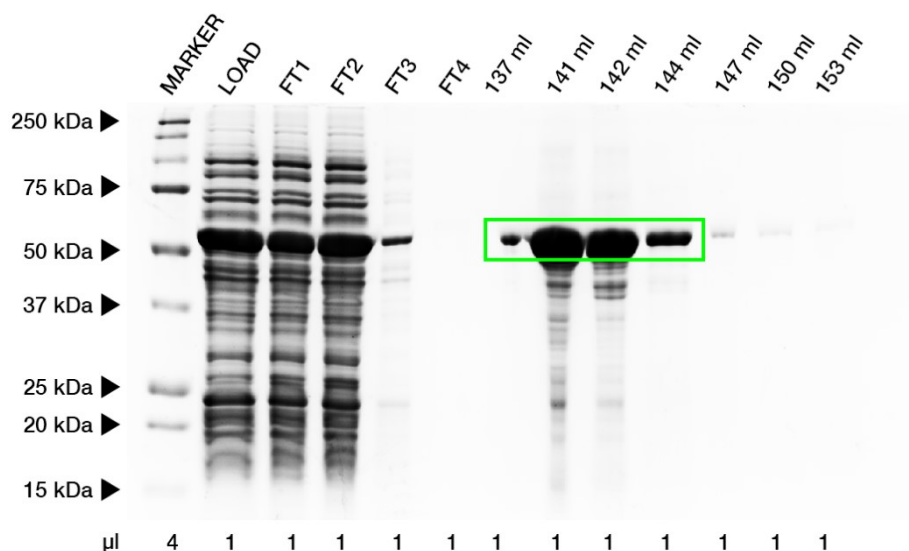


**Figure 21: SDS-PAGE TbBILBO421-EFh MBP-Trap**

17.5% SDS-PAGE of TbBILBO421-EFh MBP-Trap affinity purification fractions. Protein size: 56.9 kDa; Elution between 137-146 ml (green box). Fractions 137-143 ml and 143-146 ml were pooled respectively.

#### 4.4.3. TbBILBO421-EFh – Tag-Removal

In preparation of size-exclusion chromatography the combined MBP-His<sub>10</sub>-tag of the protein was to be removed. As TbBILBO421-EFh was expressed using the MalpET vector it is conjugated to a combined MBP-His<sub>10</sub>-tag as described in section 3.2.2.1. To cut off both tags utilizing the TEV cutting-site of the MalpET vector, HisTrap affinity purification fractions 109.5-129 ml and MBP-tag affinity purification fractions 137-143 ml were processed as described in section 3.3.7. Samples were treated with varying TEV concentrations and temperatures for 24 h in case of the MBP-Trap samples and 48 h for the HisTrap samples, as depicted in Figure 22. None of the TEV treatments were successful. Purification was continued using uncut MBP-tag affinity purification fractions 143-146 ml.



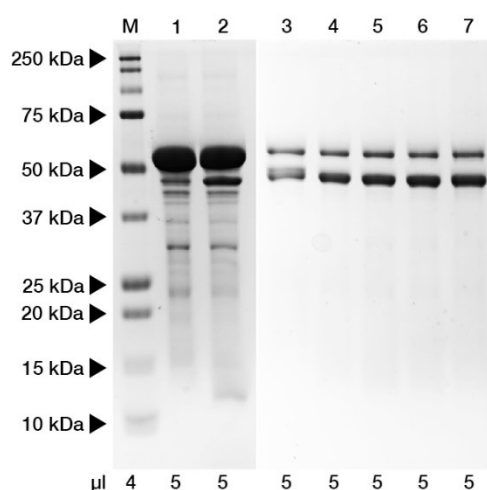


**Figure 22: *TbBILBO421-EFh* Uncut/Cut**  
 17.5% SDS-PAGE of *TbBILBO421-NTD* HisTrap affinity purification fractions 109.5-129 ml and MBP-tag affinity purification fractions 137-143 ml before and after TEV treatment. Uncut protein: 56.93 kDa; Cut protein: Protein: 9.99 kDa; Tag: 46.94 kDa. **M:** Marker; **1:** MBP-Trap 16.7% (v/v) TEV, 4°C, 24 h; **2:** MBP-Trap 16.7% (v/v) TEV, RT, 24 h; **3:** HisTrap 0% (v/v) TEV, 4°C, 48 h; **4:** HisTrap 2.5% (v/v) TEV, 4°C, 48 h; **5:** HisTrap 7.5% (v/v) TEV, 4°C, 48 h; **6:** HisTrap 7.5% (v/v) TEV, RT, 48 h; **7:** HisTrap 7.5% (v/v) TEV, 37°C, 48 h.

#### 4.4.4. *TbBILBO421-EFh* – SEC

To investigate the influence of  $\text{CaCl}_2$  on the EFh-motif of the protein, uncut MBP-tag affinity purification fraction 143-146 ml (3 ml) was split into two distinct samples. To one sample  $\text{CaCl}_2$  was added to a final concentration of 10 mM, to the second sample EDTA, likewise to a final concentration of 10 mM. With each sample size-exclusion chromatography using a Cytiva Life Sciences™ HiLoad Superdex 200pg 16/600 preparative SEC column was performed (Sample  $\text{CaCl}_2$ : Figure 23; Sample EDTA: Figure 25) as described in chapter 3.3.10. The buffers for each SEC contained additional  $\text{CaCl}_2$  or EDTA with a concentration of 5 mM accordingly.

Elution of sample  $\text{CaCl}_2$  (Figure 23) resulted in one major peak (45.54 ml) and two smaller peaks (89.14 ml, 111.77 ml). Presence of the protein of interest could only be verified in the first peak via SDS-PAGE (Figure 24). When compared to a HiLoad Superdex 200pg 16/600 SEC column protein standard supplied by the manufacturer (Cytiva, 2020), the elution volume of the first peak corresponds to a protein size of >440 kDa, indicating oligomerization of the protein.

Elution of sample EDTA (Figure 25) resulted in one major peak (45.54 ml) and three smaller peaks (89.1 ml, 113 ml, 121 ml). Again, the presence of the protein of interest could only be verified in the first peak via SDS-PAGE (Figure 26). When also compared to a HiLoad Superdex 200pg 16/600 SEC column protein standard, the elution volume of the first peak is as well corresponds to a protein size of >440 kDa, indicating oligomerization of the protein.

When overlaying both elution profiles (Figure 27) only a small variance can be observed in peak 1 (45.5 ml). Peak 3 (113 ml) and peak 4 (121 ml) are significantly

more prominent in sample EDTA. Compared to the SEC column protein standard peak 3 and peak 4 correspond to proteins significantly smaller than 17 kDa, excluding the protein of interest (56.9 kDa).

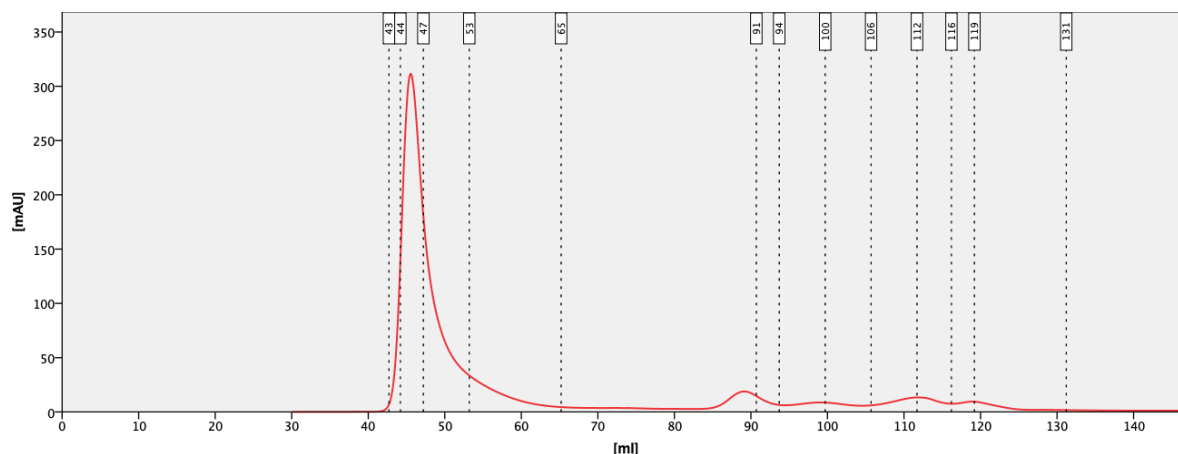


**Figure 23: Elution Profile TbBILBO421-EFh SEC (CaCl<sub>2</sub>)**

Elution profile of size-exclusion chromatography (CaCl<sub>2</sub>) of TbBILBO421-EFh (aa210-295, 56.9 kDa). Peak 1: 45.54 ml, Peak 2: 89.14 ml, Peak 3: 111.77 ml; Red line: A<sub>280</sub>.

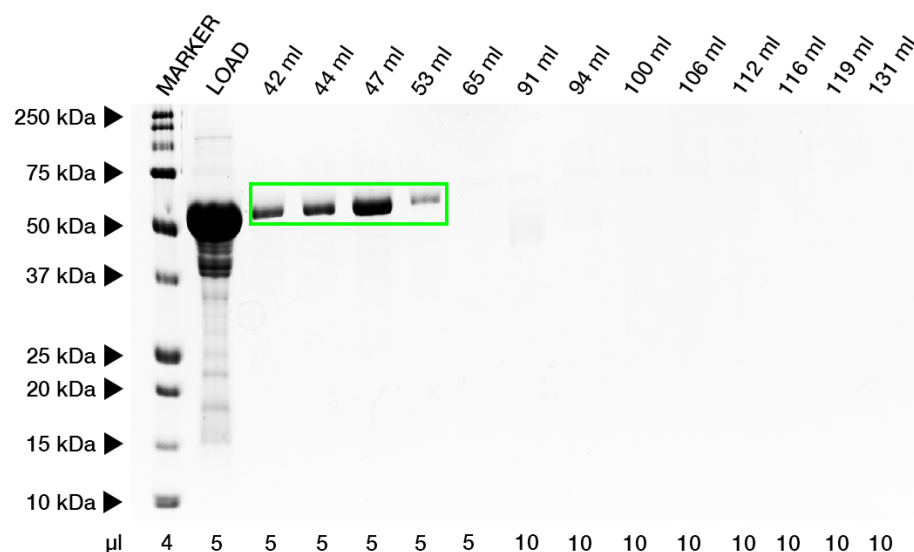


**Figure 24: SDS-PAGE TbBILBO421-EFh SEC (CaCl<sub>2</sub>)**

17.5% SDS-PAGE of TbBILBO421-EFh size-exclusion chromatography (CaCl<sub>2</sub>) fractions. Protein size: 56.9 kDa; Peak of elution: Peak 1 (45.54 ml; green box).

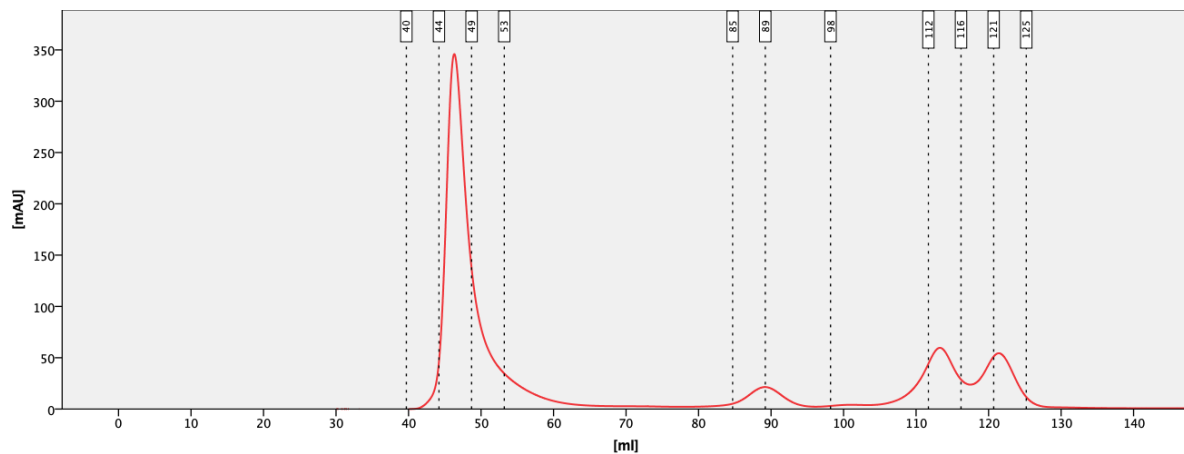


**Figure 25: Elution Profile TbBILBO421-EFh SEC (EDTA)**

Elution profile of size-exclusion chromatography (EDTA) of TbBILBO421-EFh (aa210-295, 56.9 kDa).  
Peak 1: 45.54 ml, Peak 2: 89.1 ml, Peak 3: 113 ml, Peak 4: 121 ml; Red line:  $A_{280}$ .

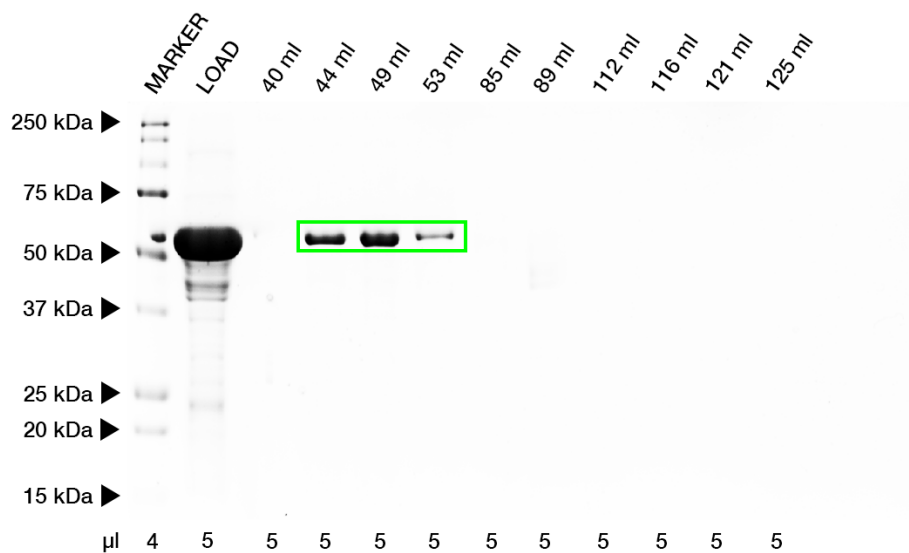


**Figure 26: SDS-PAGE TbBILBO421-EFh SEC (EDTA)**

17.5% SDS-PAGE of TbBILBO421-EFh size-exclusion chromatography (EDTA) fractions.  
Protein size: 56.9 kDa; Peak of elution: Peak 1 (45.54 ml; green box).

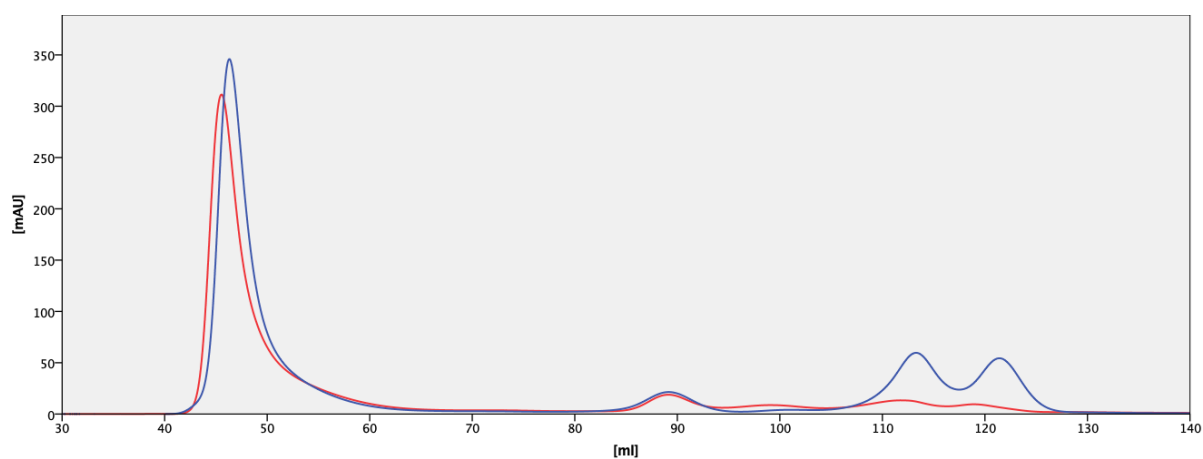


**Figure 27: Elution Profiles TbBILBO421-EFh SEC (CaCl<sub>2</sub>/EDTA)**  
 Elution profiles of size-exclusion chromatographies (CaCl<sub>2</sub>/EDTA) of TbBILBO421-EFh (aa210-295, 56.9 kDa) overlaid. Red line: Sample CaCl<sub>2</sub>, Blue line: Sample EDTA.

## 4.5. TbBILBO421-EFh-CCD – Purification and Results

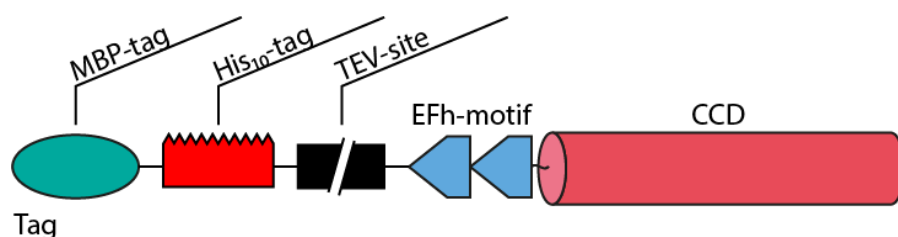


**Figure 28: Construct TbBILBO421-EFh-CCD – Illustration**

*Illustration of TbBILBO421-EFh-CCD construct features relevant for purification.*

*Depicted is the N-terminal conjugated MalpET tag and the proteins EFh-motif (aa210-295), CCD (aa296-404).*

### 4.5.1. TbBILBO421-EFh-CCD – Ni-Bead Purification

After cell lysis sample TbBILBO421-EFh-CCD was too viscous to be filtered, rendering further processing using any automated FPLC methods unfeasible. Therefore, the MBP-His<sub>10</sub>-tagged sample was purified via Ni-bead purification as described in section 3.3.5. Fractions were analyzed via SDS-PAGE (Figure 29). The protein of interest eluted throughout fractions F1-6. Fraction F1 was saved for size-exclusion chromatography.

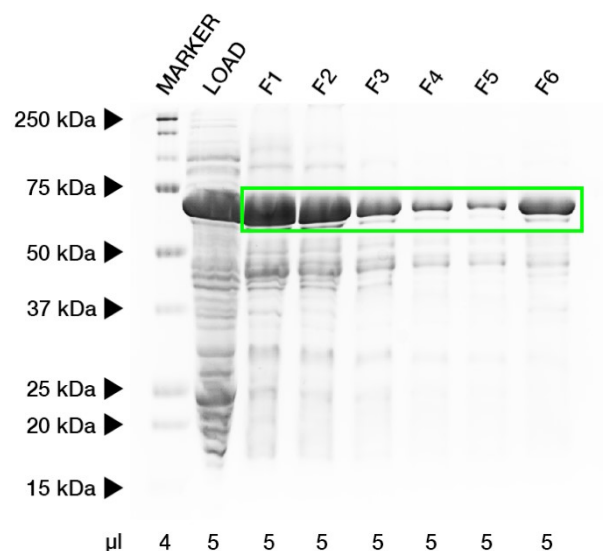


**Figure 29: SDS-PAGE TbBILBO421-EFh-CCD Ni-Bead Purification**

*17.5% SDS-PAGE of TbBILBO421-EFh-CCD – Ni-Bead Purification fractions. Protein size: 70.2 kDa; Elution between F1-F6 (green box). Fraction F1 saved for further analysis.*

#### 4.5.2. TbBILBO421-EFh-CCD – SEC

To investigate the influence of  $\text{CaCl}_2$  on the EFh-motif of the protein, uncut Ni-bead purification fraction F1 (1.5 ml) was split into two distinct samples. To one sample  $\text{CaCl}_2$  was added to a final concentration of 10 mM, to the second sample EDTA, likewise to a final concentration of 10 mM. With each sample size-exclusion chromatography using a Cytiva Life Sciences™ HiLoad Superdex 200pg 16/600 preparative SEC column was performed (Sample  $\text{CaCl}_2$ : Figure 30; Sample EDTA: Figure 32) as described in chapter 3.3.10. The buffers for each SEC contained additional  $\text{CaCl}_2$  or EDTA with a concentration of 5 mM accordingly.

Elution of sample  $\text{CaCl}_2$  (Figure 30) resulted in 6 distinct peaks (44 ml, 54 ml, 62 ml, 88 ml, 113 ml, 119 ml). The presence of the protein of interest could only be verified in peaks 1-3 via SDS-PAGE (Figure 31).

Elution of sample EDTA (Figure 32) also resulted in 6 distinct peaks (44 ml, 54 ml, 62 ml, 88 ml, 113 ml, 119 ml). Again, the presence of the protein of interest could only be verified in peaks 1-3 via SDS-PAGE (Figure 33), with peak 1 (44 ml) exhibiting a much weaker signal when compared to sample  $\text{CaCl}_2$ .

When compared to a HiLoad Superdex 200pg 16/600 SEC column protein standard provided by the manufacturer (Cytiva, 2020), the elution volume of peaks 1-3 correlate to proteins of 158 kDa and above, hinting at oligomerization of the protein of interest. By overlaying both elution profiles (Figure 34) a stark difference can be observed. Peak 1 (44 ml) displays a 1.5-fold stronger absorbance ( $A_{280}$ ) in sample  $\text{CaCl}_2$  relative to sample EDTA, while peak 2 (54 ml) displays a 3-fold elevated absorbance of sample EDTA and peak 3 (62 ml) a 2-fold elevated absorbance in sample EDTA. This strongly suggests that the addition of  $\text{CaCl}_2$  changes the conformation of the EFh-motif, pushing the protein towards oligomerization.

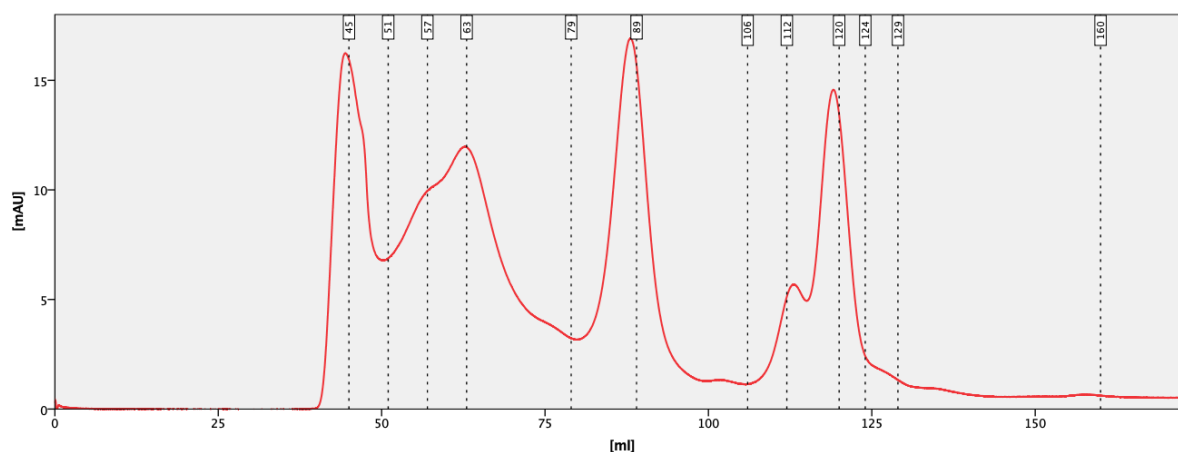


**Figure 30: Elution Profile TbBILBO421-EFh-CCD SEC (CaCl<sub>2</sub>)**  
 Elution profile of size-exclusion chromatography (CaCl<sub>2</sub>) of TbBILBO421-EFh-CCD (aa210-404, 70.2 kDa). Peak 1: 44 ml, Peak 2: 54 ml, Peak 3: 62 ml, Peak 4: 88 ml, Peak 5: 113 ml, Peak 6: 119 ml; Red line: A<sub>280</sub>.

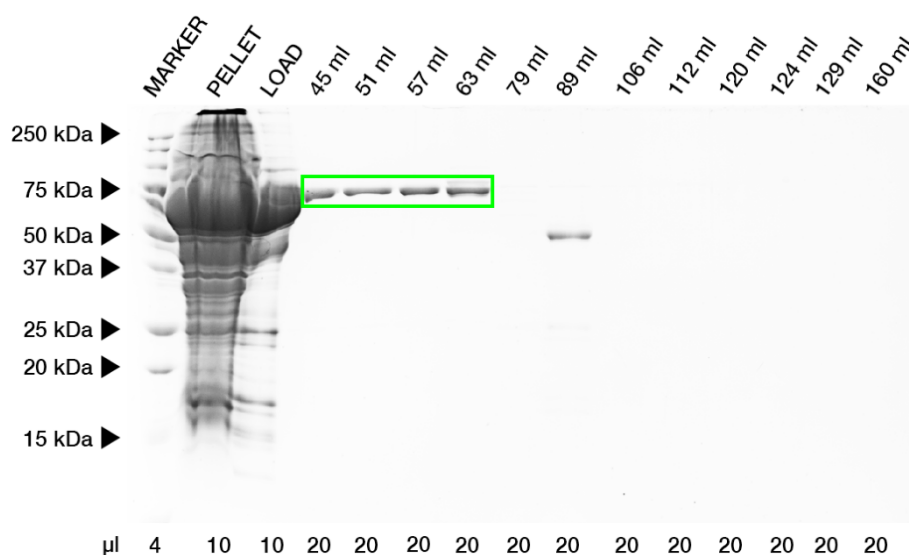


**Figure 31: SDS-PAGE TbBILBO421-EFh-CCD SEC (CaCl<sub>2</sub>)**  
 17.5% SDS-PAGE of TbBILBO421-EFh-CCD size-exclusion chromatography (CaCl<sub>2</sub>) fractions. Protein size: 70.2 kDa; Peaks of elution (green box): Peak 1 (44 ml), Peak 2 (54 ml) and Peak 3 (62 ml).

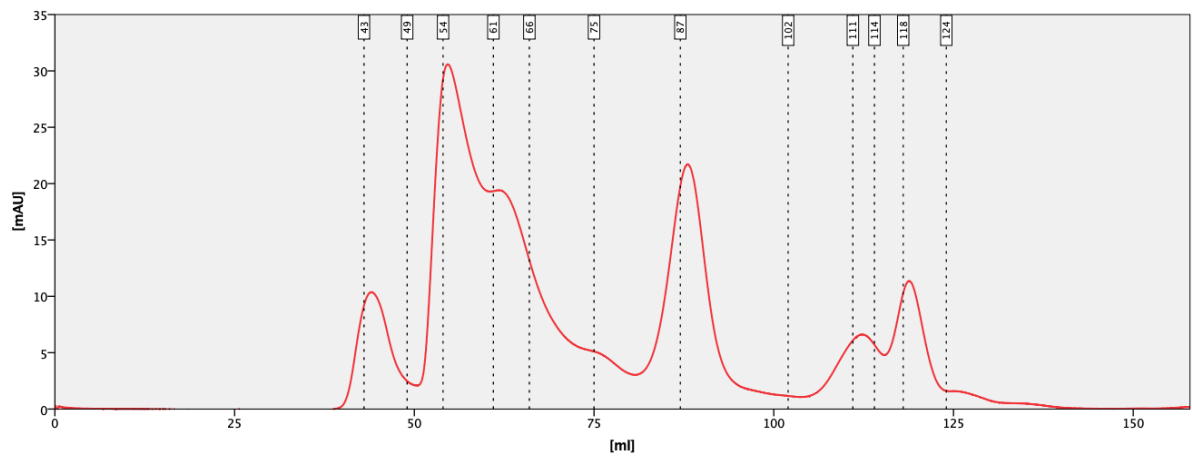


**Figure 32: Elution Profile TbBILBO421-EFh-CCD SEC (EDTA)**  
 Elution profile of size-exclusion chromatography (EDTA) of TbBILBO421-EFh-CCD (aa210-404, 70.2 kDa). Peak 1: 44 ml, Peak 2: 54 ml, Peak 3: 62 ml, Peak 4: 88 ml, Peak 5: 113 ml, Peak 6: 119 ml; Red line:  $A_{280}$ .

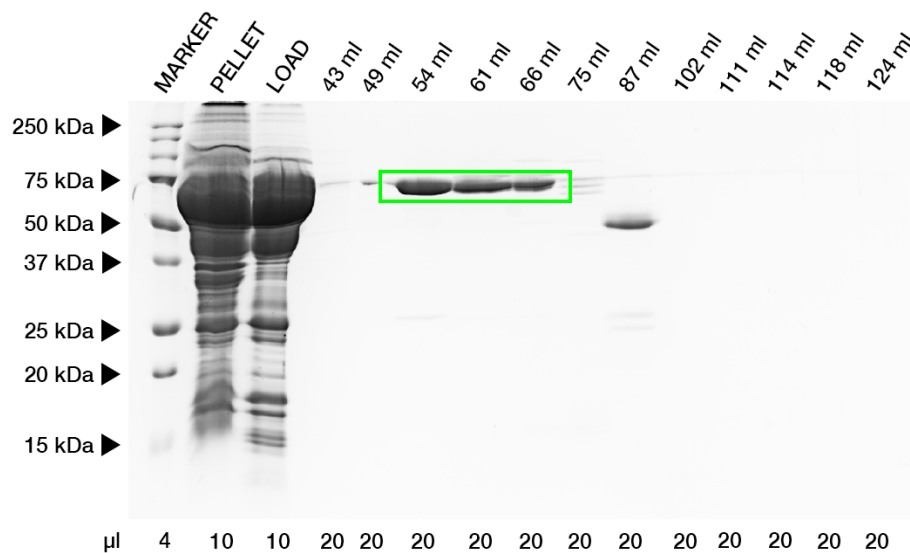


**Figure 33: SDS-PAGE TbBILBO421-EFh-CCD SEC (EDTA)**  
 17.5% SDS-PAGE of TbBILBO421-EFh-CCD size-exclusion chromatography (EDTA) fractions. Protein size: 70.2 kDa; Peaks of elution (green box): Peak 2 (54 ml) and Peak 3 (62 ml).



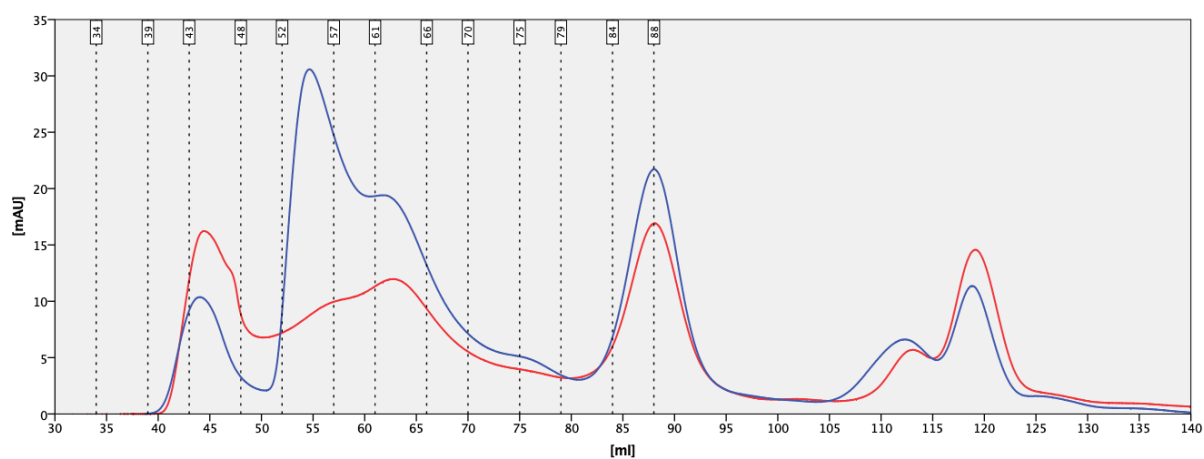


**Figure 34: Elution Profiles TbBILBO421-EFh-CCD SEC (CaCl<sub>2</sub>/EDTA)**  
 Elution profiles of size-exclusion chromatographies (CaCl<sub>2</sub>/EDTA) of TbBILBO421-EFh-CCD (aa210-404, 70.2 kDa) overlaid. Peak 1: 44 ml, Peak 2: 54 ml, Peak 3: 62 ml, Peak 4: 88 ml; Red line: Sample CaCl<sub>2</sub>, Blue line: Sample EDTA.

## 4.6. TbBILBO421-EFh-CCD-ct – Purification and Results

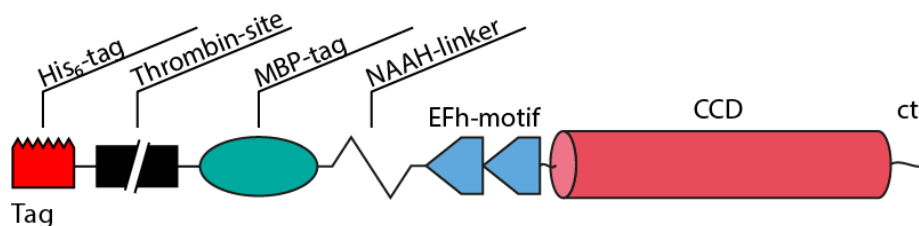


**Figure 35: Construct TbBILBO421-EFh-CCD-ct – Illustration**

*Illustration of TbBILBO421-EFh-CCD-ct construct features relevant for purification and rsEM analysis. Depicted is the N-terminal conjugated HM15b tag and the proteins EFh-motif (aa210-295), CCD (aa296-404), C-terminal tail (aa405-421).*

### 4.6.1. TbBILBO421-EFh-CCD-ct – HisTrap

In a first step the His<sub>6</sub>-tagged protein was purified via HisTrap affinity chromatography (Figure 36) as described in section 3.3.4. The flow-through and elution fractions were analyzed via SDS-PAGE (Figure 37). The protein of interest eluted in fractions 128-223 ml. Fractions 128-135.5 ml were pooled (7.5 ml).

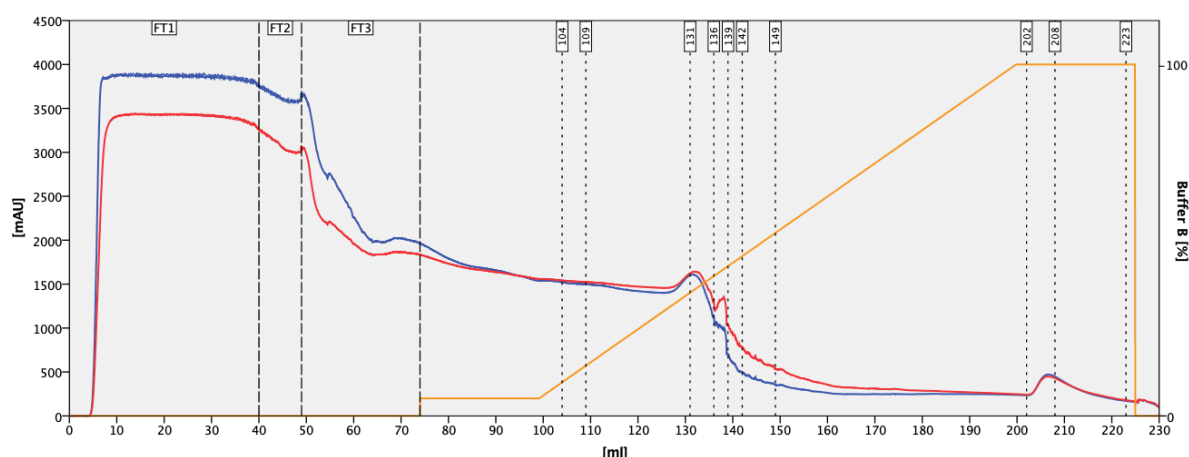


**Figure 36: Elution Profile TbBILBO421-EFh-CCD-ct HisTrap**

*Elution profile of HisTrap affinity chromatography of TbBILBO421-EFh-CCD-ct (aa210-421, 68.04 kDa). Start of elution: 128 ml (20% Buffer B); Red line: A<sub>280</sub>; Blue line: A<sub>254</sub>; Orange line: Buffer B; FT1/2: Sample loading; FT3: Column wash.*

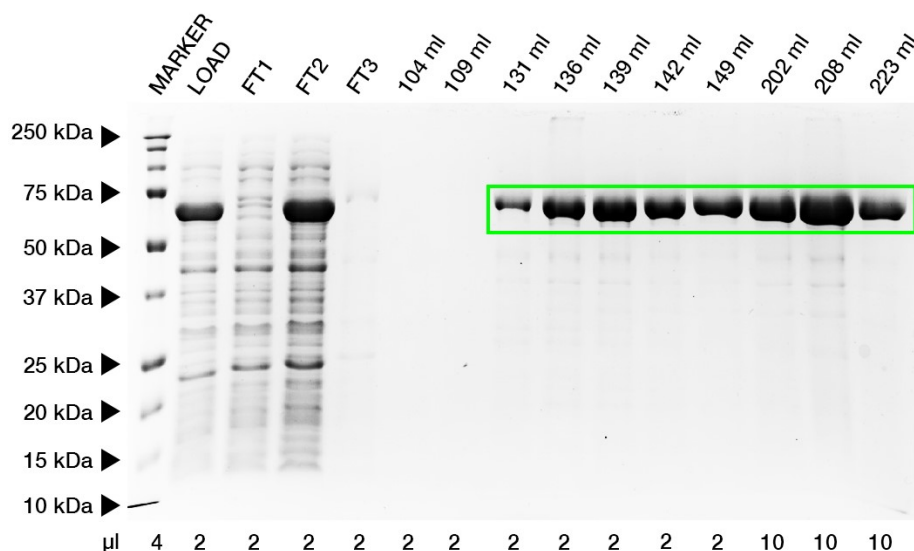


**Figure 37: SDS-PAGE TbBILBO421-EFh-CCD-ct HisTrap**

17.5% SDS-PAGE of TbBILBO421-EFh-CCD-ct HisTrap affinity purification fractions. Protein size: 68 kDa; Elution between 128-223 ml (green box). Fractions 128-135.5 ml were pooled.

#### 4.6.2. TbBILBO421-EFh-CCD-ct – SEC

To investigate the influence of  $\text{CaCl}_2$  on the EFh-motif of the protein fraction 128-135.5 ml (7.5 ml) of the HisTrap affinity chromatography was split into two separate samples. To one sample  $\text{CaCl}_2$  was added to a final concentration of 5 mM, to the second sample EDTA, likewise to a final concentration of 5 mM. With each sample size-exclusion chromatography using a Cytiva Life Sciences™ HiLoad Superdex 200pg 16/600 preparative SEC column was performed (Sample  $\text{CaCl}_2$ : Figure 38; Sample EDTA: Figure 40) as described in chapter 3.3.10. The buffers for each SEC contained additional  $\text{CaCl}_2$  or EDTA with a concentration of 1 mM accordingly.

Elution of sample  $\text{CaCl}_2$  (Figure 38) resulted in 6 distinct peaks (44 ml, 51 ml, 65 ml, 89 ml, 112 ml, 119 ml). The presence of the protein could only be verified in peaks 2 (51 ml) and 3 (65 ml) via SDS-PAGE (Figure 39).

Elution of sample EDTA (Figure 40) resulted in 5 distinct peaks (51 ml, 65 ml, 89 ml, 112 ml, 119 ml), lacking peak 1 (44 ml) of sample  $\text{CaCl}_2$ . The presence of the protein could only be verified in peaks 1 (51 ml) and 2 (65 ml) via SDS-PAGE (Figure 41).

When compared to a HiLoad Superdex 200pg 16/600 SEC column protein standard provided by the manufacturer (Cytiva, 2020), the elution volume of peaks 1-2 correlate to proteins of 158 kDa and above, hinting at oligomerization of the protein of interest.

Comparing both elution profiles by superimposition (Figure 42) reveals no significant difference in the peaks verified to contain protein by SDS-PAGE.

Fraction 51-52.5 ml was saved for rsEM.

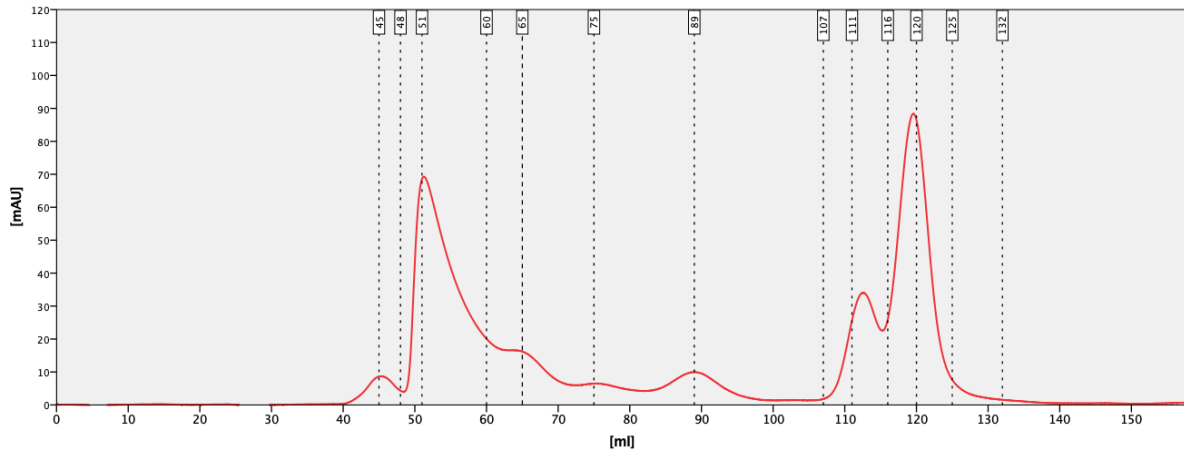


**Figure 38: Elution Profile TbBILBO421-EFh-CCD-ct SEC (CaCl<sub>2</sub>)**

Elution profile of size-exclusion chromatography (CaCl<sub>2</sub>) of TbBILBO421-EFh-CCD-ct (aa210-421, 66.5 kDa). Peak 1: 45 ml, Peak 2: 51 ml, Peak 3: 65 ml, Peak 4: 89 ml, Peak 5: 112 ml, Peak 6: 119 ml; Red line: A<sub>280</sub>.

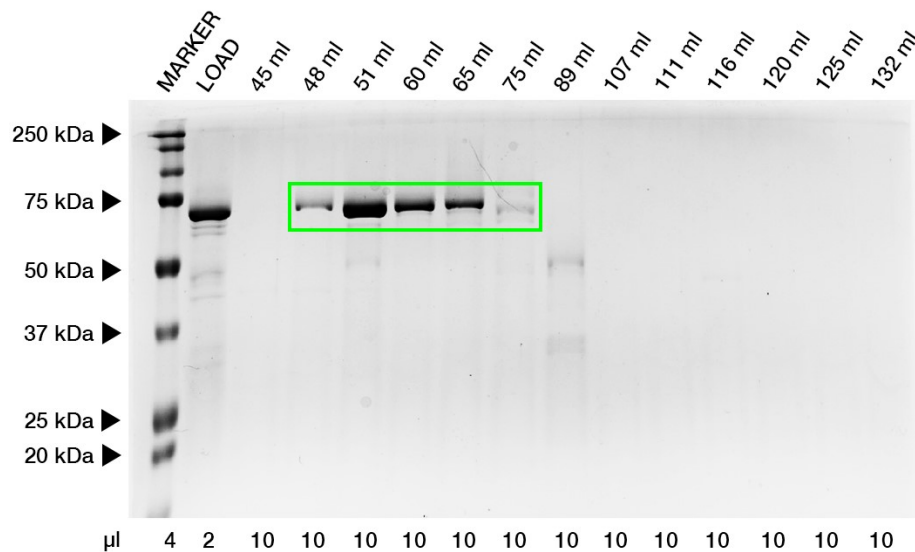


**Figure 39: SDS-PAGE TbBILBO421-EFh-CCD-ct SEC (CaCl<sub>2</sub>)**

17.5% SDS-PAGE of TbBILBO421-EFh-CCD-ct size-exclusion chromatography (CaCl<sub>2</sub>) fractions. Protein size: 66.5 kDa; Peak of elution: Peak 2 (51 ml; green box). Fraction 51-52.5 ml was saved.

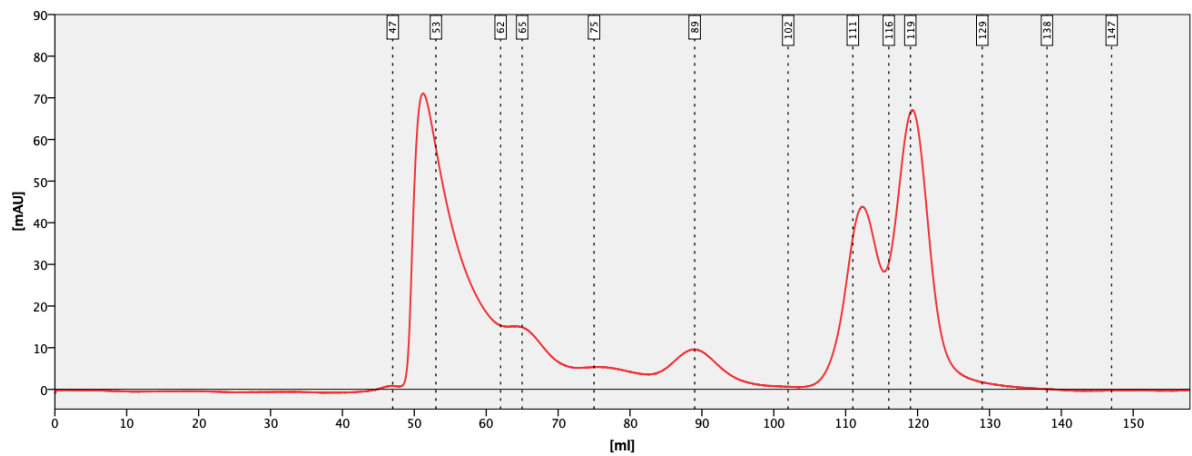


**Figure 40: Elution Profile TbBILBO421-EFh-CCD-ct SEC (EDTA)**  
 Elution profile of size-exclusion chromatography (EDTA) of TbBILBO421-EFh-CCD-ct (aa210-421, 66.5 kDa). Peak 1: 51 ml, Peak 2: 65 ml, Peak 3: 89 ml, Peak 4: 112 ml, Peak 5: 119 ml; Red line:  $A_{280}$ .

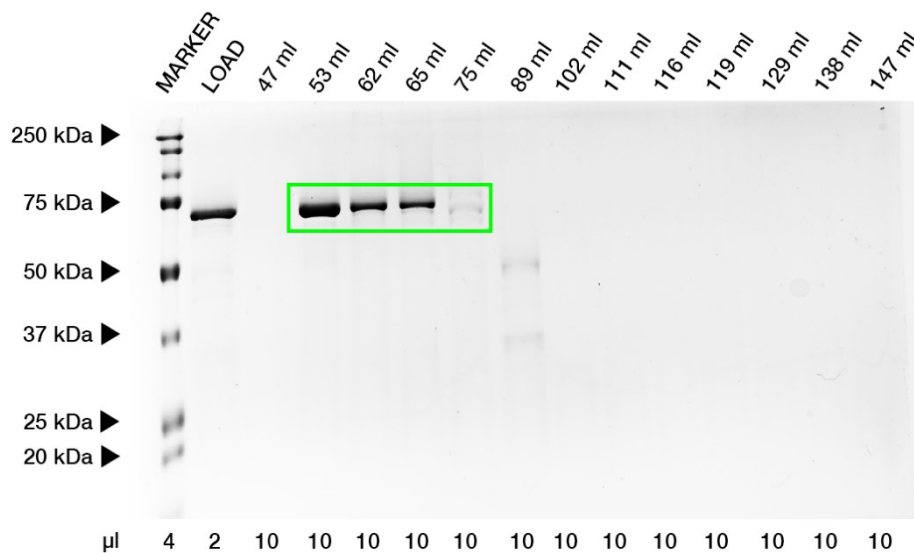


**Figure 41: SDS-PAGE TbBILBO421-EFh-CCD-ct SEC (EDTA)**  
 17.5% SDS-PAGE of TbBILBO421-EFh-CCD-ct size-exclusion chromatography (EDTA) fractions. Protein size: 66.5 kDa; Peaks of elution (green box): Peak 1 (51 ml) and Peak 2 (65 ml).

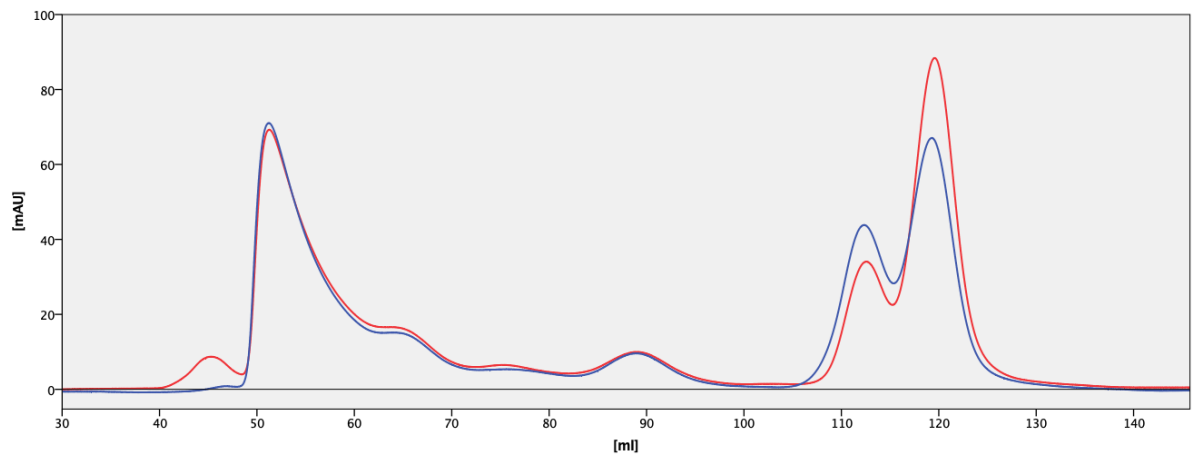


**Figure 42: Elution Profiles TbBILBO421-EFh-CCD-ct SECs (CaCl<sub>2</sub>/EDTA)**  
 Elution profile of size-exclusion chromatography (CaCl<sub>2</sub>/EDTA) of TbBILBO421-EFh-CCD-ct (aa210-421, 66.5 kDa) overlaid. Red line: Sample CaCl<sub>2</sub>, Blue line: Sample EDTA.

#### 4.6.3. TbBILBO421-EFh-CCD-ct – rsEM

Fraction 51-52.5 ml (3 ml) of TbBILBO421-EFh-CCD-ct SEC ( $\text{CaCl}_2$ ) was prepared for rsEM (Figure 44) as depicted in section 3.3.15. The concentration of the sample was 0.6 mg/ml (MW 66502.19 Da,  $\epsilon$  79885  $\text{M}^{-1}\text{cm}^{-1}$ ) as determined by microvolume measurement.

Rotary shadowing EM (Figure 44) revealed that TbBilbo421-EFh-CCD-ct forms an antiparallel dimer via its coiled-coil domain (Figure 43). The images clearly show two globular domains (MBP-tag) linked by a thin line (CCD) in multiple instances. With 15 nm the distance between the globular domains matches the theoretical length of the CCD.

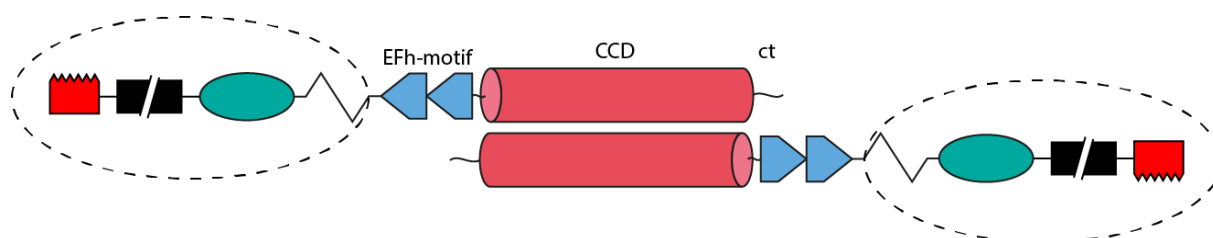


**Figure 43: TbBILBO421-EFh-CCD-ct – Antiparallel Dimer**

Theoretical illustration of TbBILBO421-EFh-CCD-ct forming an antiparallel dimer. Image shows the CCD with the C-terminal tail and N-terminal EFh-motif. The dashed circle resembles the globular MBP-tag.

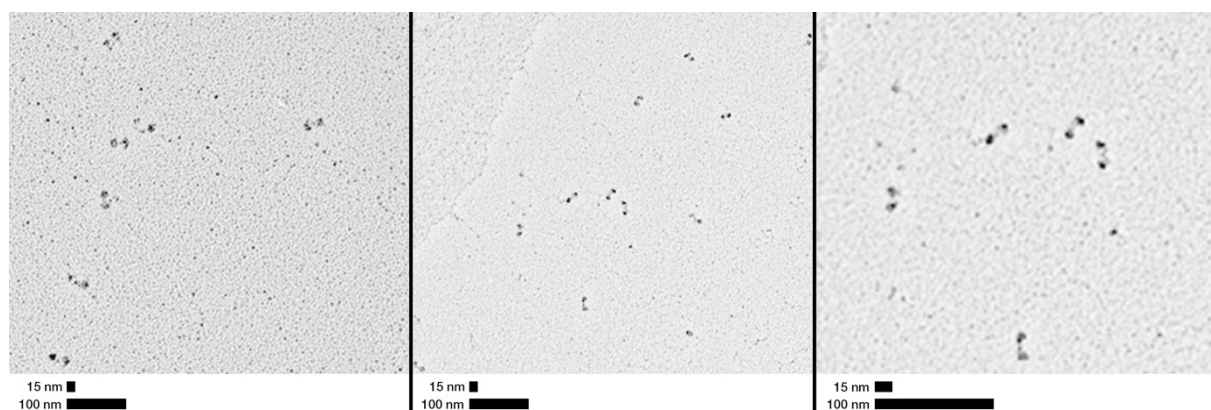


**Figure 44: rsEM of TbBILBO421-EFh-CCD-ct SEC ( $\text{CaCl}_2$ )**

Rotary shadowing electron microscopy images of TbBILBO421-EFh-CCD-ct size-exclusion chromatography ( $\text{CaCl}_2$ ) sample. Sample concentration 0.6 mg/ml.

## 4.7. TbBILBO421-CCD-ct – Purification and Results

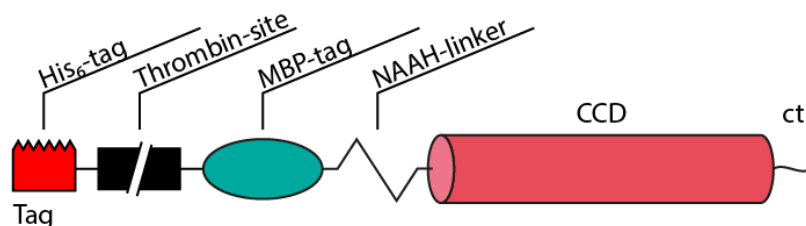


**Figure 45: Construct TbBILBO421-CCD-ct – Illustration**

*Illustration of TbBILBO421-CCD-ct construct features relevant for purification and rsEM analysis. Depicted is the N-terminal conjugated HM15b tag and the proteins CCD (aa296-404), C-terminal tail (aa405-421).*

### 4.7.1. TbBILBO421-CCD-ct – HisTrap

The His<sub>6</sub>-MBP-tagged protein was purified via HisTrap affinity chromatography (Figure 46) as described in section 3.3.4. The flow-through and fractions spanning the resulting peak were analyzed via SDS-PAGE (Figure 47). The protein eluted between fractions 145-155 ml. Fractions 150-153 ml were pooled for size-exclusion chromatography.

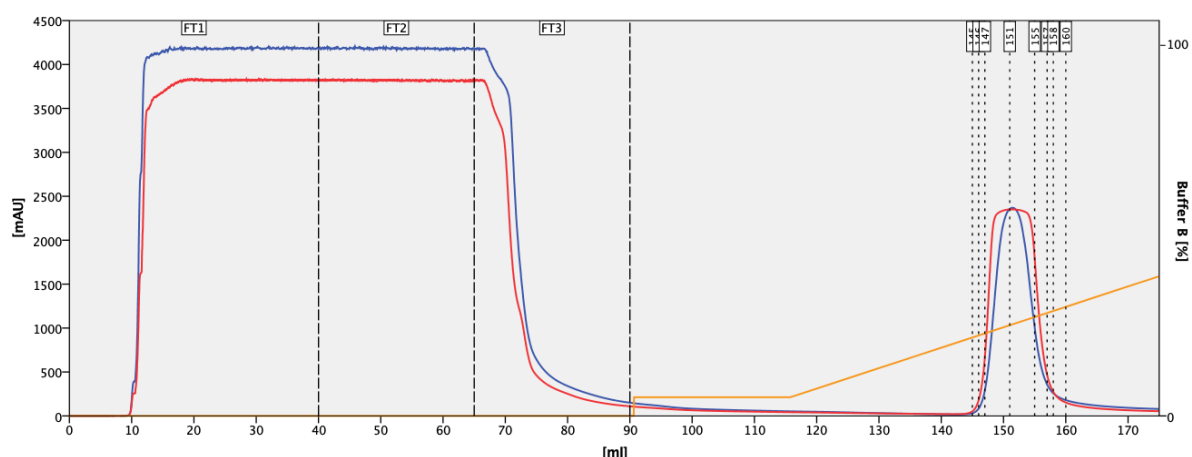


**Figure 46: Elution Profile TbBILBO421-CCD-ct HisTrap**

*Elution profile of HisTrap affinity chromatography of TbBILBO421-CCD-ct (aa296-421, 58.09 kDa) uncut. Elution between 144-158 ml (20-30% Buffer B); Red line:  $A_{280}$ ; Blue line:  $A_{254}$ ; Orange line: Buffer B; FT1/2: Sample loading, FT3: Column wash.*



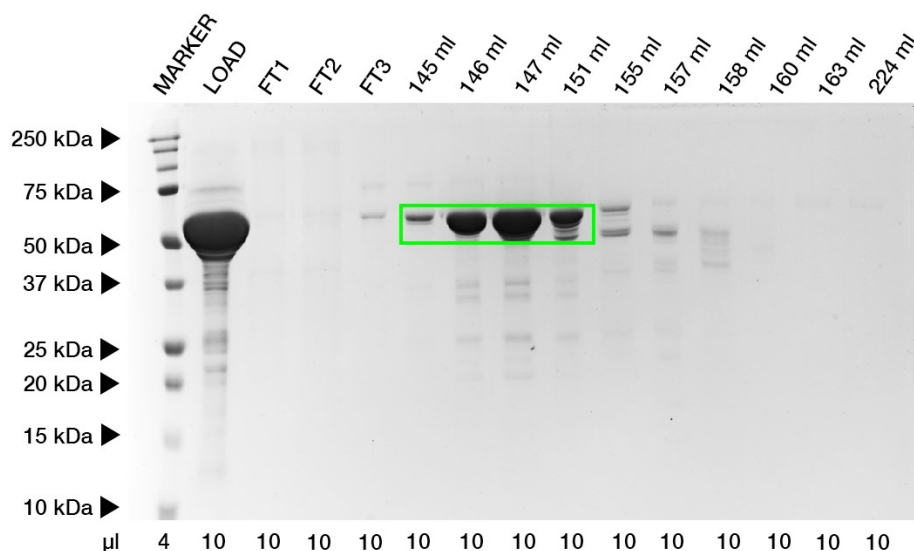


**Figure 47: SDS-PAGE TbBILBO421-CCD-ct HisTrap**

17.5% SDS-PAGE of TbBILBO421-CCD-ct HisTrap affinity purification fractions. Protein size: 58 kDa; Elution between 145-155 ml (green box). Fractions 150-153 ml were pooled.

#### 4.7.2. TbBILBO421-CCD-ct – SEC (1)

To further purify the sample fractions 150-153 ml size-exclusion chromatography using a Cytiva Life Sciences™ HiLoad Superdex 200pg 16/600 preparative SEC column was performed (Figure 48) as described in chapter 3.3.10.

The protein eluted in one distinct peak (74.77 ml), which, when compared to the before mentioned HiLoad Superdex 200pg 16/600 SEC column protein standard supplied by the manufacturer (Cytiva, 2020), roughly corresponds to the theoretical elution volume, suggesting the protein eluted as a monomer. The identity of the protein was verified via SDS-PAGE (Figure 49).

Fractions 73.5-78 ml were pooled for Thrombin treatment. Fraction 69-70.5 ml was saved for rsEM. Its concentration was determined to be 1.2 mg/ml (MW 57,688.38 Da,  $\epsilon$  72310 M<sup>-1</sup>cm<sup>-1</sup>) via microvolume measurement.

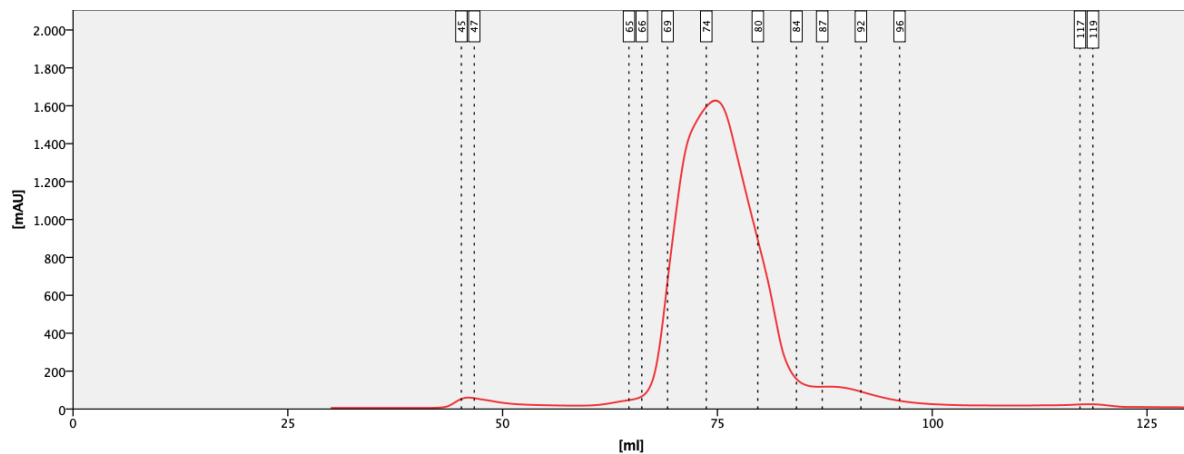


**Figure 48: Elution Profile TbBILBO421-CCD-ct SEC (1)**  
 Elution profile of size-exclusion chromatography (1) of TbBILBO421-CCD-ct (aa296-421, 57.7 kDa) uncut. Peak: 74.77 ml; Red line:  $A_{280}$ .

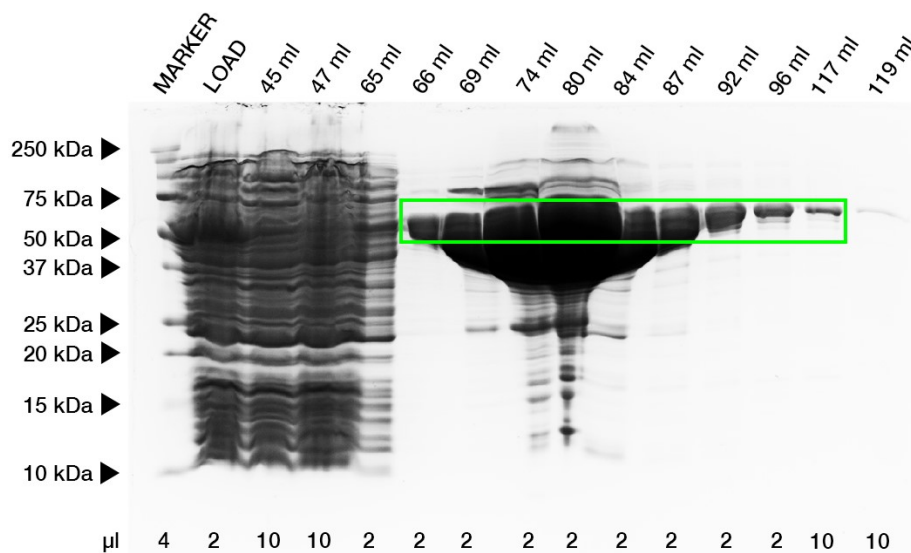


**Figure 49: SDS-PAGE TbBILBO421-CCD-ct SEC (1)**  
 17.5% SDS-PAGE of TbBILBO421-CCD-ct size-exclusion chromatography (1) fractions. Protein size: 57.7 kDa; Peak of elution: 74.77 ml (green box). Fractions 69-70.5 ml (rsEM) and 73.5-78 ml (Thrombin treatment) were pooled respectively.

#### 4.7.3. TbBILBO421-CCD-ct – rsEM

Fraction 69-70.5 ml (3 ml) of TbBILBO421-CCD-ct SEC (1) was prepared for rsEM (Figure 51) as depicted in section 3.3.15. The concentration of the sample was measured to be 1.2 mg/ml (MW 57688.38 Da,  $\epsilon$  72310 M<sup>-1</sup>cm<sup>-1</sup>) as determined by microvolume measurement and diluted to 1 mg/ml prior to rsEM.

Rotary shadowing EM (Figure 51) revealed that TbBilbo421-CCD-ct forms an antiparallel dimer via its coiled-coil domain (Figure 50). The images clearly show two globular domains (MBP-tag) linked by a thin line (CCD) in multiple instances.

When compared to rsEM images of TbBILBO421-EFh-CCD-ct (Figure 44), the distance between the globular domains seems to be shorter.

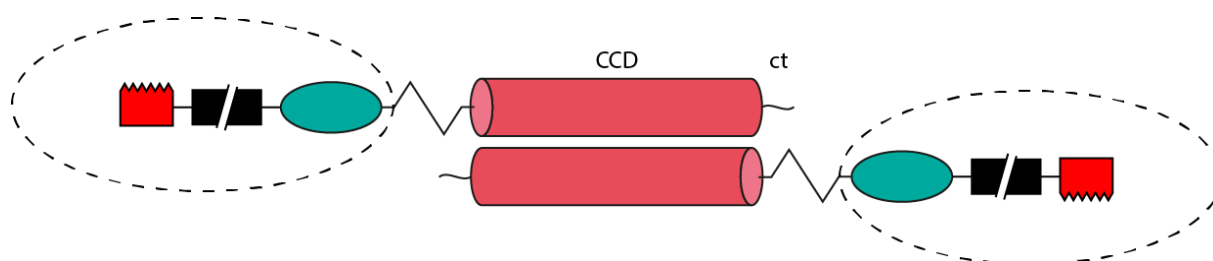


**Figure 50: TbBILBO421-CCD-ct – Antiparallel Dimer**

Theoretical illustration of TbBILBO421-CCD-ct forming an antiparallel dimer. Image shows the CCD with the C-terminal tail. The dashed circle resembles the globular MBP-tag.

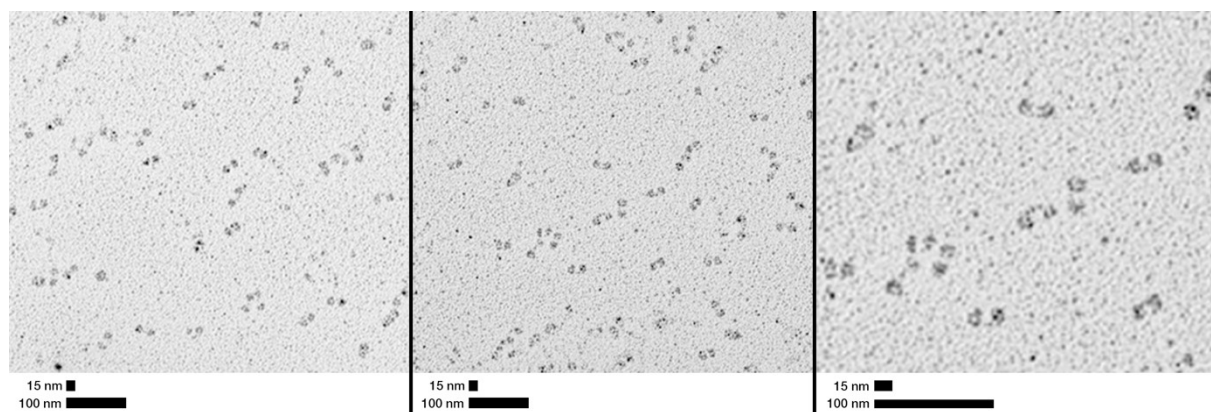


**Figure 51: rsEM of TbBILBO421-CCD-ct SEC (1)**

Rotary shadowing electron microscopy images of TbBILBO421-CCD-ct size-exclusion chromatography (1). Sample concentration 1.0 mg/ml.

#### 4.7.4. TbBILBO421-CCD-ct – Tag-Removal

As TbBILBO421-CCD-ct was expressed using the HM15b vector it is conjugated to a combined His<sub>6</sub>-MBP-tag as described in section 3.2.2.1. As the vector provides a Thrombin cleavage-site between the His<sub>6</sub>- and MBP-tag, SEC fraction 73.5-78 ml was treated with Thrombin as described in section 3.3.7. to eliminate the His<sub>6</sub>-tag. To verify successful cleavage of the tag SDS-PAGE was performed (Figure 52). The removal of the His<sub>6</sub>-tag has been successful. The gel does not show the removed His<sub>6</sub>-tag as it is only of 1.83 kDa and lost during dialysis as a dialysis filter of higher MWCO was used.

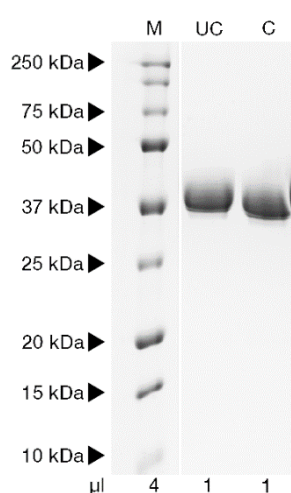


Figure 52: TbBILBO421-CCD-ct Uncut/Cut

*17.5% SDS-PAGE of TbBILBO421-CCD-ct HisTrap (1) Size-exclusion chromatography fractions 73.5-78 ml before (UC) and after (C) Thrombin treatment. UC: uncut protein (57.69 kDa); C: cut protein and tag (Protein+MBP-tag: 55.86 kDa; Tag: 1.83 kDa).*

#### 4.7.5. TbBILBO421-CCD-ct – SEC (2)

After the His<sub>6</sub>-tag was removed from the protein in SEC fraction 73.5-78 ml, as a last purification step, size-exclusion chromatography using a Cytiva Life Sciences™ HiLoad Superdex 200pg 16/600 preparative SEC column was performed (Figure 53), as described in section 3.3.10.

The protein eluted in one distinct peak (70.72 ml), which, when compared to the before mentioned HiLoad Superdex 200pg 16/600 SEC column protein standard supplied by the manufacturer (Cytiva manual, p.52), roughly corresponds to the theoretical elution volume, suggesting the protein eluted as a monomer. The identity of the protein was verified via SDS-PAGE (Figure 54).

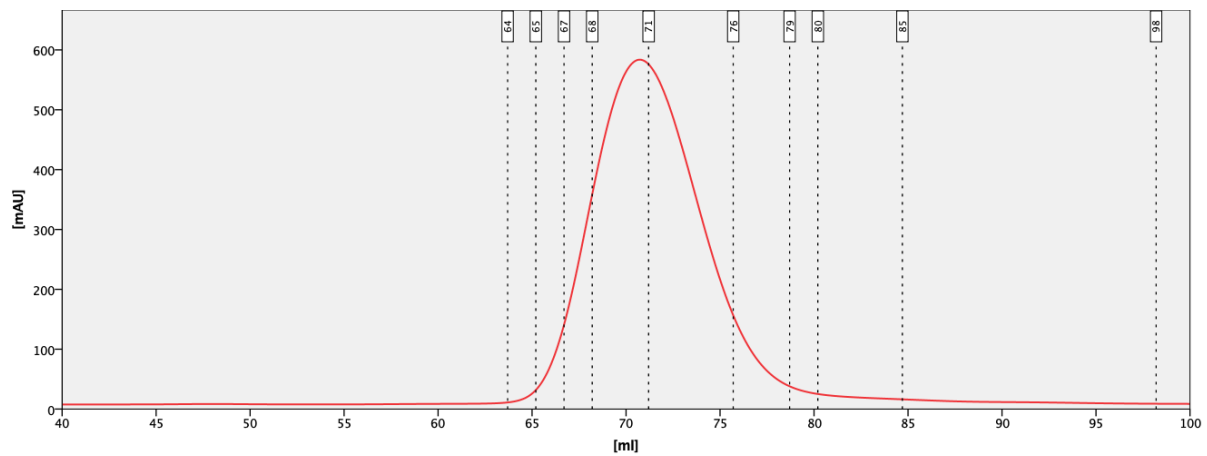


**Figure 53: Elution Profile TbBILBO421-CCD-ct SEC (2)**  
 Elution profile of size-exclusion chromatography (2) of TbBILBO421-CCD-ct (aa296-421, 55.91 kDa) cut. Peak: 70.72 ml; Red line: A<sub>280</sub>.

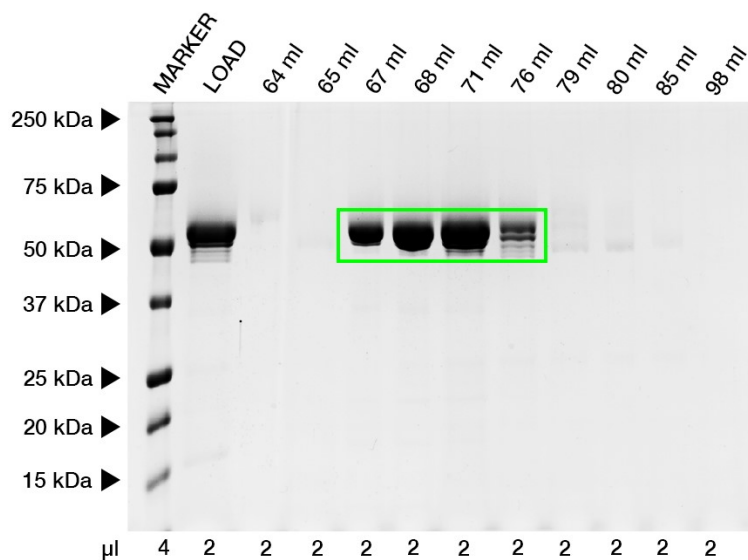


**Figure 54: Elution Profile TbBILBO421-CCD-ct SEC (2)**  
 17.5% SDS-PAGE of TbBILBO421-CCD-ct size-exclusion chromatography (2) fractions. Protein size: 55.9 kDa; Peak of elution: 70.72 ml (green box).

## 4.8. TbBILBO421-CCD – Purification and Results

### 4.8.1. TbBILBO421-CCD (HM15b)

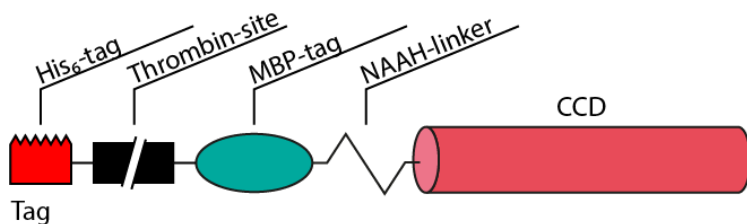


**Figure 55: Construct TbBILBO421-CCD (HM15b) – Illustration**

Illustration of TbBILBO421-CCD construct features relevant for purification and rsEM analysis. Depicted is the N-terminal conjugated HM15b tag and the proteins CCD (aa296-404).

#### 4.8.1.1. TbBILBO421-CCD – HisTrap

Initial purification of the His<sub>6</sub>-MBP-tagged protein was performed via HisTrap affinity chromatography (Figure 56) as described in section 3.3.4. The flow-through and fractions spanning the resulting peak were analyzed via SDS-PAGE (Figure 57). The protein eluted in fractions 83-135 ml. Fractions 110-128 ml were pooled for size-exclusion chromatography.

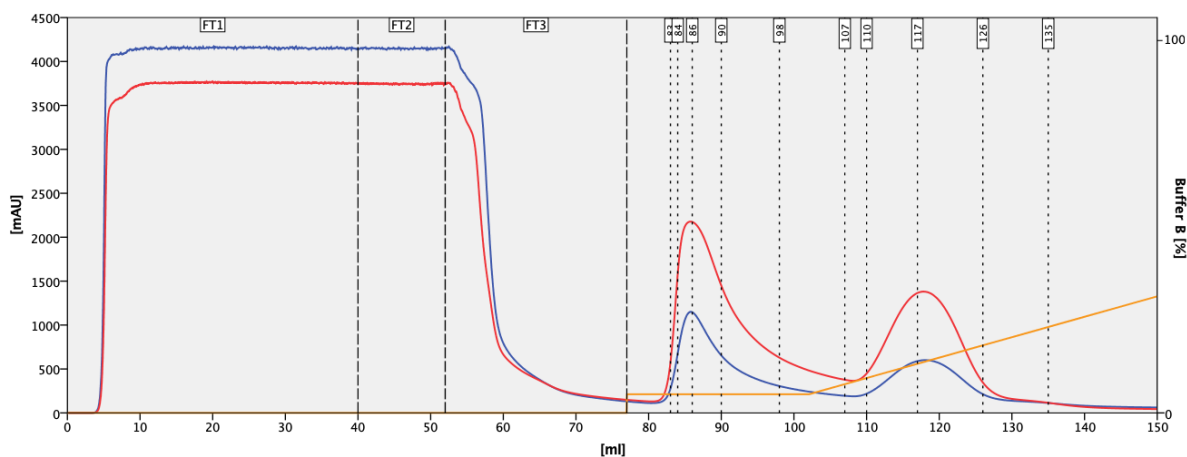


**Figure 56: Elution Profile TbBILBO421-CCD (HM15b) HisTrap**

Elution profile of HisTrap affinity chromatography of TbBILBO421-CCD (HM15b) (aa296-404, 55.99 kDa) uncut. Elution starting at 83 ml (5% Buffer B); Red line: A<sub>280</sub>; Blue line: A<sub>254</sub>; Orange line: Buffer B; FT1/2: Sample loading; FT3: Column wash.

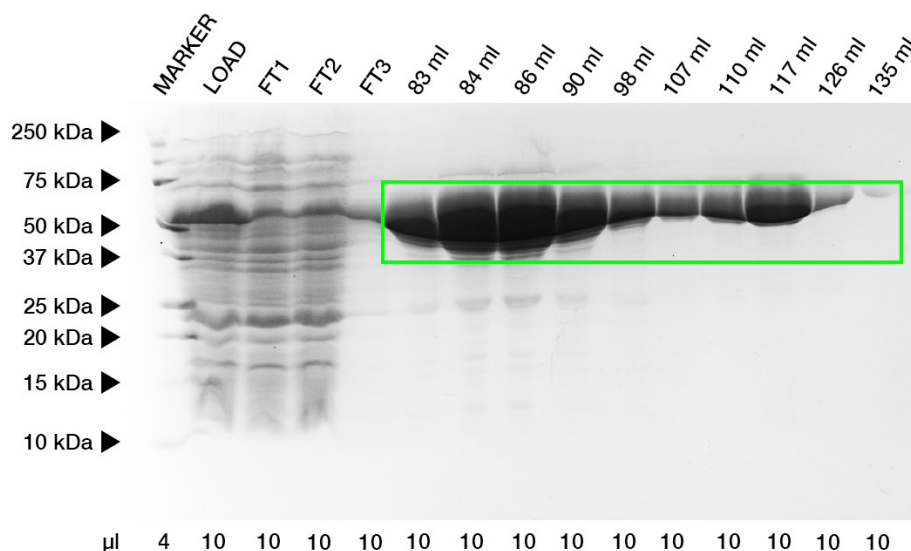


**Figure 57: SDS-PAGE TbBILBO421-CCD (HM15b) HisTrap**  
 17.5% SDS-PAGE of TbBILBO421-CCD (HM15b) HisTrap affinity purification fractions. Protein size: 56 kDa; Elution between 83-135 ml (green box). Fractions 110-128 ml were pooled.

#### 4.8.1.2. TbBILBO421-CCD – SEC (1)

Fraction 110-128 ml (18 ml) of the preliminary HisTrap purification was concentrated down to 3 ml and size-exclusion chromatography using a Cytiva Life Sciences™ HiLoad Superdex 200pg 16/600 preparative SEC column was performed (Figure 58), as described in section 3.3.10.

The protein eluted in 2 distinct peaks (45.8 ml, 66.91 ml). The elution volumes of both peaks indicate oligomerization in both cases, when compared to the before mentioned HiLoad Superdex 200pg 16/600 SEC column protein standard supplied by the manufacturer (Cytiva, 2020). The identity of the protein could be verified in both peaks via SDS-PAGE (Figure 59).

Fractions 64.5-66 ml were pooled for Thrombin treatment, with fraction 66-67.5 ml being excluded and saved separately for rsEM. The concentration of fraction 66-67.5 ml (rsEM) was determined to be 4.8 mg/ml (MW 55612.02 Da,  $\epsilon$  69330 M<sup>-1</sup>cm<sup>-1</sup>) via microvolume measurement.

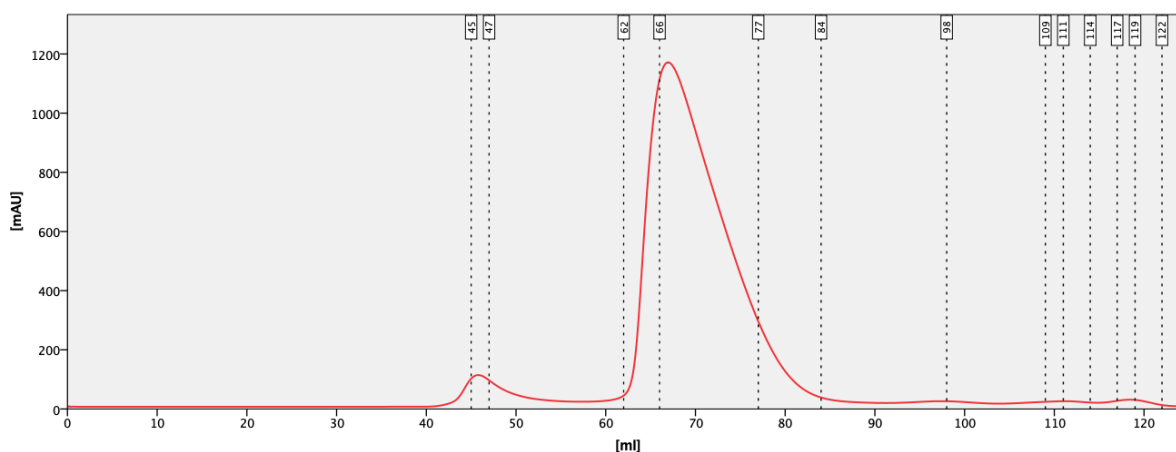


**Figure 58: Elution Profile TbBILBO421-CCD (HM15b) SEC (1)**  
 Elution profile of size-exclusion chromatography (1) of TbBILBO421-CCD (HM15b) (aa296-404, 55.6 kDa) uncut. Peak 1: 45.8 ml, Peak 2: 66.91 ml; Red line:  $A_{280}$ .

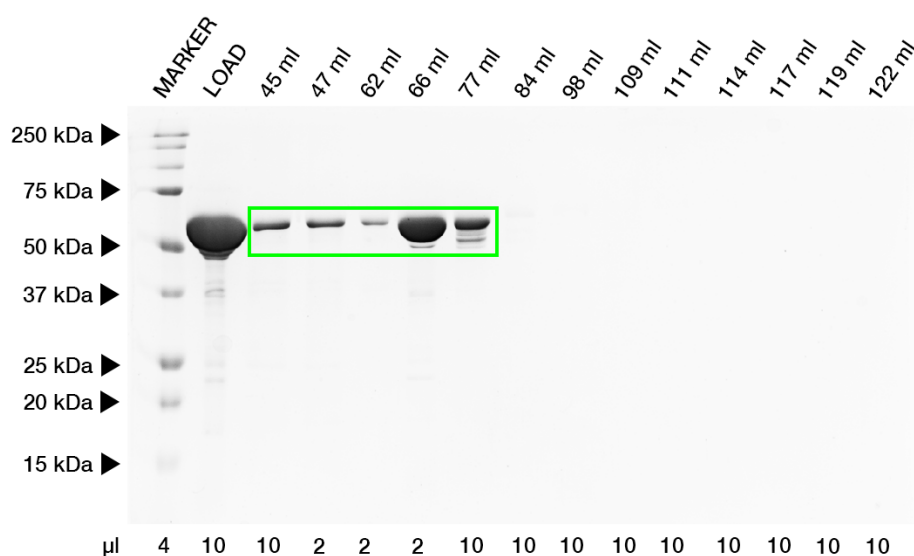


**Figure 59: SDS-PAGE TbBILBO421-CCD (HM15b) SEC (1)**  
 17.5% SDS-PAGE of TbBILBO421-CCD (HM15b) size-exclusion chromatography (1) fractions. Protein size: 56 kDa; Elution in Peak 1 (45.8 ml) and Peak 2 (66.91 ml) (green box). Fractions 64.5-66 ml were pooled (Thrombin treatment) with fraction 66-67.5 ml (rsEM) being excluded and saved separately.



#### 4.8.1.3. TbBILBO421-CCD – rsEM

Fraction 66-67.5 ml (3 ml) of TbBILBO421-CCD (HM15b) SEC (1) was prepared for rsEM (Figure 61) as described in section 3.3.15. The concentration of the sample was measured to be 4.8 mg/ml (MW 55,612.02 Da,  $\epsilon$  69330 M<sup>-1</sup>cm<sup>-1</sup>) as determined by microvolume measurement and diluted to 1 mg/ml prior to rsEM.

Rotary shadowing EM (Figure 61) revealed that TbBilbo421-CCD forms an antiparallel dimer via its coiled-coil domain (Figure 60). The images clearly show two globular domains (MBP-tag) linked by a thin line (CCD) in multiple instances.

When compared to rsEM images of TbBILBO421-EFh-CCD-ct (Figure 44), the distance between the globular domains seems to be shorter, matching those of TbBILBO421-CCD-ct (Figure 51).

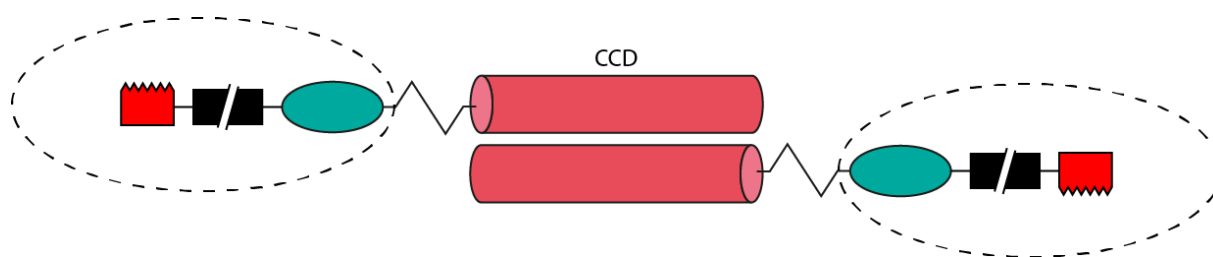


**Figure 60: TbBILBO421-CCD – Antiparallel Dimer**

*Theoretical illustration of TbBILBO421-CCD forming an antiparallel dimer. Image shows the proteins CCD. The dashed circle resembles the globular MBP-tag.*

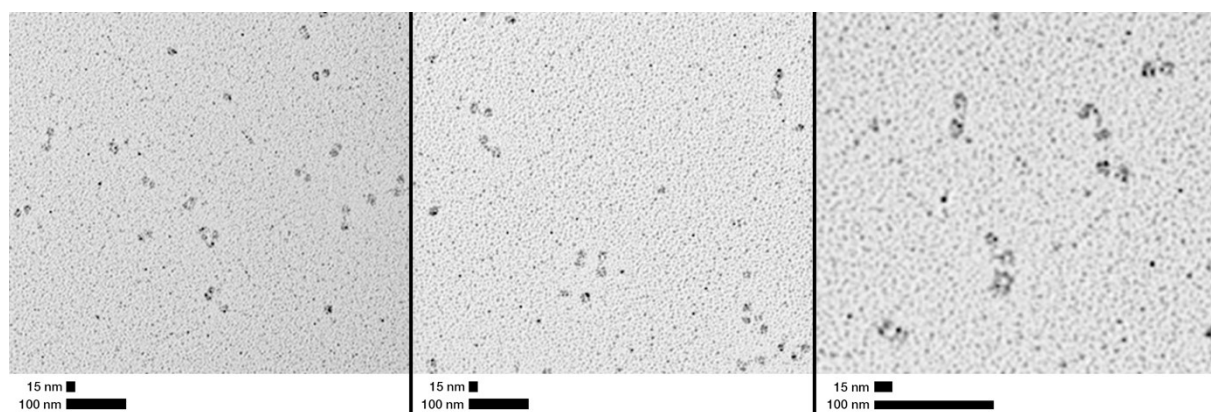


**Figure 61: rsEM of TbBILBO421-CCD SEC (1)**

*Rotary shadowing electron microscopy images of TbBILBO421-CCD size-exclusion chromatography (1). Sample concentration 1.0 mg/ml.*

#### 4.8.1.4. TbBILBO421-CCD – Tag-Removal

As TbBILBO421-CCD was expressed using the HM15b vector it is conjugated to a combined His<sub>6</sub>-MBP-tag, with a Thrombin cleavage-site in between both tags, as described in section 3.2.2.1. To cut of the His<sub>6</sub>-tag utilizing this Thrombin cleavage-site, SEC fraction 64.5-66 ml (excluding fraction 66-67.5 ml) was processed as described in section 3.3.7. To verify successful cleavage of the tag SDS-PAGE was performed (Figure 62). The removal of the His<sub>6</sub>-tag has been successful. The gel does not show the removed His<sub>6</sub>-tag as it is only of 1.83 kDa and lost during dialysis as a dialysis filter of higher MWCO was used.

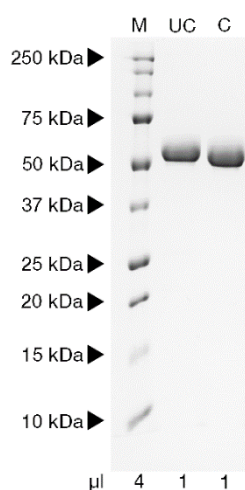
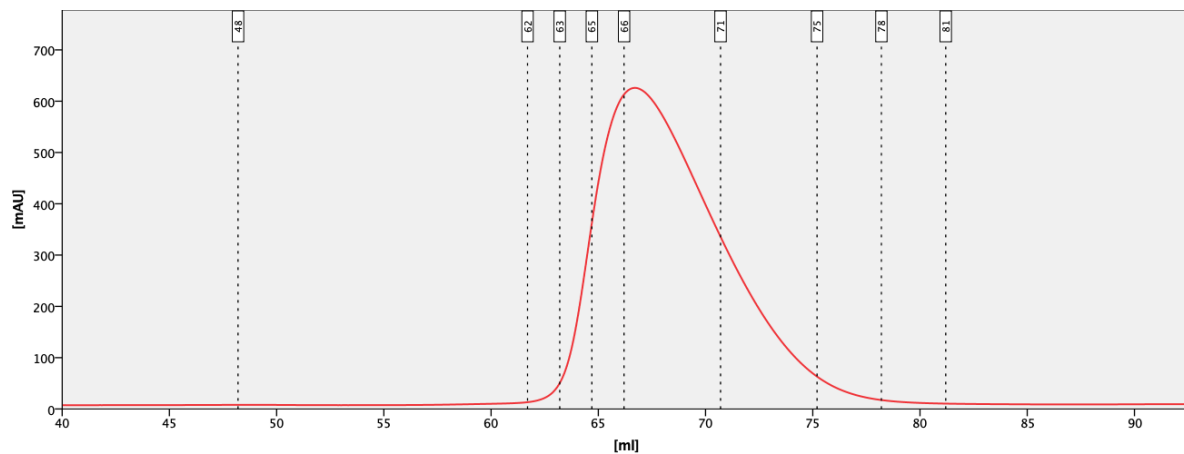


**Figure 62: TbBILBO421-CCD (HM15b) Uncut/Cut**  
17.5% SDS-PAGE of TbBILBO421-NTD (Hm15b) HisTrap (1) affinity purification fractions 64.5-66 ml (excluding fraction 66-67.5 ml) before (UC) and after (C) Thrombin treatment. UC: uncut protein (55.61 kDa); C: cut protein and tag (Protein + MBP-tag: 53.78 kDa; Tag: 1.83 kDa).

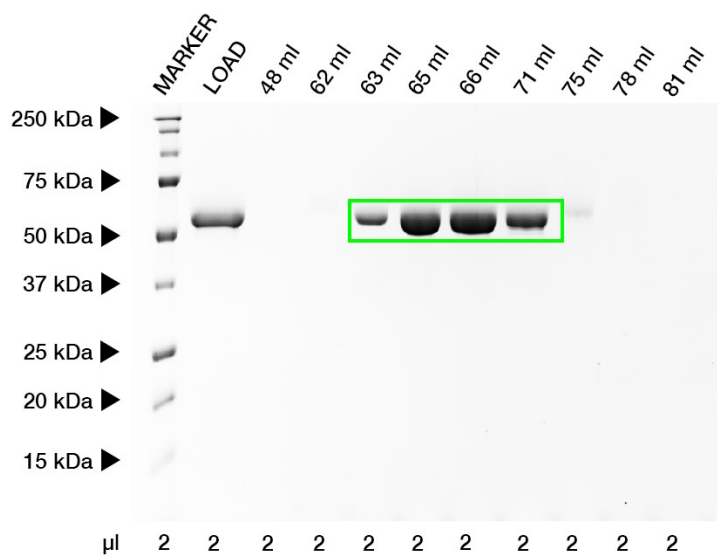
#### 4.8.1.5. TbBILBO421-CCD – SEC (2)

After the His<sub>6</sub>-tag was removed from the protein in SEC fraction 64.5-66 ml (excluding fraction 66-67.5 ml), as a last purification step size-exclusion chromatography using a Cytiva Life Sciences™ HiLoad Superdex 200pg 16/600 preparative SEC column was performed (Figure 63), as described in section 3.3.10.

The protein eluted in one distinct peak (66.7 ml), which, when compared to the before mentioned HiLoad Superdex 200pg 16/600 SEC column protein standard supplied by the manufacturer (Cytiva, 2020), strongly suggests dimerization of the protein. The identity of the protein was verified via SDS-PAGE (Figure 64).

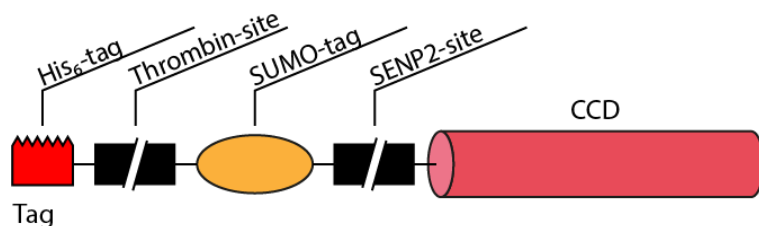


**Figure 63: Elution Profile TbBILBO421-CCD (HM15b)**  
 Elution profile of size-exclusion chromatography (2) of TbBILBO421-CCD (HM15b) (aa296-404, 53.78 kDa) cut. Peak: 66.7 ml; Red line:  $A_{280}$ .



**Figure 64: SDS-PAGE TbBILBO421-CCD (HM15b) SEC (2)**  
 17.5% SDS-PAGE of TbBILBO421-CCD (HM15b) size-exclusion chromatography (2) fractions. Protein size: 53.78 kDa; Peak of elution: 66.7 ml (green box).

#### 4.8.2. TbBILBO421-CCD (Sumo15b)



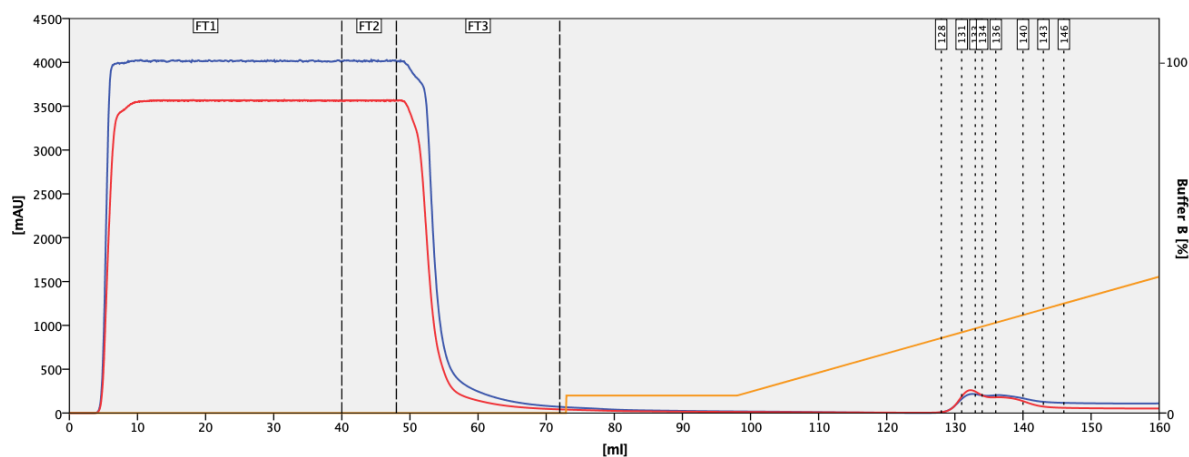
**Figure 65: Construct TbBILBO421-CCD (Sumo15b) – Illustration**

Illustration of TbBILBO421-CCD construct features relevant for purification.

Depicted is the N-terminal conjugated Sumo15b tag and the proteins CCD (aa296-404).

##### 4.8.2.1. TbBILBO421-CCD – HisTrap (1)

Initial purification of the His<sub>6</sub>-tagged protein was performed via HisTrap affinity chromatography (Figure 66), as described in section 3.3.4. The flow-through and fractions spanning the resulting peak were analyzed via SDS-PAGE (Figure 67). The protein eluted in fractions 128-143 ml. Fractions 130-145 ml were pooled for SENP2 treatment.



**Figure 66: Elution Profile TbBILBO421-CCD (Sumo15b) HisTrap (1)**

Elution profile of HisTrap affinity chromatography (1) of TbBILBO421-CCD (Sumo15b) (aa296-404, 26.7 kDa) uncut. Elution between 129.9-144.9 ml (20-30% Buffer B); Red line: A<sub>280</sub>, Blue line: A<sub>254</sub>; Orange line: Buffer B; FT1/2: Sample loading; FT3: Column wash.

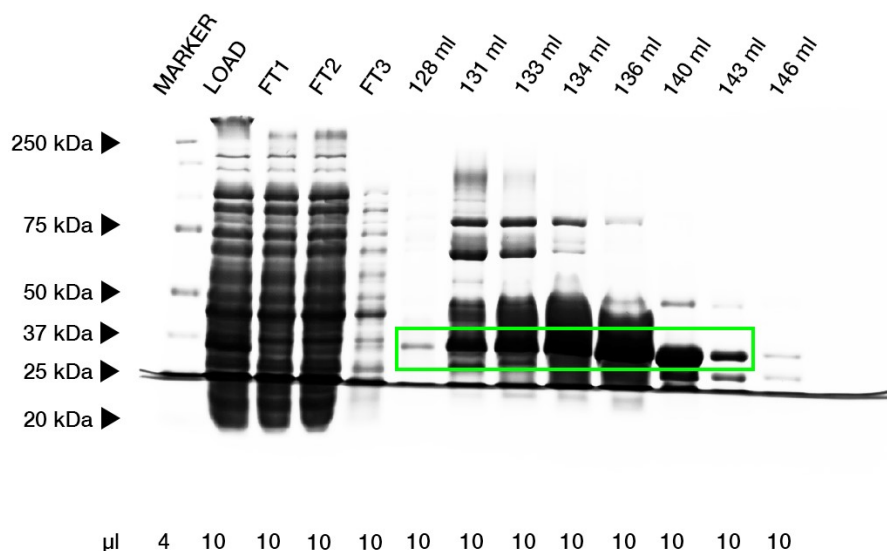


**Figure 67: SDS-PAGE TbBILBO421-CCD (Sumo15b) HisTrap (1)**  
 17.5% SDS-PAGE of TbBILBO421-CCD (Sumo15b) HisTrap affinity purification (1) fractions.  
 Protein size: 26.7 kDa; Elution between 128-143 ml (green box). Fractions 130-145 ml were pooled.

#### 4.8.2.2. TbBILBO421-CCD – Tag-Removal

As TbBILBO421-CCD was expressed using the Sumo15b vector, the protein is conjugated to a combined His<sub>6</sub>-SUMO-tag as described in section 3.2.2.1. To cut off both tags utilizing the SENP2 cutting site of the Sumo15b vector, the sample was processed as described in section 3.3.7. The tag was successfully removed as depicted in Figure 68.

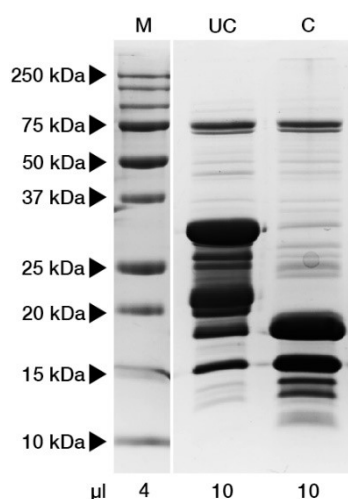


**Figure 68: TbBILBO421-CCD (Sumo15b) Uncut/Cut**  
 17.5% SDS-PAGE of TbBILBO421-CCD (Sumo15b) HisTrap (1) affinity purification fractions 130-145 ml before (UC) and after (C) SENP2 treatment. UC: uncut protein (26.7 kDa); C: cut protein and tag (Protein: 13.3 kDa; Tag: 13.4 kDa).

#### 4.8.2.3. TbBILBO421-CCD – HisTrap (2)

To separate tag and protein and further purify the protein reverse HisTrap affinity chromatography was performed (Figure 69), as described in section 3.3.4. The protein eluted in fractions FT1-2 (0-40 ml) as verified by SDS-PAGE (Figure 70). Fractions FT1-2 were pooled for size-exclusion chromatography.

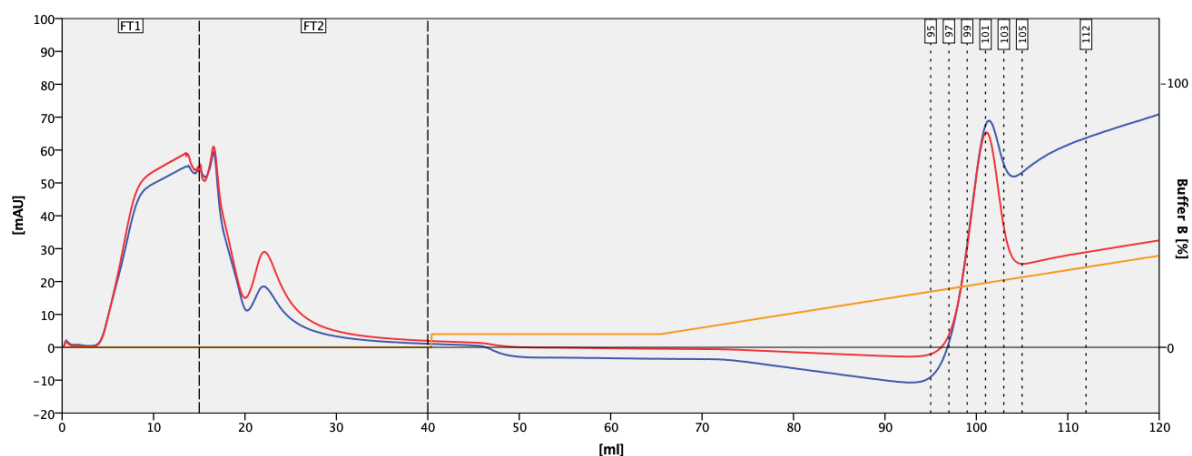


**Figure 69: Elution Profile TbBILBO421-CCD (Sumo15b) HisTrap (2)**  
Elution profile of HisTrap affinity chromatography (2) of TbBILBO421-CCD (Sumo15b) (aa296-404, 13.3 kDa) cut. Elution of tag between 95.8-106.3 ml (20-30% Buffer B); Red line: A<sub>280</sub>, Blue line: A<sub>254</sub>; Orange line: Buffer B; FT1/2: Sample loading; FT3: Column wash.

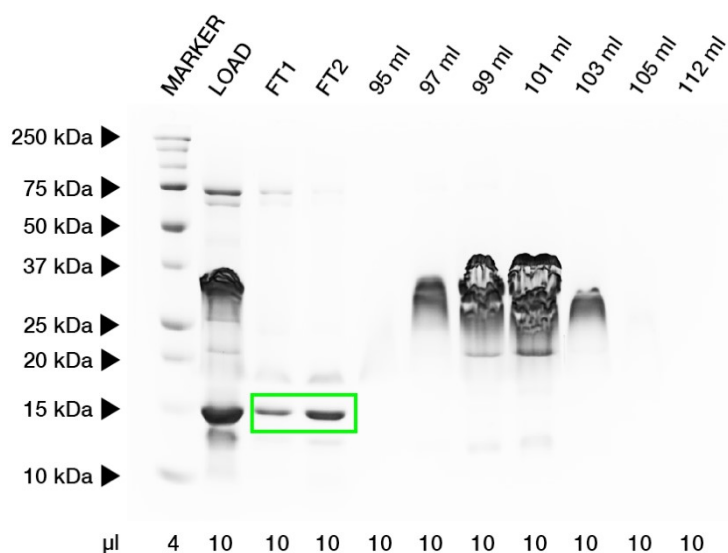


**Figure 70: SDS-PAGE TbBILBO421-CCD (Sumo15b) HisTrap (2)**  
17.5% SDS-PAGE of TbBILBO421-CCD (Sumo15b) HisTrap affinity purification (2) fractions. Protein size: 13.3 kDa; Elution: FT1-2 (green box). Fractions FT1-2 (0-40 ml) were pooled.

#### 4.8.2.4. TbBILBO421-CCD – SEC

Fractions FT1-2 (40 ml) of the reverse HisTrap affinity chromatography were concentrated down to 1.5 ml and further purified via size-exclusion chromatography (Figure 71) using a Cytiva Life Sciences™ HiLoad Superdex 200pg 16/600 preparative SEC column as described in section 3.3.10. Elution resulted in 7 peaks (44.78 ml, 63.87 ml, 74.12 ml, 84.16 ml, 92.47 ml, 111.32 ml, 117.84 ml), with the protein of interest only eluting in peak 3 (84.16 ml) as verified by SDS-PAGE (Figure 72), which, when compared to the before mentioned HiLoad Superdex 200pg 16/600 SEC column protein standard supplied by the manufacturer (Cytiva, 2020), strongly suggest dimerization of the protein.

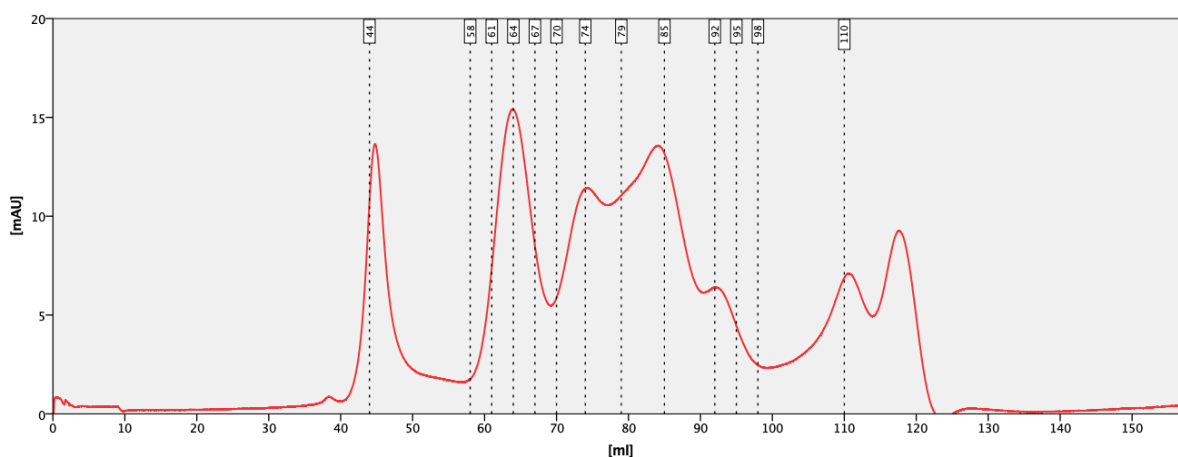


**Figure 71: Elution Profile TbBILBO421-CCD (Sumo15b) SEC**

Elution profile of size-exclusion chromatography of TbBILBO421-CCD (Sumo15b) (aa296-404, 13.3 kDa) cut. Peak 1: 44.78 ml, Peak 2: 63.87 ml, Peak 3: 74.12 ml, Peak 4: 84.16 ml, Peak 5: 92.47 ml, Peak 6: 111.32 ml, Peak 7: 117.84 ml; Red line:  $A_{280}$ .

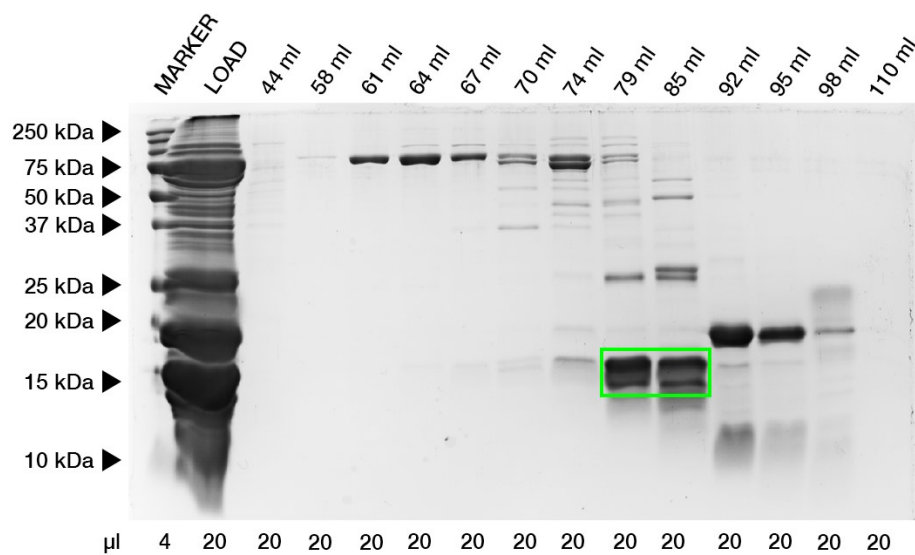


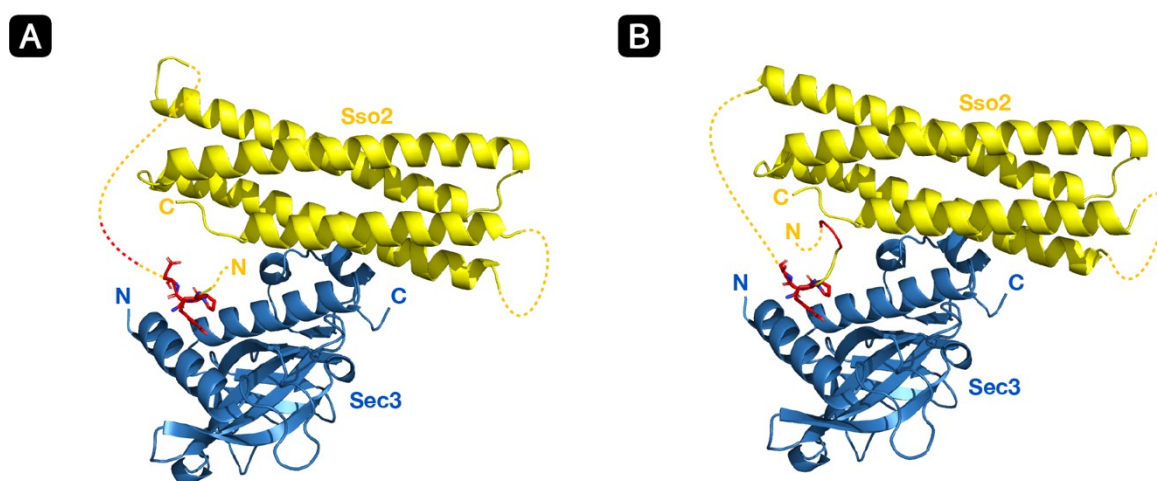
**Figure 72: SDS-PAGE TbBILBO421-CCD (Sumo15b) SEC**  
 17.5% SDS-PAGE of TbBILBO421-CCD (Sumo15b) size-exclusion chromatography fractions.  
 Protein size: 13.3 kDa; Peak of elution: Peak 3 (84.16 ml; green box).



## 4.9. Sec3(aa75-260) Sso2(aa1-270) Complex

Diffraction data, to a resolution of 2.19 Å, of the Sec3(aa75-260)/Sso2(aa1-224) complex crystal was collected as mentioned in section 3.4.1. Data collection and refinement statistics are presented in Table 22.

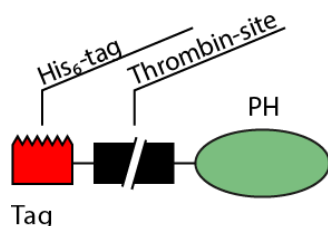
The model contains two distinct heterodimeric complexes of Sec3(aa75-260)/Sso2(aa1-224), each showing one of the two NPY motifs to be bound to a conserved hydrophobic pocket on Sec3 respectively (Figure 73). The NPY motives are connected to the helical core of Sso2 via a long flexible linker. This confirms the theory of a possible additional binding site for Sec3 on Sso2, besides the one on its four-helix bundles, located at the N-terminal end of Sso2, comprised of the two highly conserved Asn-Pro-Tyr (NPY) motifs.



**Figure 73: Crystal Structure Sec3(aa75-260)/Sso2(aa1-224) Complex**

**A:** Structure of Sec3/Sso2 complex with first NPY-motif (aa5-8) binding to Sec3. First NPY-motif marked red, with second NPY-motif indicated by red dotted line on the linker region. **B:** Structure of Sec3/Sso2 complex with second NPY-motif (aa11-14) binding to Sec3. Second NPY-motif marked red, with first NPY-motif indicated at the very N-terminal side as backbone-structure colored in red.

## 4.10. Sec3-PH – Purification and Results



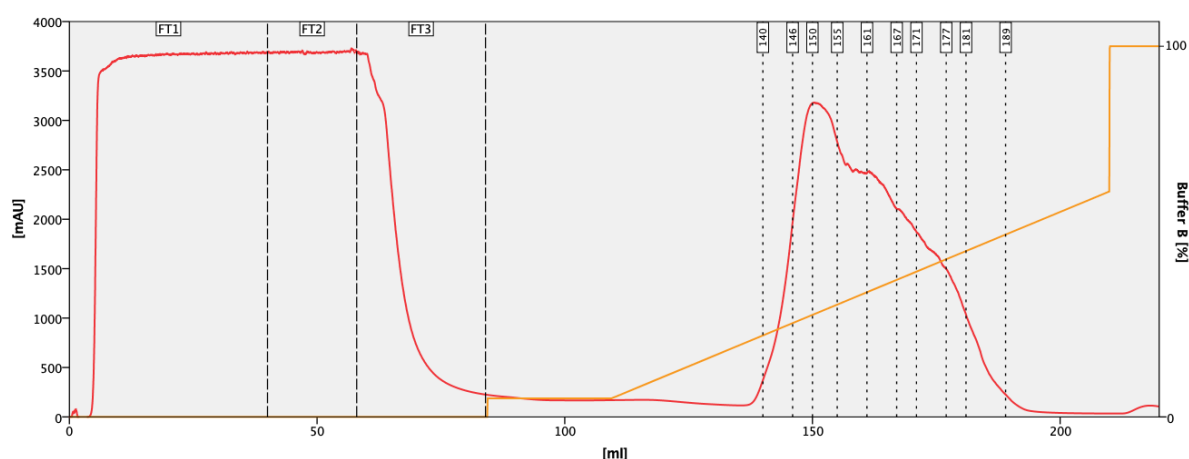
**Figure 74: Construct Sec3-PH – Illustration**

Illustration of Sec3-PH construct features relevant for purification.

Depicted is the N-terminal conjugated pET15b tag and the proteins pleckstrin homology (PH) domain (aa75-260).

### 4.10.1. Sec3-PH – HisTrap (1)

Initial purification of the His<sub>6</sub>-tagged protein was performed via HisTrap affinity chromatography (Figure 75) as described in section 3.3.4. The flow-through and fractions spanning the resulting peak were analyzed via SDS-PAGE (Figure 76). The protein eluted in fractions 140-167 ml and, as the amount of protein exceeded the binding capacity of the column, in fractions FT1-2 (0-59 ml). As not all protein bound to the column, fractions 140-167 ml were frozen to -80°C for future studies, while fractions FT1-2 (0-59 ml) were pooled for PEI-precipitation, and subsequently run in a second HisTrap in order to recover all of the protein.



**Figure 75: Elution Profile Sec3-PH HisTrap (1)**

Elution profile of HisTrap affinity chromatography (1) of Sec3-PH (aa75-260, 23.81 kDa) uncut. Elution between 140-189 ml (20-50% Buffer B); Red line: A<sub>280</sub>; Blue line: A<sub>254</sub>; Orange line: Buffer B; FT1/2: Sample loading; FT3: Column wash.

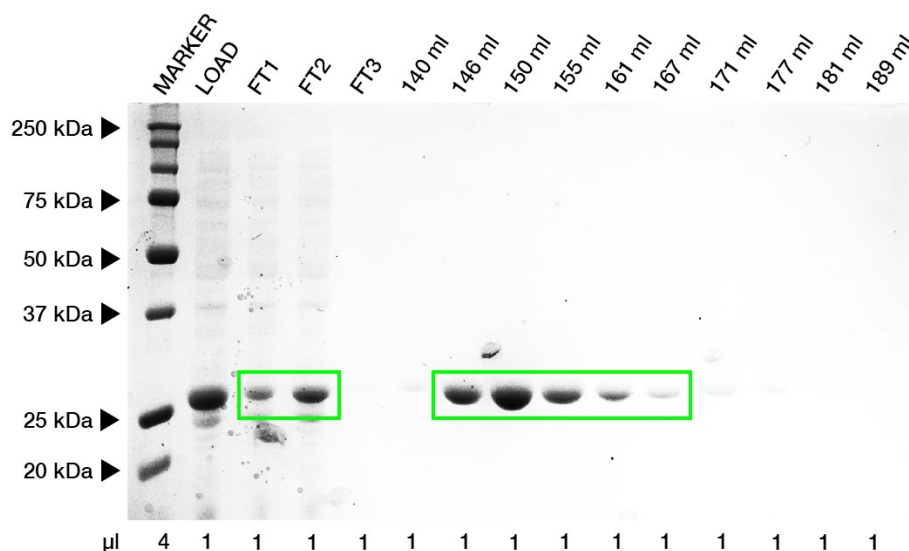


**Figure 76: SDS-PAGE Sec3-PH HisTrap (1)**

17.5% SDS-PAGE of Sec3-PH HisTrap affinity purification (1) fractions. Protein size: 23.81 kDa; Elution of protein in FT1-2 and 140-167 ml (green boxes). Fractions FT1-2 (0-59 ml) were pooled.

#### 4.10.2. Sec3-PH – PEI Nucleic Acid Precipitation

As the eluates of HisTraps of the same construct have previously shown high  $A_{254}$  signals, hinting at high nucleic acid content, the fraction FT1-2 (0-59 ml) of the first HisTrap purification was processed via PEI nucleic acid precipitation, as described in section 3.3.6.

#### 4.10.3. Sec3-PH– HisTrap (2)

To recover more of the protein of the first HisTrap's flow-through, HisTrap fractions FT1-2 were re-loaded onto a HisTrap affinity chromatography column after PEI-precipitation (Figure 77). Chromatography was performed according to section 3.3.4. The flow-through and fractions spanning the resulting peak were analyzed via SDS-PAGE (Figure 78). The protein eluted in fractions 123-138 ml, which were pooled for His<sub>6</sub>-tag removal.

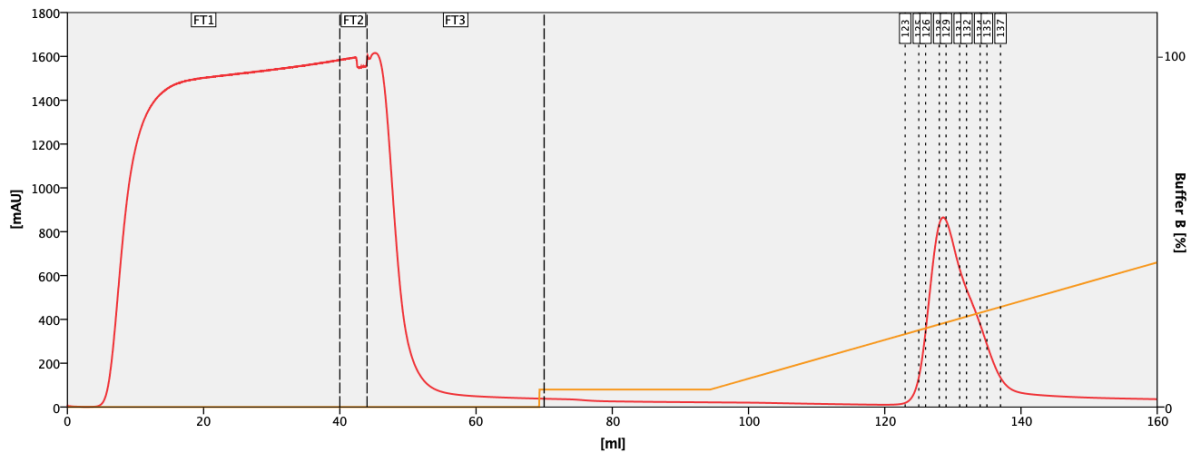


**Figure 77: Elution Profile Sec3-PH HisTrap (2)**

Elution profile of HisTrap affinity chromatography (2) of Sec3-PH (aa75-260, 23.81 kDa) uncut. Elution between 123-137 ml (20-50% Buffer B); Red line:  $A_{280}$ ; Blue line:  $A_{254}$ ; Orange line: Buffer B; FT1/2: Sample loading; FT3: Column wash.

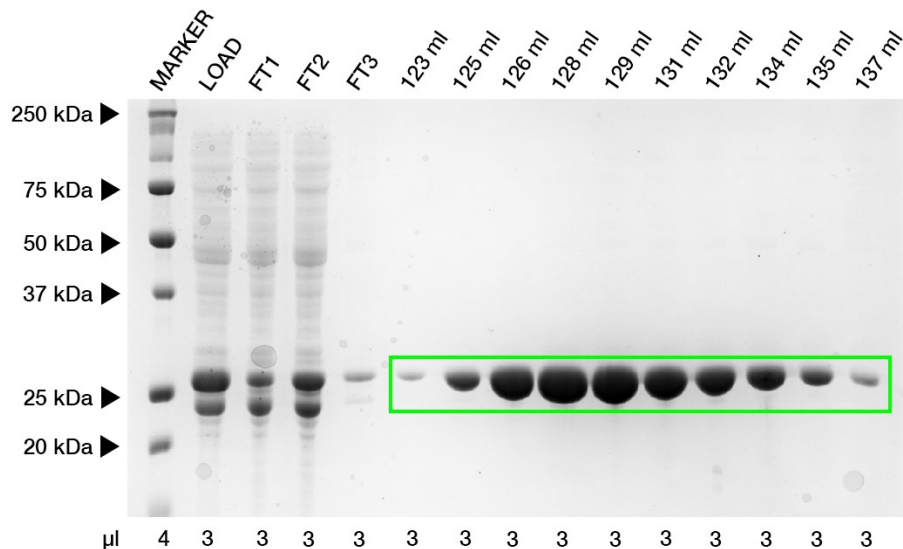


**Figure 78: SDS-PAGE Sec3-PH HisTrap (2)**

17.5% SDS-PAGE of Sec3-PH HisTrap affinity purification (2) fractions. Protein size: 23.81 kDa; Elution between 123-138 ml (green box). Fractions 123-138 ml were pooled.

#### 4.10.4. Sec3-PH – Tag-Removal

As Sec3-PH was expressed using the pET15b vector, the protein is conjugated to a His<sub>6</sub>-tag followed by a Thrombin cutting-site as described in section 3.2.2.1. To cut of the tag utilizing the Thrombin cutting site of the pET15b vector, the sample was processed as described in section 3.3.7. The tag was successfully removed as verified by SDS-PAGE (Figure 79).

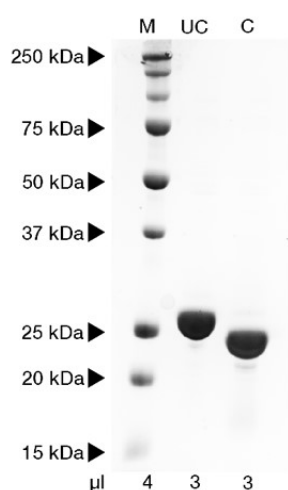


**Figure 79: Sec3-PH Uncut/Cut**  
17.5% SDS-PAGE of Sec3-PH HisTrap affinity purification (2) fractions 123-138 ml before (UC) and after (C) Thrombin treatment. UC: uncut protein (23.81 kDa); C: cut protein and tag (Protein: 22.06 kDa; Tag: 1.75 kDa).

#### 4.10.5. Sec3-PH – CEX

To further eliminate contamination cation-exchange chromatography was performed (Figure 80) as described in section 3.3.9. The protein eluted in fractions 117-131 ml as verified by SDS-PAGE (Figure 81). Fractions 119-126.5 ml were pooled for isothermal titration calorimetry.

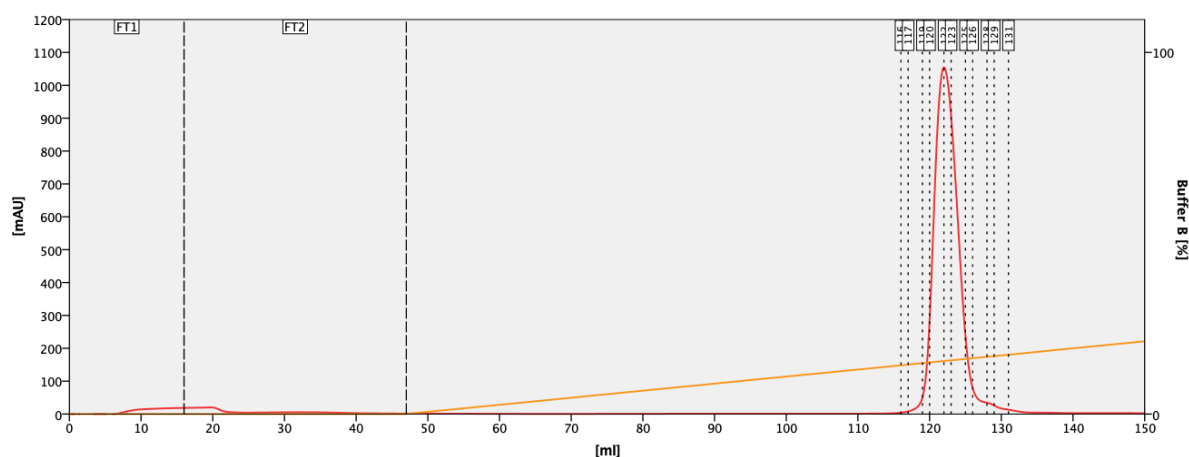


**Figure 80: Elution Profile Sec3-PH CEX**  
Elution profile of cation-exchange chromatography of Sec3-PH (aa75-260, 22.06 kDa, pI 9.28) cut. Peak: 122 ml, 150 mM NaCl (15% Buffer B); Red line:  $A_{280}$ ; Orange line: Buffer B; FT1: Sample loading; FT2: Column wash.

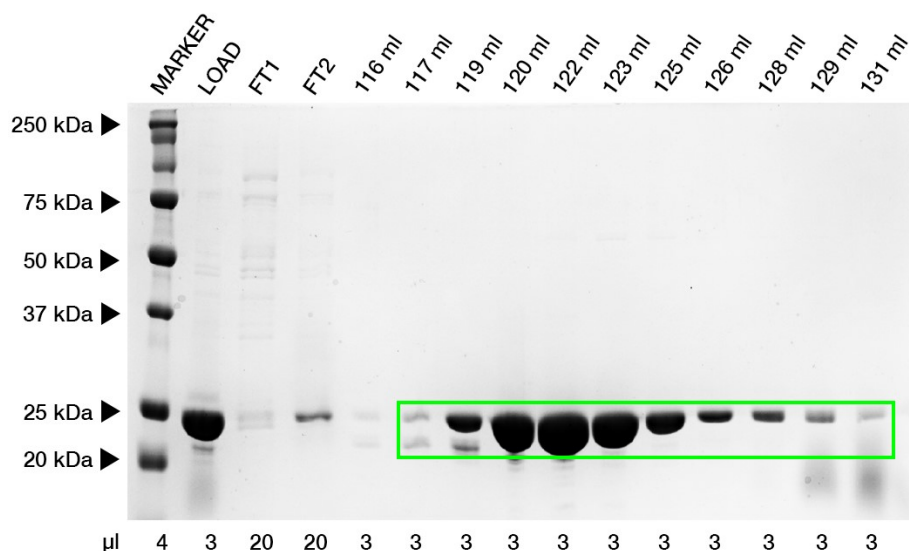


**Figure 81: SDS-PAGE Sec3-PH CEX**

17.5% SDS-PAGE of Sec3-PH cation-exchange chromatography fractions. Protein size: 22.06 kDa; Elution between 117-131 ml (green box). Fractions 119-126.5 ml were pooled.

#### 4.11. Sec3-PH – ITC

To see how both NPY motifs of Sso2 interact with the N-terminal PH domain of Sec3 isothermal titration calorimetry was carried out. Sample Sec3-PH of the previous cation-exchange chromatography and the corresponding peptides were prepared for ITC according to section 3.3.14.

Peptide Sso2-N15 (aa1-15), with both wildtype NPY motifs, bound Sec3-PH with a dissociation constant ( $K_d$ ) of 21.1  $\mu$ M, while mutation of the core residues of both NPY motifs to alanines, in peptide Sso2-N15-m1m2 (aa1-15), abolished binding of the peptide to Sec3-PH completely (Figure 82).

When measuring each NPY motif individually the dissociation constants dropped 3-4-fold, resulting in a  $K_d$  of 82.3  $\mu$ M in peptide Sso2-N9 (aa1-8) and a  $K_d$  of 63.3  $\mu$ M in peptide Sso2-1015 (aa10-15) (Figure 83).

Mutating the core residues of the first NPY motif to alanines, while retaining the second NPY motif, slightly reduces the binding affinity of peptide Sso2-N15-m1 (aa1-15) with a  $K_d$  of 34.9  $\mu$ M. In contrast, when only the second NPY motif is mutated, binding affinity was severely reduced resulting in a  $K_d$  of 188  $\mu$ M (Figure 84).

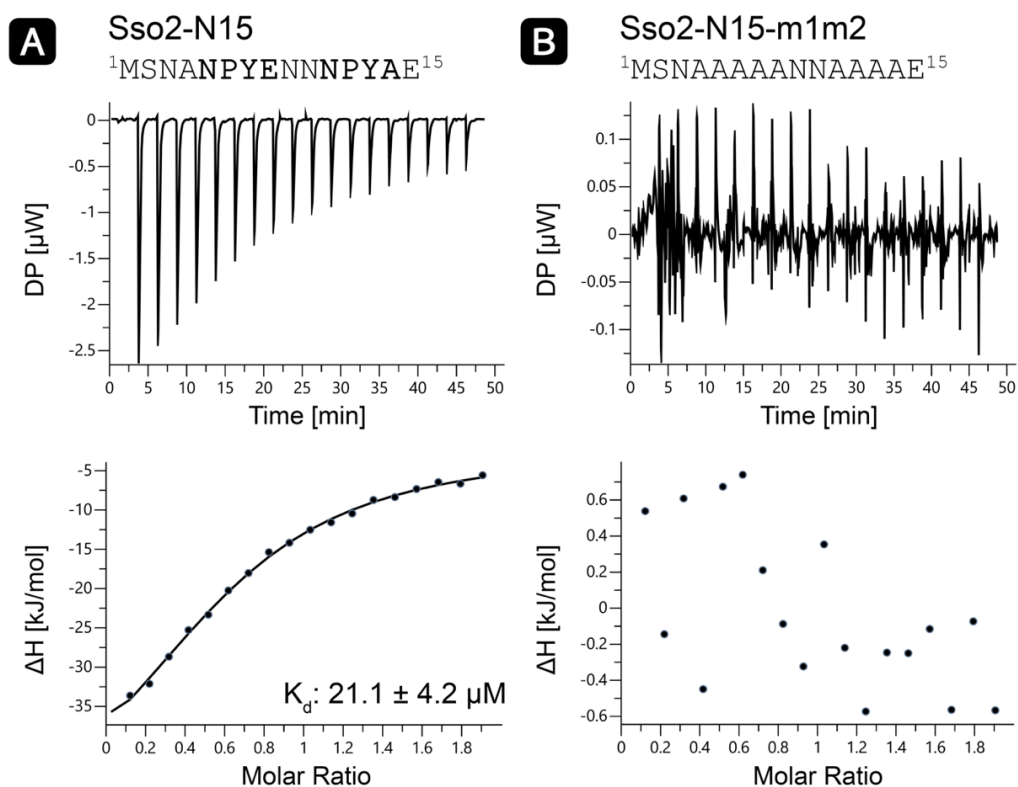


**Figure 82: Sec3-PH Sso2-N15/N15-m1m2 – ITC**

**A:** Sec3-PH (59  $\mu M$ , cell) with Sso2-N15 (590  $\mu M$ , titrant).

**B:** Sec3-PH (59  $\mu M$ , cell) with Sso2-N15-m1m2 (590  $\mu M$ , titrant).

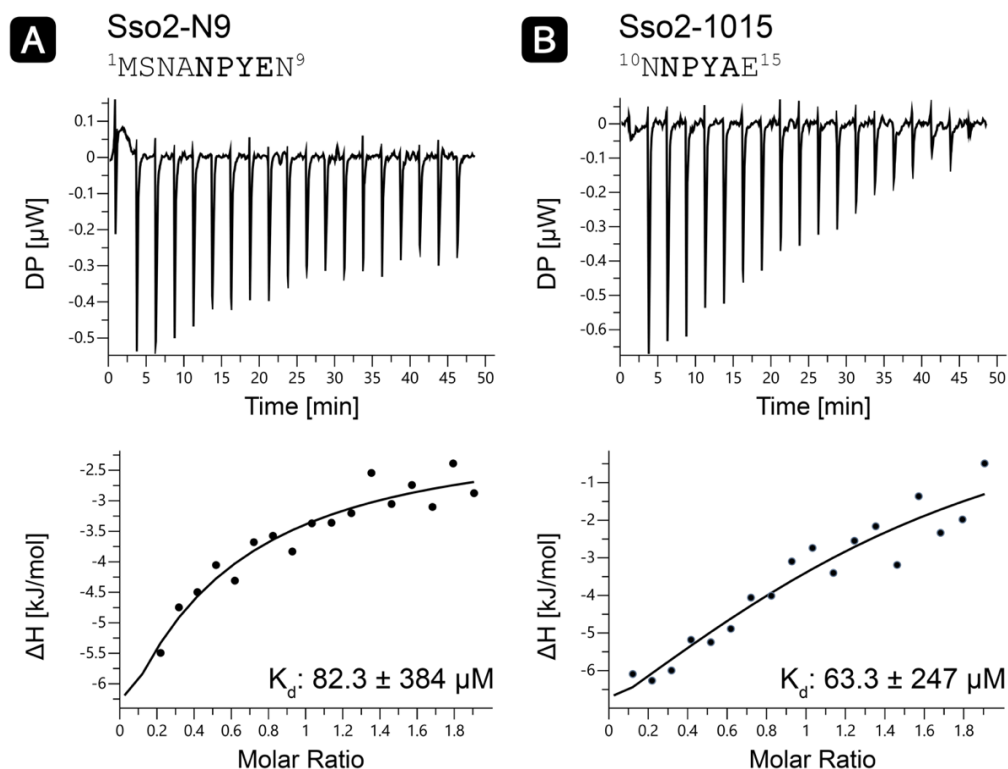


**Figure 83: Sec3-PH Sso2-N9/1015 – ITC**

**A:** Sec3-PH (59  $\mu M$ , cell) with Sso2-N9 (590  $\mu M$ , titrant).

**B:** Sec3-PH (59  $\mu M$ , cell) with Sso2-1015 (590  $\mu M$ , titrant).

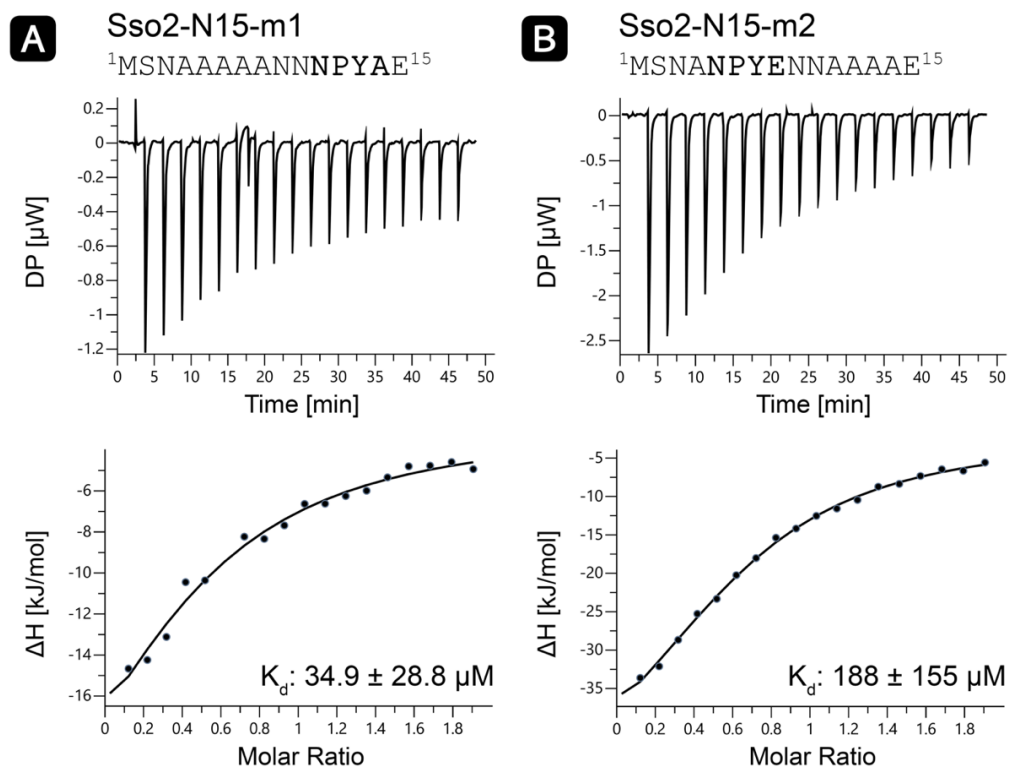


**Figure 84: Sec3-PH Sso2-N15-m1/N15-m2 – ITC**  
**A:** Sec3-PH (59  $\mu\text{M}$ , cell) with Sso2-N15-m1 (590  $\mu\text{M}$ , titrant).  
**B:** Sec3-PH (59  $\mu\text{M}$ , cell) with Sso2-N15-m2 (590  $\mu\text{M}$ , titrant).



## 4.12. SSO1Δ Sso2<sup>mut</sup> – In Vivo Results

### 4.12.1. SSO1Δ Sso2<sup>mut</sup> – Growth Test

The growth test of SSO1Δ Sso2 mutant yeast strains revealed that the complete mutation of both Sso2 NPY motifs (M7) results in growth reduction at 25 °, 34 °C and severely reduced growth at 37 °C (Figure 85, A). Mutation of all four residues of the first NPY motive (M5) resulted in reduced growth at 37 °C (Figure 85, A,B), while mutation of all four residues of the second NPY motif (M6) had no observable effect on growth at any temperature (Figure 85, A). Mutation of single, double or triple mutations (M1, M2, M3, M4) of the first NPY-motif did not affect growth as well (Figure 85, B).

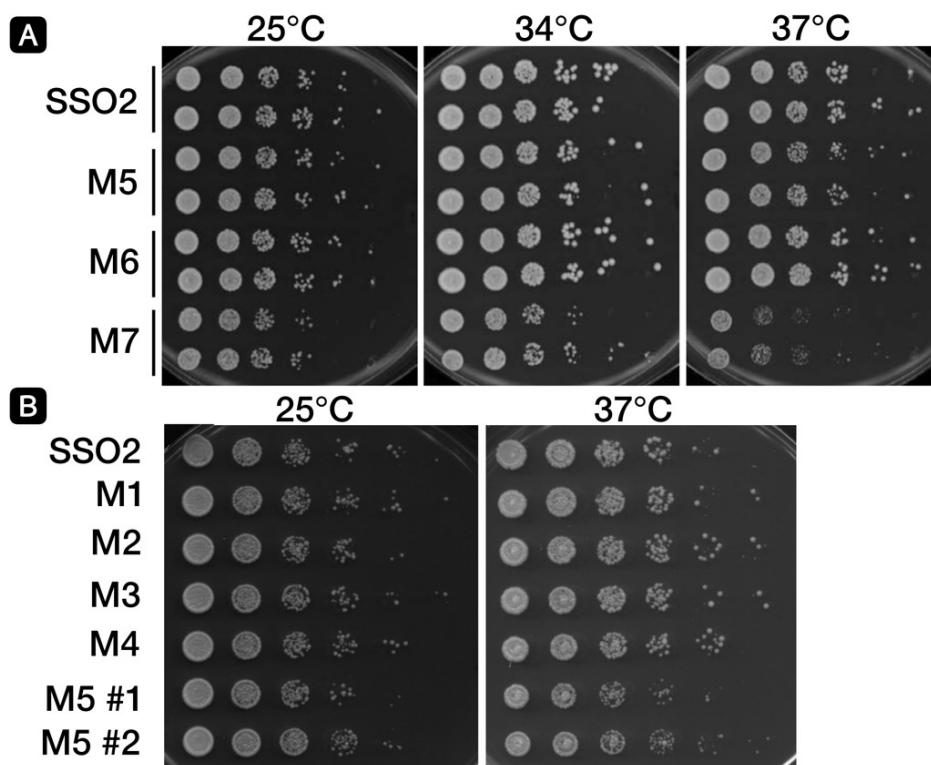


**Figure 85: SSO1Δ Sso2<sup>mut</sup> – Growth Test**

Control and mutant SSO1Δ Sso2 cells were grown overnight in YPD medium, an aliquot was drawn from each sample at OD<sub>600</sub> 0.2, serially diluted 5-fold and subsequently spotted onto YPD plates. Plates were incubated at the respective temperatures for 2 days. All data and figures were adapted from Peer et al., 2022. **A:** Mutant SSO1Δ Sso2M5 visibly affected in growth at 37 °C; mutant SSO1Δ Sso2M7 exhibits severe reduction in growth at 37°C. **B:** Mutant SSO1Δ Sso2M5 affected in growth at 37 °C.

#### 4.12.2. SSO1Δ Sso2<sup>mut</sup> – Bgl2 Secretion Assay

The Bgl2 secretion assay of SSO1Δ Sso2 mutant yeast strains revealed a significantly increased internal pool of Bgl2 in mutants with both NPY-motifs' residues being replaced for alanines (M7) (Figure 86, A, C). Mutation of single, double, triple residues and complete mutation of the first NPY-motif (M1, M2, M3, M4, M5; Figure 86, B, D) and the complete mutation of the second NPY-motif (M6; Figure 86, A, B) resulted in only modest accumulation of an internal pool, largely paralleling growth results.

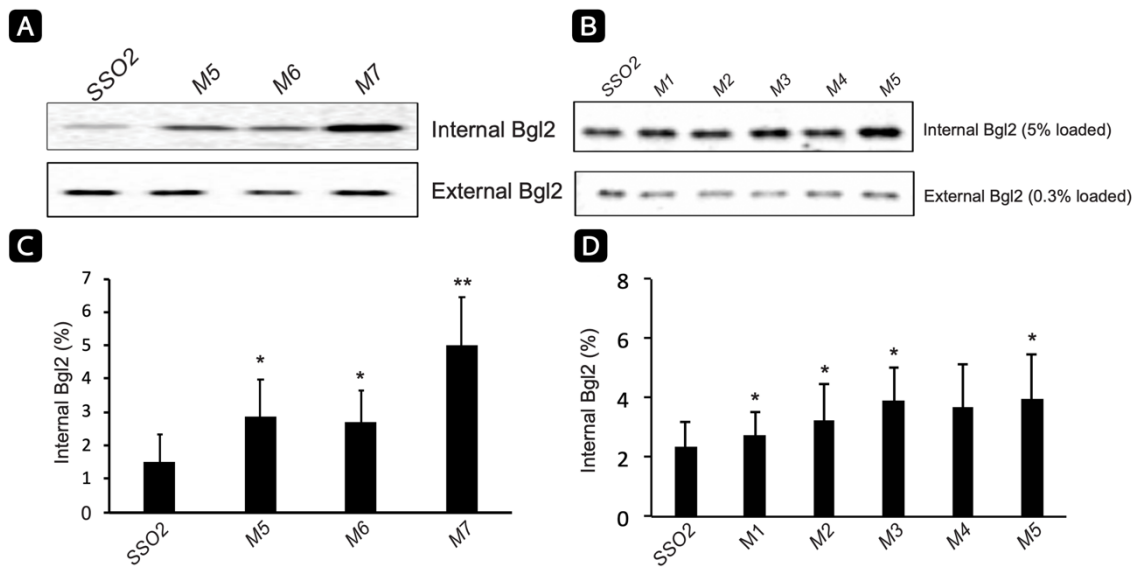


**Figure 86: SSO1Δ Sso2<sup>mut</sup> – Bgl2 Secretion Assay**

Control and mutant SSO1Δ Sso2 cells were grown overnight at 25 °C in YPD medium, until early log phase was reached and subsequently shifted to 37 °C for 90 min. The internal and external fractions were prepared as described in the corresponding paper. All data and figures were adapted from Peer et al., 2022. **A/B:** SSO1Δ Sso2 mutations cause inhibition of Bgl2 secretion as detected by western blot analysis. **C:** SSO1Δ Sso2 mutations cause accumulation of internal Bgl2 as detected by western blot analysis. Internal Bgl2 was quantified using ImageJ. Data is based on six independent experiments. Error bars represent SD, n = 7. \*p < 0.005, \*\*p < 2e5. **D:** SSO1Δ Sso2 mutations cause accumulation of internal Bgl2 as detected by western blot analysis. Internal Bgl2 was quantified using ImageJ. Data is based on four independent experiments. Error bars represent SD, n = 5. \*p < 0.05.

#### 4.12.3. SSO1Δ Sso2<sup>mut</sup> – Invertase Secretion

The Invertase secretion assay of SSO1Δ Sso2 mutant yeast strains revealed a substantial defect in secretion of invertase in mutants with both NPY-motifs' residues being replaced for alanines (M7; Figure 87, A). The complete mutation of the first NPY-motif (M5) only resulted in a minor defect in secretion (Figure 87, A, B), while mutation of single, double and triple residues of the first NPY motif (M1, M2, M3, M4; Figure 87, B, D) and the complete mutation of the second NPY-motif (M6; Figure 87, A, B) resulted in only modest accumulation of an internal pool, largely paralleling growth results.

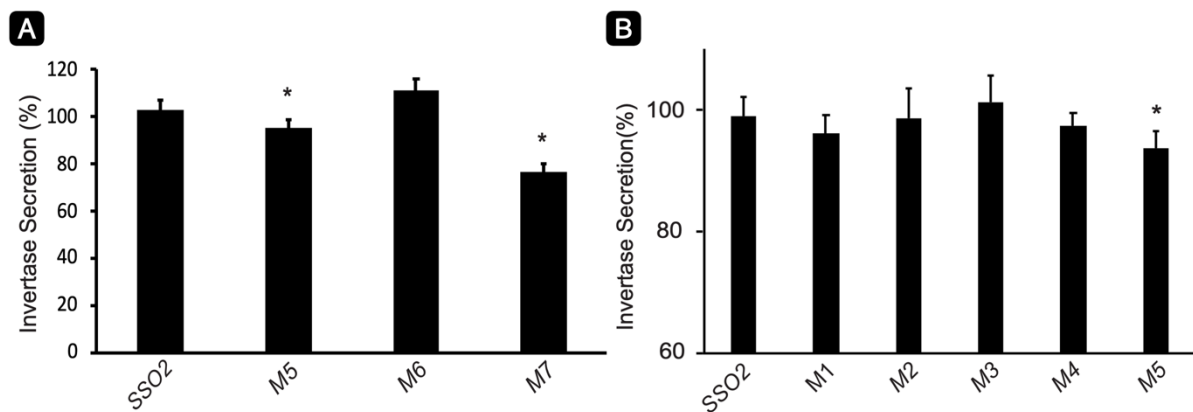


**Figure 87: SSO1Δ Sso2<sup>mut</sup> – Invertase Secretion Assay**

Control and mutant SSO1Δ Sso2 cells were grown overnight at 25 °C in YP medium containing 5% (w/v) glucose, until early log phase was reached, and subsequently shifted to YP medium containing 0.1% (w/v) glucose and incubated at 37 °C for 45 min. Invertase accumulation was calculated according to formula  $(Ext_{45m} - Ext_{0m}) / [(Ext_{45m} - Ext_{0m}) + (Int_{45m} - Int_{0m})]$ . The internal and external fractions were prepared as described in the corresponding paper. All data and figures were adapted from Peer et al., 2022. **A:** SSO1Δ Sso2 mutations M5 and M7 show a defect in secretion of invertase. Data is based on four independent experiments. Error bars represent SD,  $n = 4$ . \* $p < 0.005$ . **B:** Data is based on three independent experiments. Error bars represent SD,  $n = 3$ . \* $p < 0.05$ .

#### 4.12.4. SSO1Δ Sso2<sup>mut</sup> – Accumulation of Secretory Vesicles

Thin section electron microscopy of SSO1Δ Sso2 mutant yeast strains revealed polarized accumulation of vesicles in budding yeast. Complete mutation of either the first NPY-motif (M5, Figure 88, B) or both NPY-motifs (M7; Figure 88, D) resulted in accumulation of vesicles (Figure 88, E) preferably within the buds of small budding cells. In contrast, control cells (Sso2, Figure 88, A) and cells with only the second NPY-motif being mutated (M6, Figure 88, C) only contained a low number of vesicles per cell (Figure 88, E). The overall size of the vesicles was similar among all tested strains (Figure 88, F).

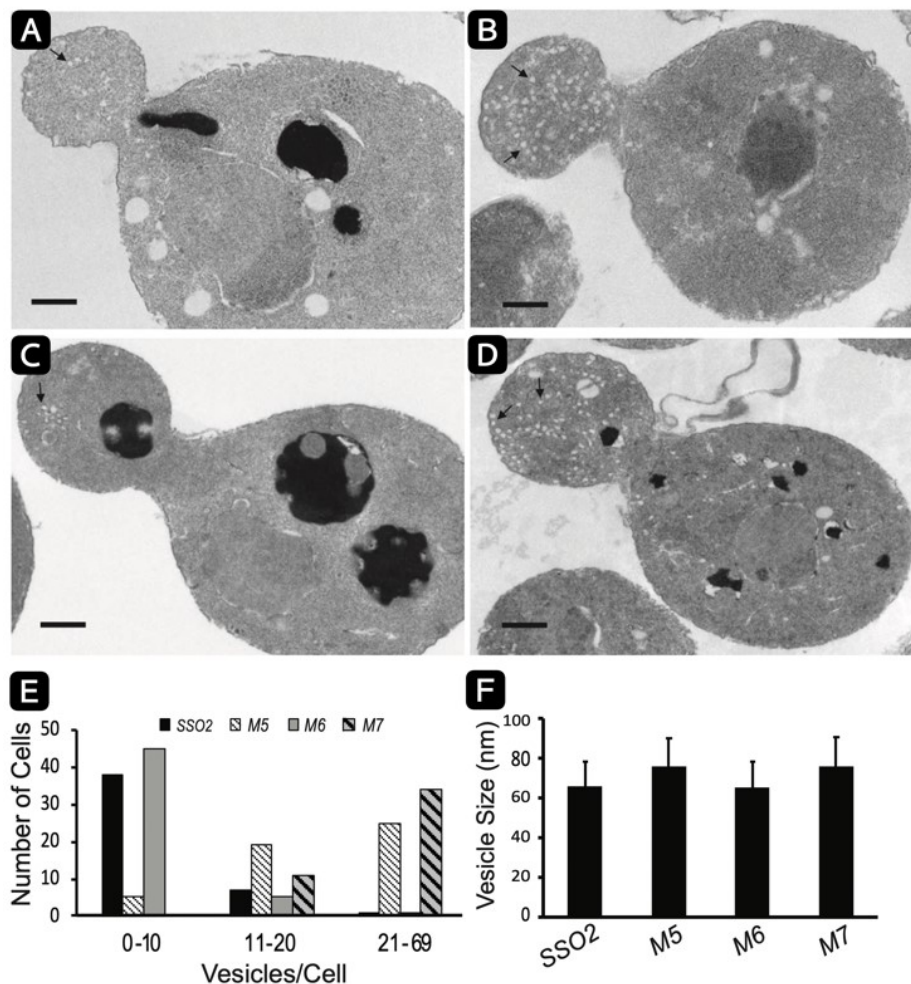


**Figure 88: SSO1Δ Sso2<sup>mut</sup> – Accumulation of Secretory Vesicles**

Control and mutant SSO1Δ Sso2 cells were grown overnight at 25 °C in YPD medium, until an OD<sub>600</sub> of ~0.5 was reached for EM analysis. All data and figures were adapted from Peer et al., 2022.

**A:** SSO1Δ Sso2. **B:** SSO1Δ Sso2M5. **C:** SSO1Δ Sso2M6. **D:** SSO1Δ Sso2M7. **A-D:** Scale bar: 0.5 μm; SSO1Δ Sso2 M5 and M7 cells display an elevated number of secretory vesicles (indicated by arrows) in the bud compared to control and M6 mutation cells. **E:** Quantification of secretory vesicles. Sample sizes: 46 SSO1Δ Sso2 cells, 49 SSO1Δ Sso2M5 cells, 51 SSO1Δ Sso2M6 cells, 45 SSO1Δ Sso2M7 cells. **F:** Average vesicle size as determined using ImageJ. Sample sizes ranged from 23-91 vesicles.

#### 4.12.5. SSO1Δ Sso2<sup>mut</sup> – Snc1 Recycling

Snc1 recycling in SSO1Δ Sso2 mutant yeast strains with all residues of the first NPY-motif of Sso2 (M5; Figure 89, B, E) and strains with all residues of the first and second NPY-motif of Sso2 (M7; Figure 89, D, E) being mutated to alanines displayed severely impaired Snc1 recycling, leading to the formation of internal Snc1 patches caused by greatly reduced relocation of Snc1 to the plasma membrane. SSO1Δ Sso2 control cells (Sso2, Figure 89, A, E) and M6 mutants with only the second NPY-motif of Sso2 being mutated (M6, Figure 89, C, E) did not display signs of impaired Snc1 recycling, with Snc1 being mostly located to the plasma membrane and only small numbers of internal patch like structures present.

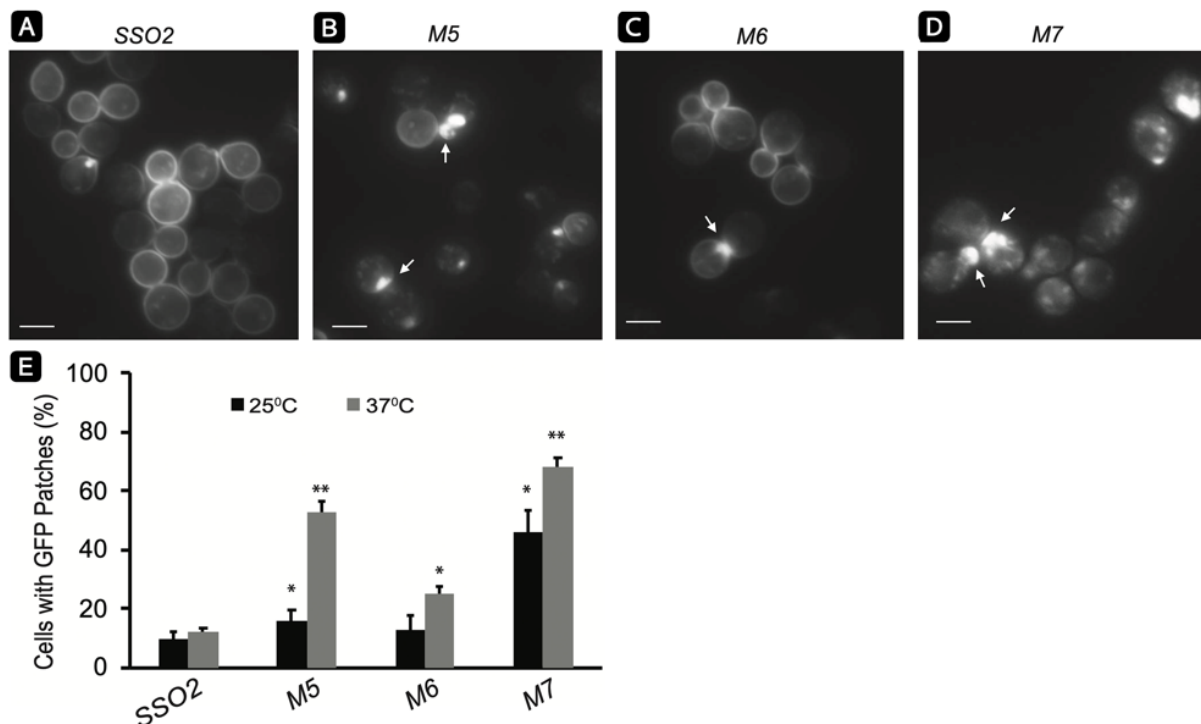


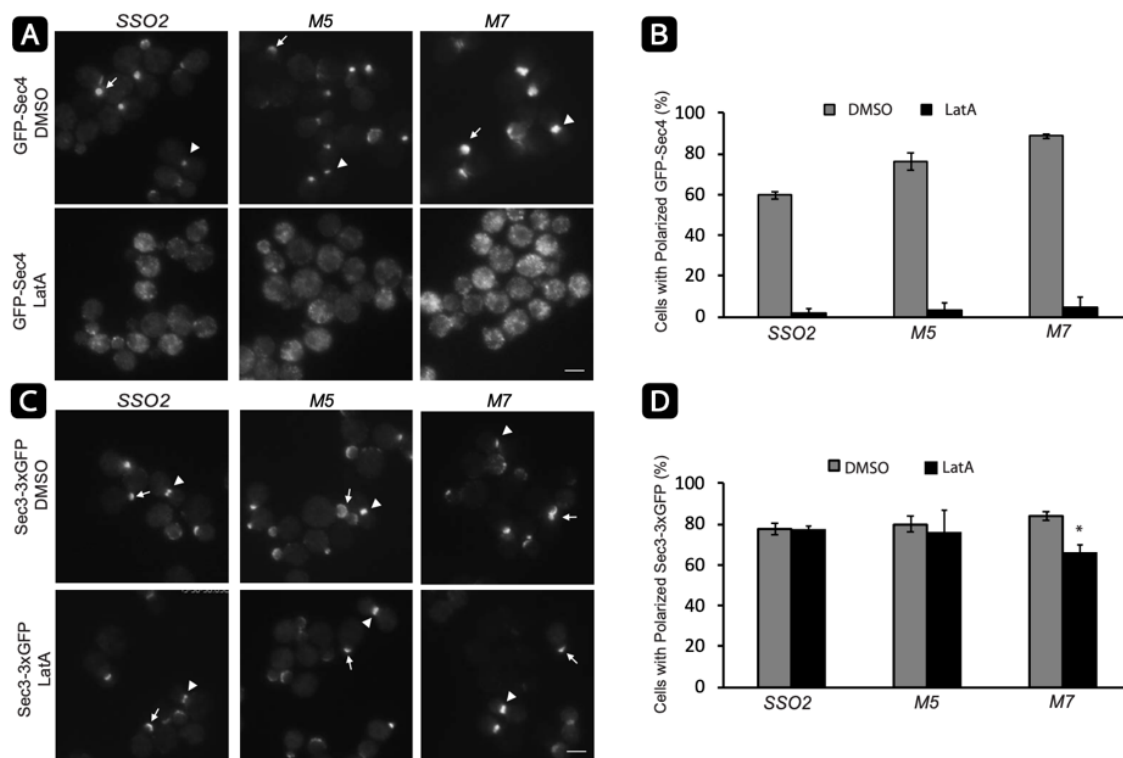
**Figure 89: SSO1Δ Sso2<sup>mut</sup> – Snc1 Recycling**

SSO1Δ Sso2 control and mutant strains expressing GFP-Snc1 were grown overnight at 25 °C in SC-Ura medium to an OD<sub>600</sub> of ~0.5, subsequently diluted and shifted to 37 °C for 90 min prior to imaging. All data and figures were adapted from Peer et al., 2022. **A-D:** Representative images of GFP-Snc1 SSO1Δ Sso2 control and mutant M5, M6 and M7 cells. Scale bar: 5 μm. GFP-Snc1 mainly localized to the plasma membrane in GFP-Snc1 SSO1Δ Sso2 control and mutant M6 cells. GFP-Snc1 SSO1Δ Sso2 M5 and M7 mutant cells displayed GFP patches (indicated by arrows) in vicinity of small buds or bud necks. **E:** Quantification of cells with GFP patches. GFP-Snc1 patches near bud tips or necks were scored. Error bar represents SD, n = 3. \*P < 0.05, \*\*P < 0.005.

#### 4.12.6. SSO1Δ Sso2<sup>mut</sup> – Sec3 Actin Independent Localization

The observation, that the polarized localization of vesicle marker Sec4 is impaired by disruption of actin filament polymerization by LatA, as described by Salminen & Novack, 1989, could be verified (Figure 90, A, B). It could also be shown that the polarization of Sec3 was unaffected by the disruption of actin polymerization via LatA treatment, as previously described by Finger *et al.*, 1998 (Figure 90, C, D). Localization of Sec3 is therefore actin independent, leaving Sec3 associated with sites of cell surface growth, regardless of actin filament status.

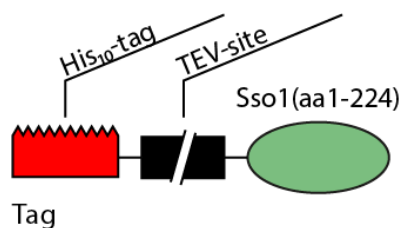
SSO1Δ Sso2 mutant yeast strains with all residues of the first NPY-motif of Sso2 (M5; Figure 90, C, D) and of the first and second NPY-motif (M7; Figure 90, C, D) being mutated to alanines, were not showing significant changes in Sec3 deployment, with mutation M7 only exhibiting a very slight reduction in polarization of Sec3 after LatA treatment (Figure 90, D). This demonstrates that recruitment of Sec3 to sites of polarized growth is largely independent of Sso2s NPY-motifs.



**Figure 90: SSO1Δ Sso2<sup>mut</sup> – Sec3 Actin Independent Localization**

GFP-Sec4 as well as Sec3-3xGFP expressing SSO1Δ Sso2 control and mutant strains were grown at 25 °C in YPD medium until reaching early log phase, subsequently 1 OD<sub>600</sub> unit of cells were collected and resuspended in 50 µl SC medium to be incubated at 25 °C for 15 min with either 200 µl DMSO or LatA, prior to fluorescence microscopy image acquisition. All data and figures were adapted from Peer et al., 2022. **A:** Scale bar: 5 µm. DMSO treatment: GFP-Sec4 is localized to the tip of small buds (arrow) and the neck of large buds (arrowhead), resembling the conventional distribution. LatA treatment: GFP-Sec4 polarization disrupted. **B:** Quantification of cells with polarized GFP-Sec4. Error bars represent SD based on three independent experiments respectively. **C:** Scale bar: 5 µm. Sec3-3xGFP polarization remains undisrupted after LatA treatment. Sec3-3xGFP remains localized to the tip of small buds (arrow) and the neck of large buds (arrowhead). **D:** Quantification of cells with polarized Sec3-3xGFP. Error bars represent SD based on three independent experiments respectively. Sso2M7 mutant cells display slightly reduced polarization after LatA treatment.

## 4.13. Sso1(aa1-224) – Purification and Results



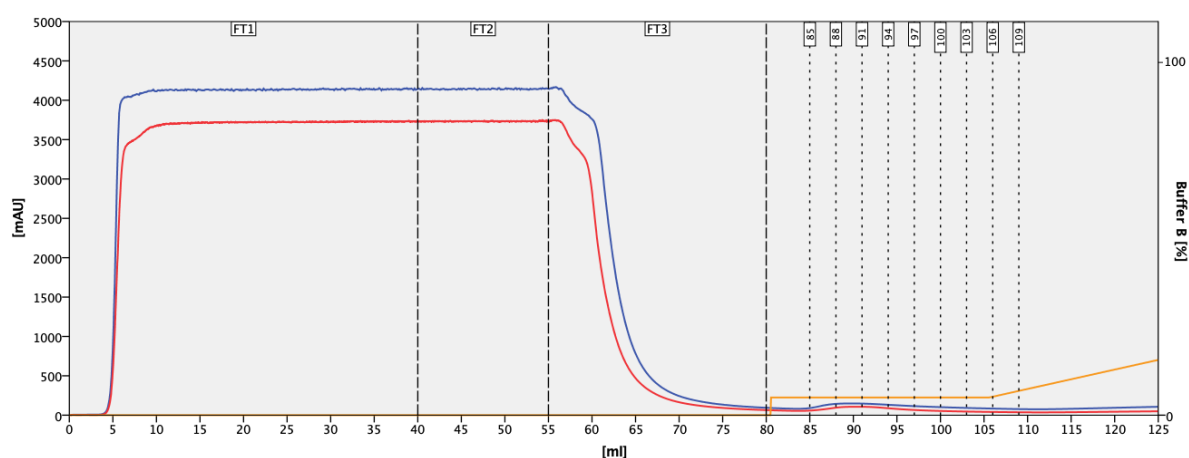
**Figure 91: Construct Sso1(aa1-224) – Illustration**

Illustration of Sso1(aa1-224) construct features relevant for purification.

Depicted is the N-terminal conjugated HT15b tag and the proteins N-terminus (aa1-224).

### 4.13.1. Sso1(aa1-224) – HisTrap

Initial purification of the His<sub>10</sub>-tagged protein was performed via HisTrap affinity chromatography (Figure 92) as described in section 3.3.4. The flow-through and fractions spanning the resulting peak were analyzed via SDS-PAGE (Figure 93). The protein eluted in fractions 83.5-104.5 ml, which were pooled for His<sub>10</sub>-tag removal.



**Figure 92: Elution Profile Sso1(aa1-224) HisTrap**

Elution profile of HisTrap affinity chromatography of Sso1 (aa1-224, 28.7 kDa) uncut. Elution between 85-106 ml (5% Buffer B); Red line: A<sub>280</sub>; Blue line: A<sub>254</sub>; Orange line: Buffer B; FT1/2: Sample loading; FT3: Column wash.



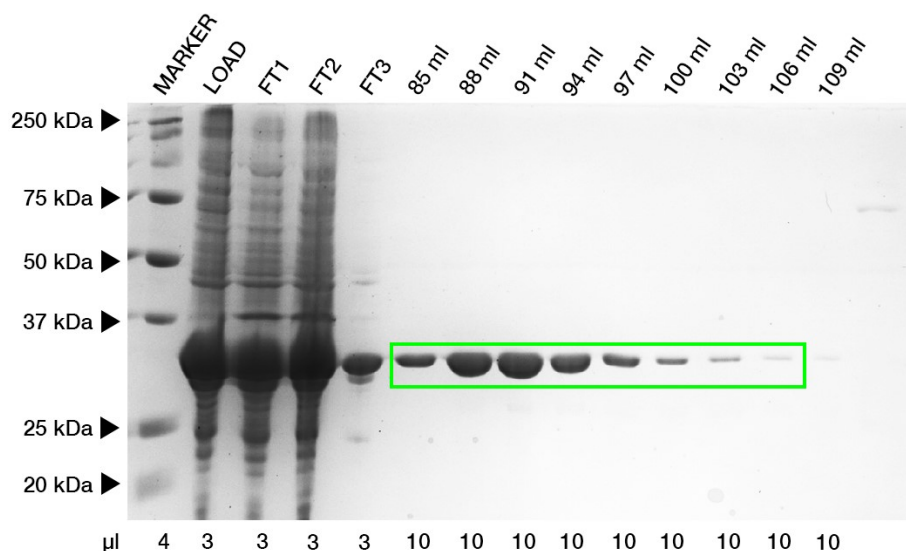


**Figure 93: SDS-PAGE Sso1(aa1-224) HisTrap**  
17.5% SDS-PAGE of Sso1(aa1-224) HisTrap affinity purification fractions. Protein size: 28.7 kDa; Elution between 83.5-104.5 ml (green box). Fractions 83.5-104.5 were pooled.

#### 4.13.2. Sso1(aa1-224) – Tag-Removal

As Sso1(aa1-224) was expressed using the HT15b vector it is conjugated to a His<sub>10</sub>-tag as described in section 3.2.2.1. To cut of the tag utilizing the TEV cutting site of the HM15b vector the sample was processed as described in section 3.3.7. The tag was successfully cleaved as depicted in Figure 94.

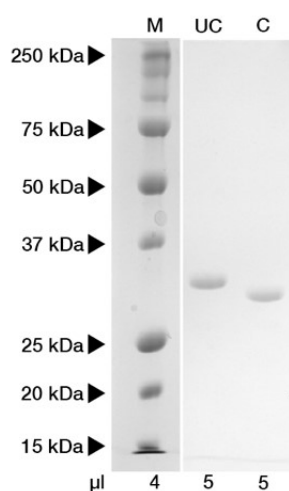


**Figure 94: Sso1(aa1-224) Uncut/Cut**  
17.5% SDS-PAGE of Sso1(aa1-224) HisTrap affinity purification fractions 83.5-104.5 ml before (UC) and after (C) TEV treatment. UC: uncut protein (28.7 kDa); C: cut protein and tag (Protein: 26.1 kDa; Tag: 2.6 kDa).

#### 4.13.3. Sso1(aa1-224) – AEX

After cleavage of the tag the sample was further purified via anion-exchange chromatography (Figure 95), as described in section 3.3.8. The protein eluted in fractions 139-148 ml, as verified by SDS-PAGE (Figure 96). Fractions 139-148 ml (9 ml) were pooled, and the concentration was determined to be 0.277 mg/ml (MW 22,058 Da,  $\epsilon$  10430 M<sup>-1</sup>cm<sup>-1</sup>) via microvolume measurement.

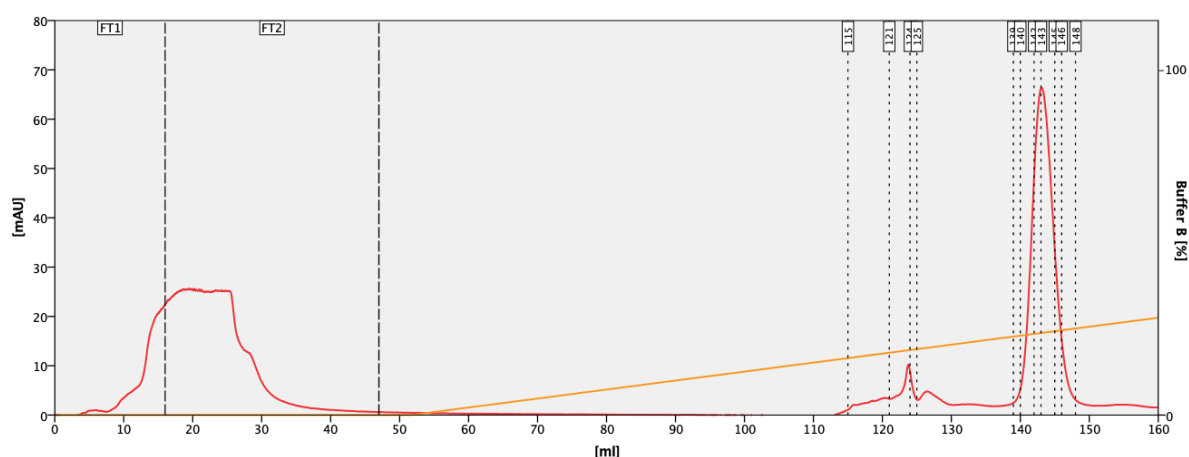


**Figure 95: Elution Profile Sso1(aa1-224) AEX**

Elution profile of anion-exchange chromatography of Sso1(aa1-224, 26.01 kDa, pI 4.91) cut. Peak: 143 ml, 240 mM NaCl (24% Buffer B); Red line: A<sub>280</sub>; Blue line: A<sub>254</sub>; Orange line: Buffer B; FT1: Sample loading; FT2: Column wash.

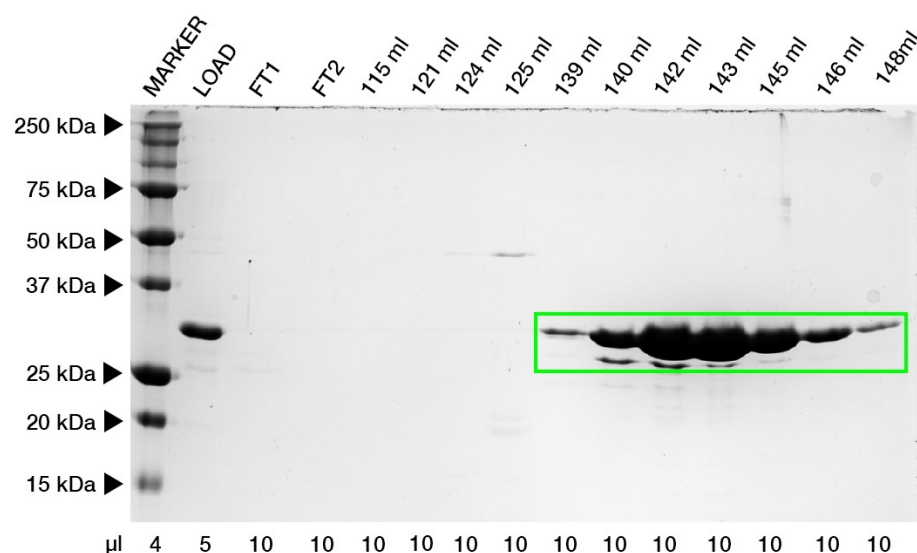


**Figure 96: SDS-PAGE Sso1(aa1-224) AEX**

17.5% SDS-PAGE of Sso1(aa1-224) anion-exchange chromatography fractions. Protein size: 26.1 kDa; Elution between 139-148 ml (green box). Fractions 139-148 ml were pooled.

## **4.14. Sec3-PH/Sso1(aa1-224) – Complex**

### **4.14.1. Sec3-PH/Sso1(aa1-224) Complex – SEC**

For complex formation 750 µl of Sec3-PH with a concentration of 2.14 mg/ml were combined with 6 ml of Sso1(aa1-224) with a concentration of 0.277 mg/ml. While sample Sec3-PH already had its buffer exchanged to standard SEC buffer in preparation of isothermal titration calorimetry, sample Sso1(aa1-224) was containing higher amounts of NaCl (~240 mM), as it eluted at approximately 24% of Buffer B during anion-exchange chromatography. To lower the total amount of NaCl in the combined samples two washing-steps were performed. During each washing-step 30 ml of a Buffer containing 1 mM DTT, 10 mM HEPES, pH 7.5 were added to the sample followed by concentration of the sample down to 1 ml using Merck Amicon™ Ultra-15 Centrifugal filter units with a MWCO of 10 kDa. After buffer exchange the sample was loaded onto a Cytiva Life Sciences™ HiLoad Superdex 200pg 16/600 preparative SEC column (Figure 97). Elution resulted in two overlapping peaks (85.71 ml, 96.64 ml) with the first peak (85.71 ml) being comprised of Sso1(aa1-224) and Sec3-PH and the second peak (96.64 ml) of solely Sec3-PH, as verified by SDS-PAGE (Figure 98). Between the bands of Sso1(aa1-224) and Sec3-PH of the first peak a third protein species can be observed, which can probably be explained by partially degraded Sso1(aa1-224). Fractions 82-91 ml of the first peak were pooled. The pooled fractions were set up for crystallization as described in section 3.4.2.1.

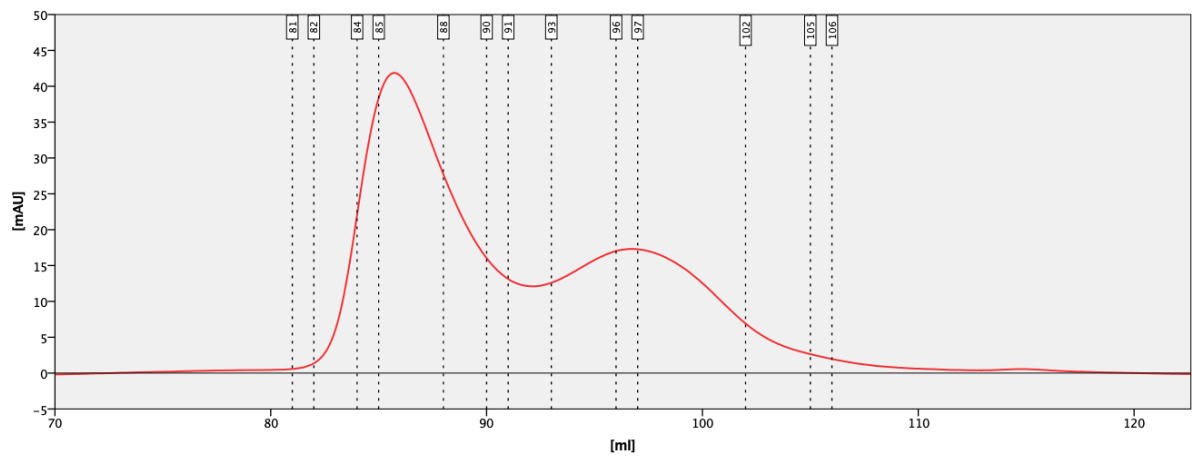


**Figure 97: Elution Profile Sec3-PH/Sso1(aa1-224) Complex SEC**  
 Elution profile of size-exclusion chromatography of Sec3-PH (aa75-260, 22.1 kDa) Sso1 (aa1-224, 26.01 kDa) Complex (48.11 kDa). Peak 1: 85.71 ml, Peak 2: 96.64 ml; Red line:  $A_{280}$ .

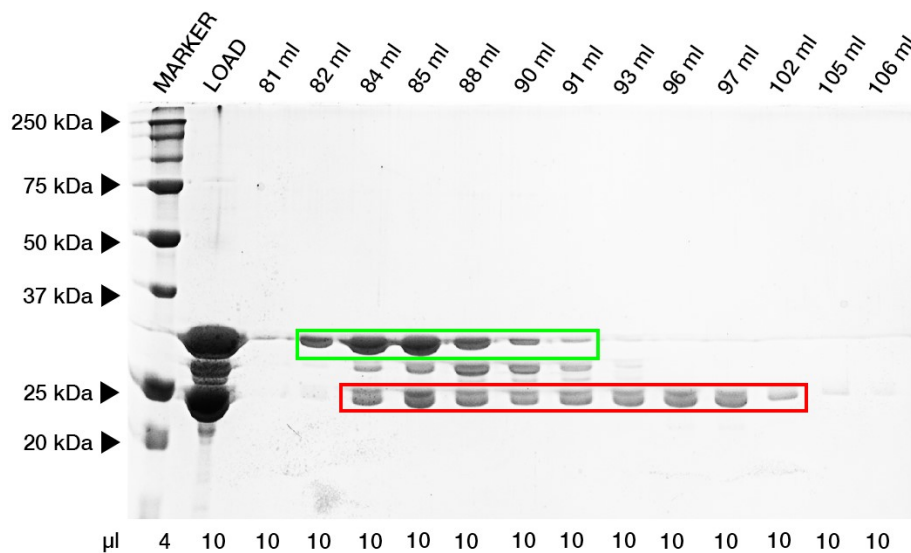
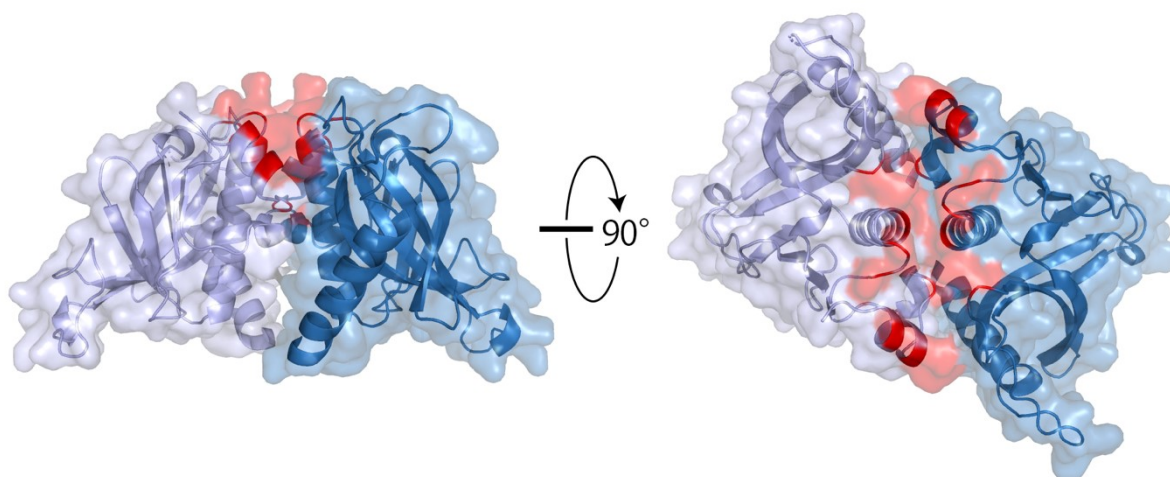


**Figure 98: SDS-PAGE Sec3-PH/Sso1(aa1-224) Complex SEC**  
 17.5% SDS-PAGE of Sec3-PH (aa75-260, 22.1 kDa; red box) Sso1 (aa1-224, 26.01 kDa; green box) Complex. Fractions 82-91 ml were pooled.

#### 4.14.2. Sec3-PH/Sso1(aa1-224) Complex – Crystallization Results

Diffraction data, to a resolution of 1.4 Å, of the Sec3-PH/Sso1(aa1-224) complex crystal was collected as mentioned in section 3.4.2.3. The crystal belongs to the *P*1 space group. Data collection and refinement statistics are presented in Table 23. The model contains two copies of Sec3-PH (Molecule 1: spanning Sec3 aa75-249; Molecule 2: spanning Sec3 aa75-98 & aa102-249) (Figure 99). Sso1(aa1-224) did not co-crystallize, and therefore no structure could be obtained.

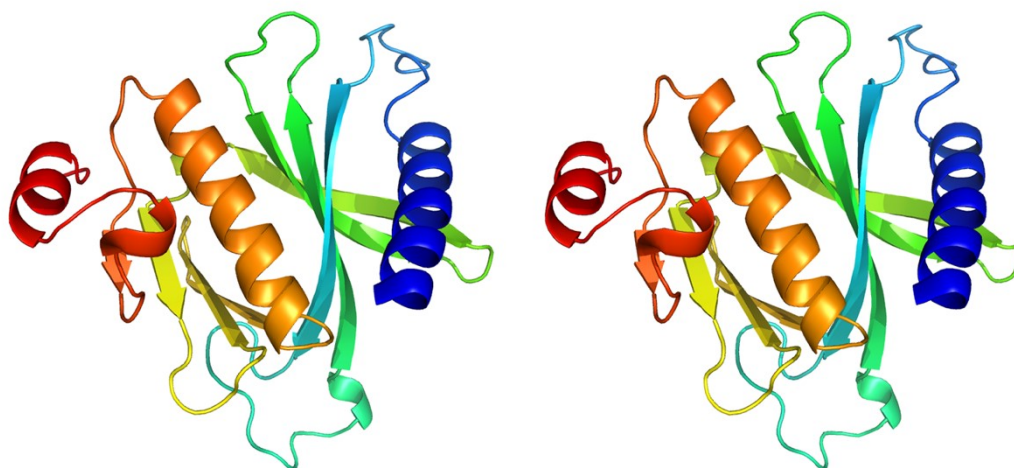
The combined crystal structure of both copies shows that the molecules border each other at the Sso1/2 binding site (Figure 99), partially covering the residues (K149, Q219, E222, H224, Y237, R241, R245) interacting with Sso2 (Yue *et al.*, 2015), possibly explaining, why Sso1 did not co-crystallize.



**Figure 99: Crystal Structure Sec3-PH**

Image shows crystal structure of both Sec3-PH copies found in the Sec3-PH/Sso1(aa1-224) complex crystal data. Molecule 1: light blue, spanning Sec3 aa75-249; Molecule 2: dark blue, spanning Sec3 aa75-98 & aa102-249. Sec3-PH residues (K149, Q219, E222, H224, Y237, R241, R245) interacting with Sso2 according to Yue *et al.* (2015) and the corresponding surface are tinted red.

The structure of a single copy (Figure 100) reveals an N-terminal pleckstrin homology domain, a central putative coiled-coil, and a C-terminal helical domain as previously described by Yue *et al.* (2015).



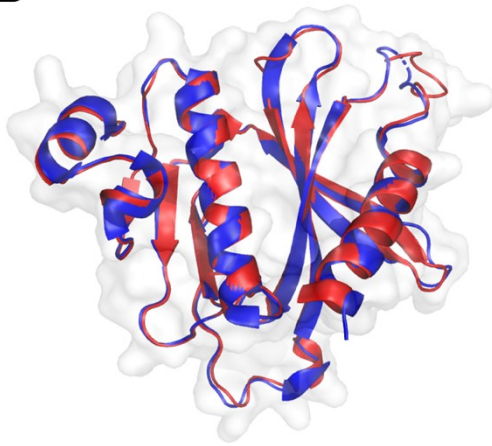
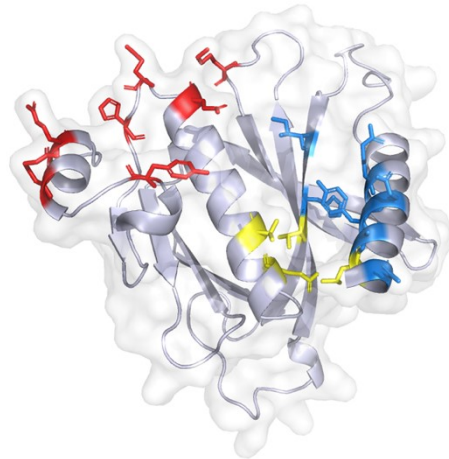
**Figure 100: Crystal Structure Sec3-PH – Autostereogram**

Image shows an autostereographic illustration of the crystal structure of Sec3-PH molecule 1 (spanning Sec3 aa75-249) contained in the Sec3-PH/Sso1(aa1-224) crystal data. The cartoon-based illustration is color-coded in a rainbow-fashion, ranging from blue (N-terminal) to red (C-terminal).

Comparing the resulting structure to a previous structure (Figure 101, A), derived from a successful co-crystallization with Sso2 (aa1-270) (PDB: 5M4Y; Yue *et al.*, 2015), reveals that the overall structures are nearly identical with an RMSD of 0.362 (1039/1039 out of 1407 atoms).

Highlighting the individual residues of Sec3-PH interacting with the H<sub>c</sub> of Sso2 (K149, Q219, E222, H224, Y237, R241, R245; Yue *et al.*, 2015) as depicted in Figure 101b, reveals that the interaction between the two proteins is concentrated to a cradle-like surface mainly formed by the central putative coiled-coil, and a C-terminal helical domain of Sec3-PH.

Highlighting Sec3-PH residues (Figure 101, B) putatively involved in Sso2 NPY-motif hydrogen-bond formation (Asn76, Ala79, Tyr82, Glu83, Arg86, Ile109, His111, based on unreleased structural data) and residues putatively involved in Sso2 NPY-motif hydrophobic interaction (Leu78, Glu205, Val208, Val112, based on unreleased structural data), reveals that the NPY-motifs interact with Sec3-PH via a hydrophobic pocket, formed mainly by the N-terminal helical domain of the pleckstrin homology domain and the central putative coiled-coil domain of Sec3-PH.

**A****B**

**Figure 101: Crystal Structure Sec3 – Comparison to Previous Structures**

**A:** Superimposition of Sec3 structural data (PDB: 5M4Y) obtained by Yue et al. (2015), spanning Sec3 aa75-249 (blue) and Sec3-PH molecule 1 (red), spanning Sec3 aa75-249, found in the Sec3-PH/Sso1(aa1-224) complex crystal data. **B:** Illustration of Sec3-PH molecule 1 (white), spanning Sec3 aa75-249, found in the Sec3-PH/Sso1(aa1-224) complex crystal data. Sec3-PH residues (K149, Q219, E222, H224, Y237, R241, R245) interacting with Sso2 according to Yue et al. (2015) tinted red. Sec3-PH residues putatively involved in Sso2 NPY-motif hydrogen-bond formation (Asn76, Ala79, Tyr82, Glu83, Arg86, Ile109, His111, based on unreleased structural data) tinted blue. Sec3-PH residues putatively involved in Sso2 NPY-motif hydrophobic interaction (Leu78, Glu205, Val208, Val112, based on unreleased structural data) tinted yellow.



## 5. Discussion

The initial aim of the study regarding *Trypanosoma brucei* flagellar pocket collar protein BILBO421 was to investigate if the BILBO421 NTD shares the ability of BILBO1 and FPC3/BILBO2 to interact with the C-terminal domain of FPC4. Via a native electrophoretic shift assay the interaction between the NTD of BILBO421 and synthetic FPC4-CTD peptides of variable length could be verified. The data suggest that the sole presence of the <sup>432</sup>VLTSVPV<sup>438</sup> motif, which was made out to be the main interacting motif of FPC4, as deduced from crystal data, is not sufficient for BILBO421 FPC4 interaction, as a peptide comprised of the <sup>432</sup>VLTSVPV<sup>438</sup> motif with a succeeding <sup>439</sup>DELLIK<sup>444</sup> motif was not sufficient for interaction establishment. Adding a preceding motif of five amino acids (<sup>427</sup>PQRRR<sup>431</sup>) to the <sup>432</sup>VLTSVPVDELLIK<sup>444</sup> sequence restored the interaction of BILBO421-NTD with the synthetic peptide.

The coiled-coil domain of BILBO421 was shown to form dimers, this was verified via SEC of a BILBO421-CCD construct. After all tags were entirely removed the elution volume of a size-exclusion chromatography matched the volume of a theoretical protein of double the molecular weight. The dimerization ability of the CCD was further confirmed via rsEM. rsEM imaging of multiple constructs (BILBO421-EFh-CCD-ct, BILBO421-CCD-ct, BILBO421-CCD) unveiled that BILBO421 forms antiparallel dimers, as previously observed in BILBO1. This was made visible by linking the constructs to a large globular MBP-tag. The images revealed two globular MBP-tags linked by a thin line. The length of this linker matched the theoretical length of the CCD (~15 nm). The length of the linker varied slightly in the observed samples, as the sample containing the BILBO421-EFh-CCD-ct construct, which was purified using buffer containing additional CaCl<sub>2</sub>, displayed a more elongated form compared to the samples containing constructs without the EFh-motif (BILBO421-CCD-ct, BILBO421-CCD). This might be explained by the ability of EFh-motifs to alter a proteins overall conformation in presence of Ca<sup>2+</sup>-ions.

This ability of the EFh-motifs to alter a proteins conformation was also verified by SEC data of a BILBO421-EFh-CCD construct. Previous to SEC the sample was split into two subsamples, to which additional CaCl<sub>2</sub> or EDTA was added respectively. Superimposing the elution profiles of both samples revealed a strong push towards oligomerization in the sample containing CaCl<sub>2</sub>. This matches the observation of



Vidilaseris *et al.* (2014c), who observed severe conformational changes based on the EFh-motifs in BILBO1, when exposed to  $\text{Ca}^{2+}$ -ions.

The main aim of the study, regarding *Saccharomyces cerevisiae* SNARE-associated proteins Sso1/2 and Sec3, was to further investigate a possible interaction of the newly identified highly conserved N-terminal NPY-motifs of Sso2 with Sec3.

By obtaining a crystal structure of the Sec3 pleckstrin homology domain in complex with a full length Sso2 protein only missing its C-terminal transmembrane region, we were able to show that both highly conserved N-terminal NPY-motifs act in a similar fashion to the N-peptides of other t-SNARE proteins such as Stx and Tlg2. These two NPY motives are connected to the helical core of Sso2 via a long flexible linker and were found to bind to a conserved hydrophobic pocket on Sec3 respectively.

By comparing the newly obtained structure with the structure of the Munc18/Stx complex (Figure 102), it becomes apparent that the much smaller interaction-site between the single globular PH-domain of Sec3 and the Sso2s four-helix bundle compared to the much larger interaction site between Munc18 and Stx, suggests a significantly weaker interaction between the two proteins. While the N-peptide of Stx binds Munc18 distally to the opposite to the interaction-site of Munc18, the double NPY-motif of Sso2 binds to the same site of Sec3 as the interaction between Sec3 and the helical bundles of Sso2.

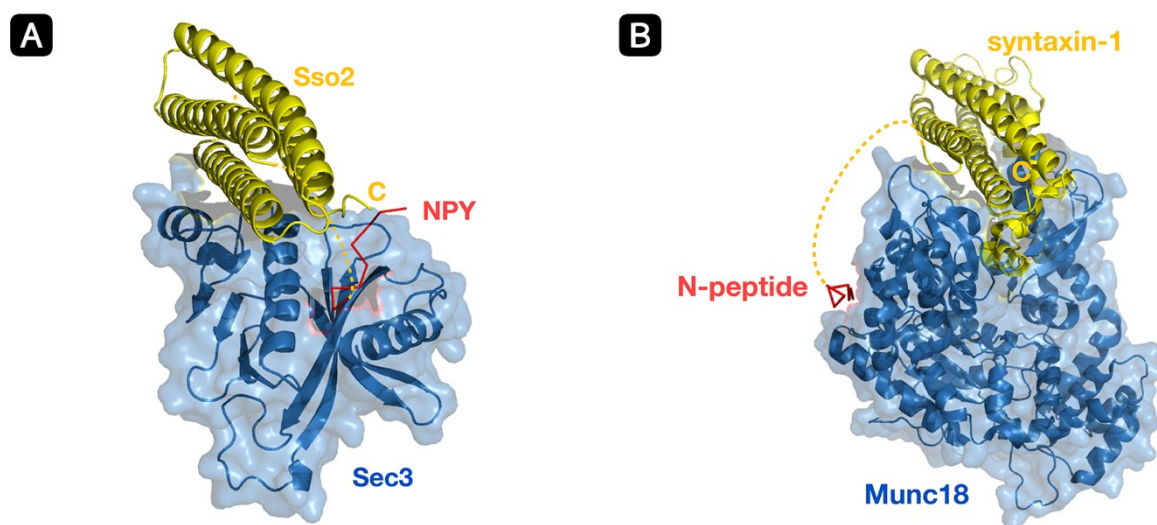


**Figure 102: Sec3/Sso2, Munc18/Stx Complex Comparison**

**A:** Structure of Sec3 PH domain in complex with Sso2(1-270). Region of Sso2 containing both NPY-motifs (aa1-14) colored red. **B:** Structure of Munc18 in complex with syntaxin-1 (PDB: 3C98). N-peptide of syntaxin-1 (aa2-9) colored red.

Additionally, the isothermal titration calorimetry essay has confirmed, that either of the NPY-motifs are able to bind Sec3. Compared to the wildtype N-terminal sequence of Sso2, with both NPY-motifs present, binding affinity dropped 3-4-fold when either of the NPY-motifs were measured individually. Mutation of either of the NPY-motifs to alanines has shown a similar effect. Mutating both NPY-motifs to alanines completely abolished the interaction. This data suggests that the NPY-motifs bind Sec3 synergistically.

Combining the data obtained from the crystal structure and the ITC assay strongly suggests that the additional binding of the NPY-motifs to a hydrophobic pocket on the same site of the Sec3 PH domain compensates for the comparatively small interaction interface between Sec3 and its t-SNARE partners. In addition, the long flexible linker-region between the helical core of Sso2 and its double NPY-motifs suggests a fishhook-like activity of the NPY-motifs, enhancing recruitment of the Sso2 t-SNARE protein to the vesicle targeting site, as depicted in Figure 103.

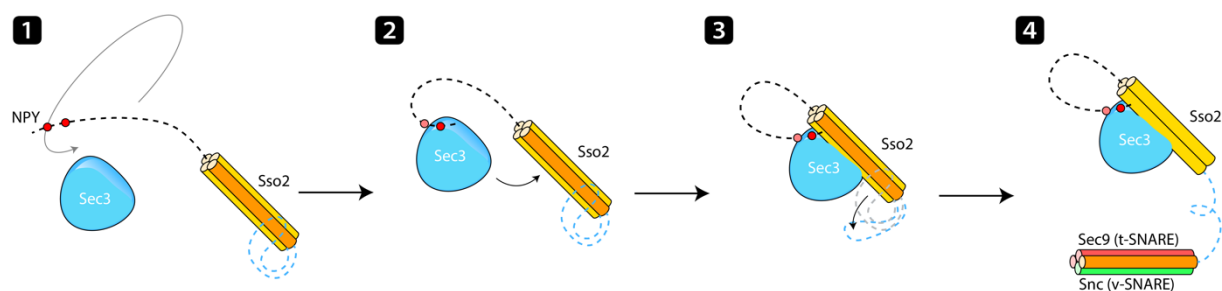


**Figure 103: Illustration of Sec3/Sso2 Interaction – NPY-motifs**

*Step-by-step illustration of the hypothetical fishhook-like recruitment of Sso2 to the site of exocytosis by Sec3 and subsequent SNARE complex assembly. 1: Fishhook-like activity of Sso2 N-terminal NPY-motifs for enhanced Sso2 recruitment to the vesicle targeting site. 2: Binding of NPY-motif to Sec3 and recruitment of Sso2 to the vesicle targeting site. 3: Sec3 PH domain promoting conformational change in the four-helix bundle of Sso2. 4: Release of H3 from the inhibitory domain and formation of an initial binary complex between H3 of Sso2 and the two helices of Sec9 with subsequent interaction of this new complex with v-SNARE Snc, initiating membrane fusion.*

The in vivo data obtained by the growth test, Bgl2 and invertase secretory efficiency assay and data on secretory vesicle accumulation in budding yeast, generally parallels the results obtained by isothermal titration calorimetry.

We were able to show that growth inhibition, disruption in Bgl2 and invertase secretion and the vesicle accumulation were mainly caused by simultaneous mutation of both of Sso2s NPY-motifs (M7). While mutation of the first NPY-motif (M5) did have an effect as well, it was significantly less pronounced. Mutation of the second NPY-motif (M6) did generally not show significant effects. This data supports the observation that both

NPY-motifs bind Sec3 synergistically, with the first NPY-motif playing a more important role in Sec3 binding.

We were also able to show that recruitment of Sec3 to sites of polarized growth is largely independent of the Sso2 NPY-motifs.

A novel structure of the Sec3-PH/Sso1(aa1-224) complex could not be obtained, as Sso1(aa1-224) did not co-crystallize with Sec3-PH and therefore only a structure covering Sec3 aa75-249 could be reproduced.

## 6. References

- Aalto, M. K., Ronne, H., & Keränen, S. (1993). Yeast syntaxins Sso1p and Sso2p belong to a family of related membrane proteins that function in vesicular transport. *EMBO J.* 1993; 12(11) 4095-104.
- Adams, P. D., Afonine, P. V., Bunkoczi, G., Chen, V. B., Davis, I. W., Echols, N., Headd, J. J., Hung, L. W., Kapral, G. J., Grosse-Kunstleve, R. W., *et al.* (2010). PHENIX: a comprehensive Python-based system for macromolecular structure solution. *Acta Crystallogr D Biol Crystallogr* 2010;66 213-221.
- Albisetti, A., Florimond, C., Landrein, N., Vidilaseris, K., Eggenspieler, M., Lesigang, J., Dong, G., Robinson, D. R., & Bonhivers, M. (2017). Interaction between the flagellar pocket collar and the hook complex via a novel microtubule-binding protein in *Trypanosoma brucei*. *PLoS Pathog* 2017;13(11) e1006710.
- Blum, J., Schmid, C., & Burri, C. (2005). Clinical aspects of 2541 patients with second stage human African trypanosomiasis. *Acta Tropica* 2006;97 55-64.
- Brun, R., Blum, J., Chappuis, F., & Burri, C. (2009). Human African trypanosomiasis. *Lancet* 2010;375 148-59.
- Burkhardt, P., Hattendorf, D. A., Weis, W. I., & Fasshauer, D. (2008). Munc18a controls SNARE assembly through its interaction with the syntaxin N-peptide. *EMBO J.* 2008;27(7) 923-933.
- Cytiva (2020). Size Exclusion Chromatography Principles and Methods Handbook. Available at: <https://cdn.cytivalifesciences.com/dmm3bwsv3/AssetStream.aspx?mediaformatid=10061&destinationid=10016&assetid=11639> (Accessed: January 10<sup>th</sup>, 2022).
- Eisemann, J. T., Allen, F., Lau, K., Shimamura, G. R., Jeffrey, P. D., & Hughson, F. M. (2020). The Sec1/Munc18 protein Vps45 holds the Qa-SNARE Tlg2 in an open conformation. *eLife* 2020;9 e60724.
- Emsley, P., Lohkamp, B., Scott, W. G., & Cowtan, K. (2010). Features and Development of Coot. *Acta Crystallographica Section D – Biological Crystallography* 2010;66 486-501.
- Fiebig, K. M., Rice, L. M., Pollock, E., & Brunger, A. T. (1999). Folding intermediates of SNARE complex assembly. *Nat Struct Biol.* 1999;6(2) 117-23.
- Finger, F. P., Hughes, T. E., & Novick, P. (1998). Sec3p Is a Spatial Landmark for Polarized Secretion in Budding Yeast. *Cell* 1998;92 559-571.
- Franco, J. R., Simarro, P. P., Diarra, A., & Jannin, J. G. (2014). Epidemiology of human African trypanosomiasis. *Clinical Epidemiology* 2014;6 257-275.
- Gibson, W. (2007). Resolution of the species problem in African trypanosomes. *International Journal for Parasitology* 2007;37 829-838.
- Hampton Research (2021). HR2-130 Crystal Screen HT Documents. Available at: [https://hamptonresearch.com/uploads/support\\_materials/HR2-130\\_Binder.pdf](https://hamptonresearch.com/uploads/support_materials/HR2-130_Binder.pdf) (Accessed: January 10<sup>th</sup>, 2022).
- Isch, C., Majneri, P., Landrein, N., Pivovarov, Y., Lesigang, J., Lauruol, F., Robinson, D. R., Dong, G., & Bonhivers, M. (2021). Structural and functional studies of the first tripartite protein complex at the *Trypanosoma brucei* flagellar pocket collar. *PLoS Pathog* 2021;17(8) e1009329

- Kantardjieff, K. A., & Rupp, B. (2003). Matthews coefficient probabilities: Improved estimates for unit cell contents of proteins, DNA, and protein-nucleic acid complex crystals. *Protein Science* 2003:12 1865-1871.
- Langousis, G., & Hill, K. L. (2014). Motility and more: the flagellum of *Trypanosoma brucei*. *Nat Rev Microbiol* 2014:12 505-518.
- Lewis, M. J., Nichols, B. J., Prescianotto-Baschong, C., Riezman, H., & Pelham, H. R. B. (2000). Specific Retrieval of the Exocytic SNARE Snc1p from Early Yeast Endosomes. *Mol Biol Cell*. 2000:11(1) 23-38.
- Lipschutz, J. H., & Mostov, K. E. (2002). Exocytosis: The Many Masters of the Exocyst. *Current Biology* 2002:12 R212-R214.
- Marcello, L., & Barry, J. D. (2017). From silent genes to noisy populations – dialogue between the genotype and phenotypes of antigenic variation. *J Eukaryot Microbiol*. 2007:54(1) 14-17.
- Matthews, B. W. (1968). Solvent content of protein crystals. *J Mol Biol* 1968:33 491-497.
- Matthews, K. R. (2005). The developmental cell biology of *Trypanosoma brucei*. *Journal of Cell Science* 2005:118 283-290.
- McCoy, A. J., Grosse-Kunstleve, R. W., Adams, P. D., Winn, M. D. Storoni, L. C., & Read, R. J. (2007). Phaser crystallographic software. *J Appl Cryst* 2007:40 658-674.
- Panavas, T., Sanders, C., & Butt, T. R. (2009). SUMO Fusion Technology for Enhanced Protein Production in Prokaryotic and Eukaryotic Expression Systems. *Methods Mol Biol*. 2009:497 303-17.
- Peer, M., Yuan, H., Zhang, Y., Korbula, K., Novick, P. J., & Dong, G. (2022). Double NPY motifs at the N-terminus of Sso2 synergistically bind Sec3 to promote membrane fusion. *bioRxiv* 2022.03.11.483902.
- Pelham, H. R. B. (1999). SNAREs and the Secretory Pathway-Lessons from Yeast. *Experimental Cell Research* 1999:247(1) 1-8.
- Promega (2009a). Wizard® Plus SV Minipreps DNA Purification System Quick Protocol. Available at: <https://promega.com/-/media/files/resources/protcards/wizard-plus-sv-minipreps-dna-purification-system-quick-protocol.pdf> (Accessed: January 10<sup>th</sup>, 2022).
- Promega (2009b). Wizard® SV Gel and PCR Clean-Up System Quick Protocol. Available at: <https://promega.com/-/media/files/resources/protcards/wizard-sv-gel-and-pcr-clean-up-system-quick-protocol.pdf> (Accessed: January 10<sup>th</sup>, 2022).
- Pruyne, D., Legesse-Miller, A., Gao, L., Dong, Y., & Bretscher, A. (2004). Mechanisms of polarized growth and organelle segregation in yeast. *Annu Rev Cell Dev Biol*. 2004:20 559-91.
- Salminen, A., & Novick, P. J. (1989). The Sec15 protein responds to the function of the GTP binding protein, Sec4, to control vesicular traffic in yeast. *J Cell Biol*. 1989:109(3) 1023-1036.
- Schrödinger, LLC. The PyMOL Molecular Graphics System, Version 2.5.2. <https://pymol.org/>.
- Vidilaseris, K., Lesigang, J., Morriswood, B., & Dong, G. (2014a). Assembly mechanism of *Trypanosoma brucei* BILBO1 at the flagellar pocket collar. *J. Biol. Chem*. 2014:289(34) 23870-81.

Vidilaseris, K., Morriswood, B., Kontaxis, G., & Dong, G. (2014b). Structure of the TbBILBO1 Protein N-terminal Domain from *Trypanosoma brucei* Reveals an Essential Requirement for a Conserved Surface Patch. *J. Biol. Chem.* 2014:289(6) 3724-3735.

Vidilaseris, K., Landrein, N., Pivovarova, Y., Lesigang, J., Aeksiri, N., Robinson, D. R., Bonhivers, M., & Dong, G. (2019). Crystal structure of the N-terminal domain of the trypanosome flagellar protein BILBO1 reveals a ubiquitin fold with a long structured loop for protein binding. *J. Biol. Chem.* 2020:295(6) 1489-1499.

Vidilaseris, K., Shimanovskaya, E., Esson, H. J., Morriswood, B., & Dong, G. (2014c). Assembly Mechanism of *Trypanosoma brucei* BILBO1, a Multidomain Cytoskeletal Protein. *J. of Biol. Chem.* 2014:289(34) 23870-23881.

Weichenberger, C. X., & Rupp, B. (2014). Ten years of probabilistic estimates of biocrystal solven content: New insights via nonparametric kernel density estimate. *Acta Crystallogr* 2014:D70(6) 1579-1588.

Wu, B., Guo, W. (2015). The Exocyst at a Glance. *J Cell Sci.* 2015:128(16) 2957-2964.

Yuan, H., Davis, S., Ferro-Novick, S., & Novick, P. (2017). Rewiring a Rab regulatory network reveals a possible inhibitory role for the vesicle tether, Uso1. *PNAS* 2017:114(41) E8637-E8645.

Yue, P., Zhang, Y., Mei, K., Wang, S., Lesigang, J., Zhu, Y., Dong, G., & Guo, W. (2017). Sec3 promotes the initial binary t-SNARE complex assembly and membrane fusion. *Nat Commun.* 2017:23(8) 14236.

## 7. List of Figures

Figure 1: BILBO1-Like Proteins.....	- 12 -
Figure 2: Illustration of Sec3/Sso2 Interaction.....	- 14 -
Figure 3: Structural Information Sec3/Sso2 and Homologues.....	- 15 -
Figure 4: Sso2 N-terminal Region Multiple Sequence Alignment of Multiple Species.....	- 15 -
Figure 5: PCR Insert Amplification Gel.....	- 39 -
Figure 6: Construct TbBILBO421-NTD – Illustration.....	- 41 -
Figure 7: Elution Profile TbBILBO421-NTD HisTrap (1).....	- 41 -
Figure 8: SDS-PAGE TbBILBO421-NTD HisTrap (1).....	- 42 -
Figure 9: TbBILBO421-NTD Uncut/Cut.....	- 42 -
Figure 10: Elution Profile TbBILBO421-NTD HisTrap (2).....	- 43 -
Figure 11: SDS-PAGE TbBILBO421-NTD HisTrap (2).....	- 44 -
Figure 12: Elution Profile TbBILBO421-NTD AEX.....	- 44 -
Figure 13: SDS-PAGE TbBILBO421-NTD AEX.....	- 45 -
Figure 14: Elution Profile TbBILBO421-NTD SEC.....	- 46 -
Figure 15: SDS-PAGE TbBILBO421-NTD SEC.....	- 46 -
Figure 16: TbBILBO421-NTD FPC4-CTD Electrophoretic Shift Assay.....	- 47 -
Figure 17: Construct TbBILBO421-EFh – Illustration.....	- 48 -
Figure 18: Elution Profile TbBILBO421-EFh HisTrap.....	- 48 -
Figure 19: SDS-PAGE TbBILBO421-EFh HisTrap.....	- 49 -
Figure 20: Elution Profile TbBILBO421-EFh MBP-Trap.....	- 49 -
Figure 21: SDS-PAGE TbBILBO421-EFh MBP-Trap.....	- 50 -
Figure 22: TbBILBO421-EFh Uncut/Cut.....	- 51 -
Figure 23: Elution Profile TbBILBO421-EFh SEC (CaCl <sub>2</sub> ).....	- 52 -
Figure 24: SDS-PAGE TbBILBO421-EFh SEC (CaCl <sub>2</sub> ).....	- 52 -
Figure 25: Elution Profile TbBILBO421-EFh SEC (EDTA).....	- 53 -
Figure 26: SDS-PAGE TbBILBO421-EFh SEC (EDTA).....	- 53 -
Figure 27: Elution Profiles TbBILBO421-EFh SEC (CaCl <sub>2</sub> /EDTA).....	- 54 -
Figure 28: Construct TbBILBO421-EFh-CCD – Illustration.....	- 55 -
Figure 29: SDS-PAGE TbBILBO421-EFh-CCD Ni-Bead Purification.....	- 55 -
Figure 30: Elution Profile TbBILBO421-EFh-CCD SEC (CaCl <sub>2</sub> ).....	- 57 -
Figure 31: SDS-PAGE TbBILBO421-EFh-CCD SEC (CaCl <sub>2</sub> ).....	- 57 -
Figure 32: Elution Profile TbBILBO421-EFh-CCD SEC (EDTA).....	- 58 -
Figure 33: SDS-PAGE TbBILBO421-EFh-CCD SEC (EDTA).....	- 58 -
Figure 34: Elution Profiles TbBILBO421-EFh-CCD SEC (CaCl <sub>2</sub> /EDTA).....	- 59 -
Figure 35: Construct TbBILBO421-EFh-CCD-ct – Illustration.....	- 60 -
Figure 36: Elution Profile TbBILBO421-EFh-CCD-ct HisTrap.....	- 60 -
Figure 37: SDS-PAGE TbBILBO421-EFh-CCD-ct HisTrap.....	- 61 -
Figure 38: Elution Profile TbBILBO421-EFh-CCD-ct SEC (CaCl <sub>2</sub> ).....	- 62 -
Figure 39: SDS-PAGE TbBILBO421-EFh-CCD-ct SEC (CaCl <sub>2</sub> ).....	- 62 -
Figure 40: Elution Profile TbBILBO421-EFh-CCD-ct SEC (EDTA).....	- 63 -
Figure 41: SDS-PAGE TbBILBO421-EFh-CCD-ct SEC (EDTA).....	- 63 -
Figure 42: Elution Profiles TbBILBO421-EFh-CCD-ct SECs (CaCl <sub>2</sub> /EDTA).....	- 64 -
Figure 43: TbBILBO421-EFh-CCD-ct – Antiparallel Dimer.....	- 65 -
Figure 44: rsEM of TbBILBO421-EFh-CCD-ct SEC (CaCl <sub>2</sub> ).....	- 65 -
Figure 45: Construct TbBILBO421-CCD-ct – Illustration.....	- 66 -
Figure 46: Elution Profile TbBILBO421-CCD-ct HisTrap.....	- 66 -
Figure 47: SDS-PAGE TbBILBO421-CCD-ct HisTrap.....	- 67 -
Figure 48: Elution Profile TbBILBO421-CCD-ct SEC (1).....	- 68 -
Figure 49: SDS-PAGE TbBILBO421-CCD-ct SEC (1).....	- 68 -
Figure 50: TbBILBO421-CCD-ct – Antiparallel Dimer.....	- 69 -
Figure 51: rsEM of TbBILBO421-CCD-ct SEC (1).....	- 69 -
Figure 52: TbBILBO421-CCD-ct Uncut/Cut.....	- 70 -
Figure 53: Elution Profile TbBILBO421-CCD-ct SEC (2).....	- 71 -
Figure 54: Elution Profile TbBILBO421-CCD-ct SEC (2).....	- 71 -
Figure 55: Construct TbBILBO421-CCD (HM15b) – Illustration.....	- 72 -
Figure 56: Elution Profile TbBILBO421-CCD (HM15b) HisTrap.....	- 72 -
Figure 57: SDS-PAGE TbBILBO421-CCD (HM15b) HisTrap.....	- 73 -
Figure 58: Elution Profile TbBILBO421-CCD (HM15b) SEC (1).....	- 74 -

Figure 59: SDS-PAGE TbBILBO421-CCD (HM15b) SEC (1).....	- 74 -
Figure 60: TbBILBO421-CCD – Antiparallel Dimer .....	- 75 -
Figure 61: rsEM of TbBILBO421-CCD SEC (1) .....	- 75 -
Figure 62: TbBILBO421-CCD (HM15b) Uncut/Cut .....	- 76 -
Figure 63: Elution Profile TbBILBO421-CCD (HM15b) .....	- 77 -
Figure 64: SDS-PAGE TbBILBO421-CCD (HM15b) SEC (2).....	- 77 -
Figure 65: Construct TbBILBO421-CCD (Sumo15b) – Illustration.....	- 78 -
Figure 66: Elution Profile TbBILBO421-CCD (Sumo15b) HisTrap (1) .....	- 78 -
Figure 67: SDS-PAGE TbBILBO421-CCD (Sumo15b) HisTrap (1).....	- 79 -
Figure 68: TbBILBO421-CCD (Sumo15b) Uncut/Cut.....	- 79 -
Figure 69: Elution Profile TbBILBO421-CCD (Sumo15b) HisTrap (2) .....	- 80 -
Figure 70: SDS-PAGE TbBILBO421-CCD (Sumo15b) HisTrap (2).....	- 80 -
Figure 71: Elution Profile TbBILBO421-CCD (Sumo15b) SEC .....	- 81 -
Figure 72: SDS-PAGE TbBILBO421-CCD (Sumo15b) SEC .....	- 82 -
Figure 73: Crystal Structure Sec3(aa75-260)/Sso2(aa1-224) Complex .....	- 83 -
Figure 74: Construct Sec3-PH – Illustration .....	- 84 -
Figure 75: Elution Profile Sec3-PH HisTrap (1).....	- 84 -
Figure 76: SDS-PAGE Sec3-PH HisTrap (1) .....	- 85 -
Figure 77: Elution Profile Sec3-PH HisTrap (2).....	- 86 -
Figure 78: SDS-PAGE Sec3-PH HisTrap (2) .....	- 86 -
Figure 79: Sec3-PH Uncut/Cut .....	- 87 -
Figure 80: Elution Profile Sec3-PH CEX .....	- 87 -
Figure 81: SDS-PAGE Sec3-PH CEX .....	- 88 -
Figure 82: Sec3-PH Sso2-N15/N15-m1m2 – ITC .....	- 89 -
Figure 83: Sec3-PH Sso2-N9/1015 – ITC .....	- 89 -
Figure 84: Sec3-PH Sso2-N15-m1/N15-m2 – ITC .....	- 90 -
Figure 85: SSO1Δ Sso2 <sup>mut</sup> – Growth Test.....	- 91 -
Figure 86: SSO1Δ Sso2 <sup>mut</sup> – Bgl2 Secretion Assay .....	- 92 -
Figure 87: SSO1Δ Sso2 <sup>mut</sup> – Invertase Secretion Assay .....	- 93 -
Figure 88: SSO1Δ Sso2 <sup>mut</sup> – Accumulation of Secretory Vesicles .....	- 94 -
Figure 89: SSO1Δ Sso2 <sup>mut</sup> – Snc1 Recycling .....	- 95 -
Figure 90: SSO1Δ Sso2 <sup>mut</sup> – Sec3 Actin Independent Localization .....	- 97 -
Figure 91: Construct Sso1(aa1-224) – Illustration.....	- 98 -
Figure 92: Elution Profile Sso1(aa1-224) HisTrap.....	- 98 -
Figure 93: SDS-PAGE Sso1(aa1-224) HisTrap .....	- 99 -
Figure 94: Sso1(aa1-224) Uncut/Cut .....	- 99 -
Figure 95: Elution Profile Sso1(aa1-224) AEX .....	- 100 -
Figure 96: SDS-PAGE Sso1(aa1-224) AEX.....	- 100 -
Figure 97: Elution Profile Sec3-PH/Sso1(aa1-224) Complex SEC .....	- 102 -
Figure 98: SDS-PAGE Sec3-PH/Sso1(aa1-224) Complex SEC.....	- 102 -
Figure 99: Crystal Structure Sec3-PH .....	- 103 -
Figure 100: Crystal Structure Sec3-PH – Autostereogram .....	- 104 -
Figure 101: Crystal Structure Sec3 – Comparison to Previous Structures .....	- 105 -
Figure 102: Sec3/Sso2, Munc18/Stx Complex Comparison .....	- 107 -
Figure 103: Illustration of Sec3/Sso2 Interaction – NPY-motifs .....	- 108 -



## 8. List of Tables

Table 1: Competent Cells – RF1/2-Solutions .....	- 18 -
Table 2: Vector pET15b.....	- 19 -
Table 3: Vector SUMO15b .....	- 19 -
Table 4: Vector HM15b.....	- 20 -
Table 5: Vector MalpET .....	- 21 -
Table 6: Vector HT15b .....	- 21 -
Table 7: Vector Digestion Reaction .....	- 22 -
Table 8: Primer for Insert Amplification .....	- 23 -
Table 9: PCR Reaction Mix .....	- 23 -
Table 10: PCR Program .....	- 24 -
Table 11: Double Digest of Insert DNA .....	- 24 -
Table 12: Constructs .....	- 25 -
Table 13: SDS-PAGE Gel Composition .....	- 31 -
Table 14: Synthetic FPC4 Peptides .....	- 32 -
Table 15: Synthetic Sso2 Polypeptides .....	- 32 -
Table 16: Sec3-PH/Sso1(aa1-224) Complex - Crystal .....	- 34 -
Table 17: Sso2 Mutations Introduced in SSO1Δ Yeast Strain .....	- 36 -
Table 18: Insert Concentrations .....	- 39 -
Table 19: Construct Concentrations .....	- 40 -
Table 20: Sequencing Results.....	- 118 -
Table 21: Hampton Research Crystal Screen HT Formulation.....	- 121 -
Table 22: Data Collection and Refinement Statistics Sec3-PH/Sso2(aa1-270).....	- 122 -
Table 23: Data Collection and Refinement Statistics Sec3-PH/Sso1(aa1-224).....	- 122 -

## 9. Appendix

### 9.1. Protein Sequences

#### 9.1.1. TbBILBO421 [*Trypanosoma brucei* TREU927] – DNA Sequence

```
1 atgggtgttca tcctcttggc atgcagtgat atatgcggga agaaggtaaa tgtaacgttg
61 cccttcgaga ggccctcccga gtcactcgat gagctttacc gcgtcgtgga gcagttgttt
121 cgtggggagg aaacggatat aaaacgtacg gtcgacgggtg gcgaataccg gacgcgcccc
181 tctgaaccct ttacctgccg tcgcatccag cgcttcgatg atgaaacgag aacttgggtg
241 gaagtaacaa gtgagaagca gttggccccg tatgatcaat tgtatgtctt tcgaaagaac
301 gcgacgcgag ctgatatttc cactgagcgg gagctaccgg aacctcgcag cagcattcac
361 ttccccaga cggatggcag actcaatggg ttatacactt ccaatgccaa ccgacgtgcc
421 agcacggcaa cggtagagtc tttgacaagc tcgccgcaca cgcccacgac acaacaacaa
481 acggcctctt cgtcccgcgg cggtagggag agccgcaggt atagtctctc ccgagagagg
541 gaaaagagtc gcgtttacaag cagcagctgc gttcctgaat gtattggtgg aaatggttct
601 ccgcaggggt ttgatattaa tgcgcgtgct gataaagtgg tgaggaagca cgtagaggct
661 gtttactcca ttggagacgc atgcaagaaa ggttatctaa ccgcacgaga gtttcagggc
721 atttttcggg cctgccatat agacttcccc ttcgatgcta ttgatgatat atatcgggtg
781 ttcgctgatg accgcgacgg ggatcggggc atgacaattc ggaacttcta cgagttcgcg
841 catagtttca accaaactgt taatattgct tatgcgcgct tcagcaacga aaggagacag
901 caagttgtgg agcaggaaca gcgtggggcg gagtctgcgc ttgaagaact gcaaaagcag
961 aaacgaatac ttgaagagcg gttggaggaa atgcagaagc aaatagttaa ggagcaggag
1021 aggcggggcg gtttgcagaa tgaagcagat gaattacgta tgtccaggga tccgtctttg
1081 cgggaagaag aacaacgatt actcgagaag gaagtgagtg tgtccaata caggaagaaa
1141 cttctgcaag aagaagtgga ttatgagaaa ctggtagcag agcgtcgtcg ccggtcggcg
1201 gctgtaatgg gtcacactaa aatgcttccc caaacattca aatatgggta cgacattcat
1261 gactga
```

#### 9.1.2. TbBILBO421 [*Trypanosoma brucei* TREU927] – Protein sequence

```
1 MVFILLACSD ICGKKVNVTL PFERPPESLD ELYRVVEQLF RGEETDIKRT VDGGEYRTRP
61 SEPFTCRRIQ RFDDETRTRWV EVTSEKQLAP YDQLYVFRKN ATRADISTER ELPEPRSSIH
121 FPQTDGRLNG LYTSNANRRA STATVSHLTS SPHTPTTQQQ TASSSRRGGE SRRYSLSRER
181 EKSRTSSSC VPECIGNGS PQGFDINARA DKVVRKHVEA VYSIGDACKK GYLTAREFQG
241 IFRSCHIDFP FDAIDDIYRV FADDRDGDRA MTIRNFYEFA HSFNQTVNIA YARFSNERRQ
301 QVVEQEQRGA ESALEELQKQ KRILEERLEE MQQIVKEQE RRARLQNEAD ELRMSRDPSL
361 REEEQRLLEK EVSVFQYRKK LLQEEVDYEK LVAERRRRSA AVMGHTKMLP QTFKYGYDIH
421 D
```

### 9.1.3. Sec3 [*Saccharomyces cerevisiae* S288C] – Protein Sequence

```
1 MRSSKSPFKR KSHSRETSHD ENTSFFHKRT ISGSSAHHSR NVSQGAVPSS APPVSGGNYS
61 HKRNVSRASN SSQTSNFLAE QYERDRKAI I NCCFSRPDHK TGEPPNNYIT HVRIIEDSKF
121 PSSRPPPSK LENKKKRLLI LSAKPNNAKL IQIHKARENS DGSFQIGRTW QLTELVRVEK
181 DLEISEGFIL TMSKKYYWET NSAKERTVFI KSLITLYIQT FEGHVPPELVN WDLSLFYLDE
241 RSYQRAVITN RPGSVSPIKS PTSNFTTNTT QSVGSVPFSA PTERTRRSET ESVNPVSTPA
301 SVEYHAGMKS LNKAPYSSNS TLNEVNKRYE LEQQQQQEEA ELRRLEEQKR LQLQKENEMK
361 RLEEERRIKQ EERKRQMELE HQRQLEEEER KRQMELEAKK QMELKRQRQF EEEQRLKKER
421 ELLEIQRKQR EQETAERLKK EEQEALAKKE EEEKSKRNKV DNESYTQEIN GKVDNLLLEDL
481 NAVLAEETET TPTMQNGTYV PERSTARAH D QLKKPLNIAK VESLGGSDLN DSISLSDEIA
541 GLNTSNLSGE DQDEKNDLSF EKGDEVRYSN NFEGEAPHVY HEVSIIQEEA PAVSQKLILP
601 EENNESEALI ESKEEIKTME NIDDEVLL E I LTDINWSIED DADSMIERID LRLAETEYLF
661 NQNLLSLQKI GPNIRPYEDK VNDECHRIIP TSLSLF MEMS NFSNDIENVE SQDNGLQVES
721 ANKKLLWNTL DELLKTVSLD EISLNQLLEC PIREKNLPWM ENQLNLLLKA FQAIGSDGNE
781 VEYNLREISG LKQRLQFYEK VTKIFLNRI V EEMQKKFSNI RGQDISHDQM IRILTLLIF
841 SPLILFCKEI SQKSYQAIVE NWNVSIQPVY MELWTKKISQ LQGIDTNDEK MNELSLSQLL
901 NEWDTFRKER KTNDINPVFK NSFSLLTECL QTMRQECIVY QNFVEVFFHI SSKHNFEEYI
961 KHFNPDAPP ILLDTPVKVMQ SDREAAVIET QLVSRIFQPI VTRLSSYFVE LVKAEP TVAP
1021 ALTFYLENEI KSLESSNHEF LLSAVTRMYT QIKQVWSDNV EEQVLHFERI SNATTNGEIL
1081 PGILDLPVGL KNSEDLFQFA KRSMDIKD TD EGYESIELMN SSFRKLSIAA TRSITHKEVN
1141 SSINPNLSDT AALNDYMET ISLLVNSNWL TEMLSMLNFN KDGIFDTS LQ NVKKVFDVEK
1201 ESYASFLLRD TMPKLTA FVY GVSNIIENTN NVNMTNPSRW AAYS RQNLEN ILLAYTSHEI
1261 ETLVKRLH TH MVNDFGYHQE NAINNVLC DK LWSCIQQQTV SLYLKLYTVI DKHYRG TNIR
1321 FTKNDIISAF EEEKNA
```

### 9.1.4. Sso1 [*Saccharomyces cerevisiae* S288C] – Protein Sequence

```
1 MSYNNPYQLE TPFEESYELD EGSSAIGAEG HDFVGF MNKI SQINRDL DKY DHTINQVDSL
61 HKRLLTEVNE EQASHLRHSL DNFVAQATDL QFKLKNEIKS AQRDGIHDTN KQAQAENSRQ
121 RFLKLIQDYR IVDSNYKEEN KEQAKRQYMI IQPEATEDEV EAAISDVGGQ QIFSQALLNA
181 NRRGEAKTAL AEVQARHQEL LKLEKSMAEL TQLFNDMEEL VIEQQENV DV IDKNVEDAQL
241 DVEQGVGHTD KAVKSARKAR KNKIRCWLIV FAIIVVVVVV VVVPAVVKTR
```

### 9.1.5. Sso2 [*Saccharomyces cerevisiae* S288C] – Protein Sequence

```
1 MSNANPYENN NPYAENYEMQ EDLNNAPTGH SDGSDDFVAF MNKINSINAN LSRYENIINQ
61 IDAQHKDLLT QVSEEQEMEL RRLDDYISQ ATDLQYQLKA DIKDAQRDGL HDSNKQAQAE
121 NCRQKFLKLI QDYRIIDSNY KESKEQAKR QYTIIQPEAT DEEVEAAIND VNGQQIFSQA
181 LLNANRRGEA KTALAEVQAR HQELLKLEKT MAELTQLFND MEELVIEQQE NVDVIDKNVE
241 DAQQDVEQGV GHTNKAVKSA RKARKNKIRC LIICFIIFAI VVVVVVVPSV VETRK
```

## 9.2. Sequencing Results

TbBILBO421		1	MVFILLACSD	ICGKKVNVTL	PFERPPESLD	ELYRVVEQLF	RGEETDIKRT	VDGGEYRTRP	60
TbBILBO421 (aa296-404)	Sumo15b		-----	-----	-----	-----	-----	-----	
TbBILBO421 (aa296-404)	HM15b		-----	-----	-----	-----	-----	-----	
TbBILBO421 (aa296-421)	HM15b		-----	-----	-----	-----	-----	-----	
TbBILBO421 (aa210-421)	HM15b		-----	-----	-----	-----	-----	-----	
TbBILBO421 (aa210-404)	MalpET		-----	-----	-----	-----	-----	-----	
TbBILBO421 (aa210-295)	MalpET		-----	-----	-----	-----	-----	-----	
TbBILBO421		61	SEPFTCRRIQ	RFDDETRTWV	EVTSEKQLAP	YDQLYVFRKN	ATRADISTER	ELPEPRSSIH	120
TbBILBO421 (aa296-404)	Sumo15b		-----	-----	-----	-----	-----	-----	
TbBILBO421 (aa296-404)	HM15b		-----	-----	-----	-----	-----	-----	
TbBILBO421 (aa296-421)	HM15b		-----	-----	-----	-----	-----	-----	
TbBILBO421 (aa210-421)	HM15b		-----	-----	-----	-----	-----	-----	
TbBILBO421 (aa210-404)	MalpET		-----	-----	-----	-----	-----	-----	
TbBILBO421 (aa210-295)	MalpET		-----	-----	-----	-----	-----	-----	
TbBILBO421		121	FPQTDGRLNG	LYTSNANRRA	STATVSHLTS	SPHTPTTQQQ	TASSSRRGGE	SRYSLSRER	180
TbBILBO421 (aa296-404)	Sumo15b		-----	-----	-----	-----	-----	-----	
TbBILBO421 (aa296-404)	HM15b		-----	-----	-----	-----	-----	-----	
TbBILBO421 (aa296-421)	HM15b		-----	-----	-----	-----	-----	-----	
TbBILBO421 (aa210-421)	HM15b		-----	-----	-----	-----	-----	-----	
TbBILBO421 (aa210-404)	MalpET		-----	-----	-----	-----	-----	-----	
TbBILBO421 (aa210-295)	MalpET		-----	-----	-----	-----	-----	-----	
TbBILBO421		181	EKSRVTSSSC	VPECIGNGS	PQGFDINARA	DKVVRKHVEA	VYSIGDACKK	GYLTAREFQG	240
TbBILBO421 (aa296-404)	Sumo15b		-----	-----	-----	-----	-----	-----	
TbBILBO421 (aa296-404)	HM15b		-----	-----	-----	-----	-----	-----	
TbBILBO421 (aa296-421)	HM15b		-----	-----	-----	-----	-----	-----	
TbBILBO421 (aa210-421)	HM15b		-----	-----	-----A	DKVVRKHVEA	VYSIGDACKK	GYLTAREFQG	
TbBILBO421 (aa210-404)	MalpET		-----	-----	-----A	DKVVRKHVEA	VYSIGDACKK	GYLTAREFQG	
TbBILBO421 (aa210-295)	MalpET		-----	-----	-----A	DKVVRKHVEA	VYSIGDACKK	GYLTAREFQG	
TbBILBO421		241	IFRSCHIDFP	FDAIDDIYRV	FADDRDGDRA	MTIRNFYEFA	HSFNQTVNIA	YARFSNERRQ	296  300
TbBILBO421 (aa296-404)	Sumo15b		-----	-----	-----	-----	-----	-----NERRQ	
TbBILBO421 (aa296-404)	HM15b		-----	-----	-----	-----	-----	-----NERRQ	
TbBILBO421 (aa296-421)	HM15b		-----	-----	-----	-----	-----	-----NERRQ	
TbBILBO421 (aa210-421)	HM15b		IFRSCHIDFP	FDAIDDIYRV	FADDRDGDRA	MTIRNFYEFA	HSFNQTVNIA	YARFSNERRQ	
TbBILBO421 (aa210-404)	MalpET		IFRSCHIDFP	FDAIDDIYRV	FADDRDGDRA	MTIRNFYEFA	HSFNQTVNIA	YARFSNERRQ	
TbBILBO421 (aa210-295)	MalpET		IFRSCHIDFP	FDAIDDIYRV	FADDRDGDRA	MTIRNFYEFA	HSFNQTVNIA	YARFS-----	
TbBILBO421		301	QVVEQEQRGA	ESALEELQKQ	KRILEERLEE	MQKQIVKEQE	RRARLQNEAD	ELRMSRDPSL	360
TbBILBO421 (aa296-404)	Sumo15b		QVVEQEQRGA	ESALEELQKQ	KRILEERLEE	MQKQIVKEQE	RRARLQNEAD	ELRMSRDPSL	
TbBILBO421 (aa296-404)	HM15b		QVVEQEQRGA	ESALEELQKQ	KRILEERLEE	MQKQIVKEQE	RRARLQNEAD	ELRMSRDPSL	
TbBILBO421 (aa296-421)	HM15b		QVVEQEQRGA	ESALEELQKQ	KRILEERLEE	MQKQIVKEQE	RRARLQNEAD	ELRMSRDPSL	
TbBILBO421 (aa210-421)	HM15b		QVVEQEQRGA	ESALEELQKQ	KRILEERLEE	MQKQIVKEQE	RRARLQNEAD	ELRMSRDPSL	
TbBILBO421 (aa210-404)	MalpET		QVVEQEQRGA	ESALEELQKQ	KRILEERLEE	MQKQIVKEQE	RRARLQNEAD	ELRMSRDPSL	
TbBILBO421 (aa210-295)	MalpET		-----	-----	-----	-----	-----	-----	
TbBILBO421		361	REEEQRLLEK	EVSVFYRKK	LLQEEVDYEK	LVAERRRRSA	AVMGHTKMPL	QTFKYGYDIH	421
TbBILBO421 (aa296-404)	Sumo15b		REEEQRLLEK	EVSVFYRKK	LLQEEVDYEK	LVAERRRRSA	AVMG-----	-----	-
TbBILBO421 (aa296-404)	HM15b		REEEQRLLEK	EVSVFYRKK	LLQEEVDYEK	LVAERRRRSA	AVMG-----	-----	-
TbBILBO421 (aa296-421)	HM15b		REEEQRLLEK	EVSVFYRKK	LLQEEVDYEK	LVAERRRRSA	AVMGHTKMPL	QTFKYGYDIH	-
TbBILBO421 (aa210-421)	HM15b		REEEQRLLEK	EVSVFYRKK	LLQEEVDYEK	LVAERRRRSA	AVMGHTKMPL	QTFKYGYDIH	-
TbBILBO421 (aa210-404)	MalpET		REEEQRLLEK	EVSVFYRKK	LLQEEVDYEK	LVAERRRRSA	AVMG-----	-----	-
TbBILBO421 (aa210-295)	MalpET		-----	-----	-----	-----	-----	-----	-

**Table 20: Sequencing Results**

### 9.3. Hampton Research Crystal Screen HT Formulation

Well	Formulation
A1	0.02 M Calcium chloride dihydrate, 0.1 M Sodium acetate trihydrate pH 4.6, 30% v/v (+/-)-2-Methyl-2,4-pentanediol
A2	0.4 M Potassium sodium tartrate tetrahydrate
A3	0.4 M Ammonium phosphate monobasic
A4	0.1 M TRIS hydrochloride pH 8.5, 2.0 M Ammonium sulfate
A5	0.2 M Sodium citrate tribasic dihydrate, 0.1 M HEPES sodium pH 7.5, 30% v/v (+/-)-2-Methyl-2,4-pentanediol
A6	0.2 M Magnesium chloride hexahydrate, 0.1 M TRIS hydrochloride pH 8.5, 30% w/v Polyethylene glycol 4,000
A7	0.1 M Sodium cacodylate trihydrate pH 6.5, 1.4 M Sodium acetate trihydrate
A8	0.2 M Sodium citrate tribasic dihydrate, 0.1 M Sodium cacodylate trihydrate pH 6.5, 30% v/v 2-Propanol
A9	0.2 M Ammonium acetate, 0.1 M Sodium citrate tribasic dihydrate pH 5.6, 30% w/v Polyethylene glycol 4,000
A10	0.2 M Ammonium acetate, 0.1 M Sodium acetate trihydrate pH 4.6, 30% w/v Polyethylene glycol 4,000
A11	0.1 M Sodium citrate tribasic dihydrate pH 5.6, 1.0 M Ammonium phosphate monobasic
A12	0.2 M Magnesium chloride hexahydrate, 0.1 M HEPES sodium pH 7.5, 30% v/v 2-Propanol
B1	0.2 M Sodium citrate tribasic dihydrate, 0.1 M TRIS hydrochloride pH 8.5, 30% v/v Polyethylene glycol 400
B2	0.2 M Calcium chloride dihydrate, 0.1 M HEPES sodium pH 7.5, 28% v/v Polyethylene glycol 400
B3	0.2 M Ammonium sulfate, 0.1 M Sodium cacodylate trihydrate pH 6.5, 30% w/v Polyethylene glycol 8,000
B4	0.1 M HEPES sodium pH 7.5, 1.5 M Lithium sulfate monohydrate
B5	0.2 M Lithium sulfate monohydrate, 0.1 M TRIS hydrochloride pH 8.5, 30% w/v Polyethylene glycol 4,000
B6	0.2 M Magnesium acetate tetrahydrate, 0.1 M Sodium cacodylate trihydrate pH 6.5, 20% w/v Polyethylene glycol 8,000
B7	0.2 M Ammonium acetate, 0.1 M TRIS hydrochloride pH 8.5, 30% v/v 2-Propanol
B8	0.2 M Ammonium sulfate, 0.1 M Sodium acetate trihydrate pH 4.6, 25% w/v Polyethylene glycol 4,000
B9	0.2 M Magnesium acetate tetrahydrate, 0.1 M Sodium cacodylate trihydrate pH 6.5, 30% v/v (+/-)-2-Methyl-2,4-pentanediol
B10	0.2 M Sodium acetate trihydrate, 0.1 M TRIS hydrochloride pH 8.5, 30% w/v Polyethylene glycol 4,000
B11	0.2 M Magnesium chloride hexahydrate, 0.1 M HEPES sodium pH 7.5, 30% v/v Polyethylene glycol 400
B12	0.2 M Calcium chloride dihydrate, 0.1 M Sodium acetate trihydrate pH 4.6, 20% v/v 2-Propanol
C1	0.1 M Imidazole pH 6.5, 1.0 M Sodium acetate trihydrate
C2	0.2 M Ammonium acetate, 0.1 M Sodium citrate tribasic dihydrate pH 5.6, 30% v/v (+/-)-2-Methyl-2,4-pentanediol
C3	0.2 M Sodium citrate tribasic dihydrate, 0.1 M HEPES sodium pH 7.5, 20% v/v 2-Propanol
C4	0.2 M Sodium acetate trihydrate, 0.1 M Sodium cacodylate trihydrate pH 6.5, 30% w/v Polyethylene glycol 8,000
C5	0.1 M HEPES sodium pH 7.5, 0.8 M Potassium sodium tartrate tetrahydrate
C6	0.2 M Ammonium sulfate, 30% w/v Polyethylene glycol 8,000
C7	0.2 M Ammonium sulfate, 30% w/v Polyethylene glycol 4,000
C8	2.0 M Ammonium sulfate
C9	4.0 M Sodium formate
C10	0.1 M Sodium acetate trihydrate pH 4.6, 2.0 M Sodium formate
C11	0.1 M HEPES sodium pH 7.5, 0.8 M Sodium phosphate monobasic monohydrate, 0.8 M Potassium phosphate monobasic
C12	0.1 M TRIS hydrochloride pH 8.5, 8% w/v Polyethylene glycol 8,000
D1	0.1 M Sodium acetate trihydrate pH 4.6, 8% w/v Polyethylene glycol 4,000
D2	0.1 M HEPES sodium pH 7.5, 1.4 M Sodium citrate tribasic dihydrate
D3	0.1 M HEPES sodium pH 7.5, 2% v/v Polyethylene glycol 400, 2.0 M Ammonium sulfate

D4	0.1 M Sodium citrate tribasic dihydrate pH 5.6, 20% v/v 2-Propanol, 20% w/v Polyethylene glycol 4,000
D5	0.1 M HEPES sodium pH 7.5, 10% v/v 2-Propanol, 20% w/v Polyethylene glycol 4,000
D6	0.05 M Potassium phosphate monobasic, 20% w/v Polyethylene glycol 8,000
D7	30% w/v Polyethylene glycol 1,500
D8	0.2 M Magnesium formate dihydrate
D9	0.2 M Zinc acetate dihydrate, 0.1 M Sodium cacodylate trihydrate pH 6.5, 18% w/v Polyethylene glycol 8,000
D10	0.2 M Calcium acetate hydrate, 0.1 M Sodium cacodylate trihydrate pH 6.5, 18% w/v Polyethylene glycol 8,000
D11	0.1 M Sodium acetate trihydrate pH 4.6, 2.0 M Ammonium sulfate
D12	0.1 M TRIS hydrochloride pH 8.5, 2.0 M Ammonium phosphate monobasic
E1	2.0 M Sodium chloride, 10% w/v Polyethylene glycol 6,000
E2	0.5 M Sodium chloride, 0.01 M Magnesium chloride hexahydrate, 0.01 M Hexadecyltrimethylammonium bromide
E3	25% v/v Ethylene glycol
E4	35% v/v 1,4-Dioxane
E5	2.0 M Ammonium sulfate, 5% v/v 2-Propanol
E6	1.0 M Imidazole pH 7.0
E7	10% w/v Polyethylene glycol 1,000, 10% w/v Polyethylene glycol 8,000
E8	1.5 M Sodium chloride, 10% v/v Ethanol
E9	0.1 M Sodium acetate trihydrate pH 4.6, 2.0 M Sodium chloride
E10	0.2 M Sodium chloride, 0.1 M Sodium acetate trihydrate pH 4.6, 30% v/v (+/-)-2-Methyl-2,4-pentanediol
E11	0.01 M Cobalt(II) chloride hexahydrate, 0.1 M Sodium acetate trihydrate pH 4.6, 1.0 M 1,6-Hexanediol
E12	0.1 M Cadmium chloride hydrate, 0.1 M Sodium acetate trihydrate pH 4.6, 30% v/v Polyethylene glycol 400
F1	0.2 M Ammonium sulfate, 0.1 M Sodium acetate trihydrate pH 4.6, 30% w/v Polyethylene glycol monomethyl ether 2,000
F2	0.2 M Potassium sodium tartrate tetrahydrate, 0.1 M Sodium citrate tribasic dihydrate pH 5.6, 2.0 M Ammonium sulfate
F3	0.5 M Ammonium sulfate, 0.1 M Sodium citrate tribasic dihydrate pH 5.6, 1.0 M Lithium sulfate monohydrate
F4	0.5 M Sodium chloride, 0.1 M Sodium citrate tribasic dihydrate pH 5.6, 2% v/v Ethylene imine polymer
F5	0.1 M Sodium citrate tribasic dihydrate pH 5.6, 35% v/v tert-Butanol
F6	0.01 M Iron(III) chloride hexahydrate, 0.1 M Sodium citrate tribasic dihydrate pH 5.6, 10% v/v Jeffamine M-600
F7	0.1 M Sodium citrate tribasic dihydrate pH 5.6, 2.5 M 1,6-Hexanediol
F8	0.1 M MES monohydrate pH 6.5, 1.6 M Magnesium sulfate heptahydrate
F9	0.1 M Sodium phosphate monobasic monohydrate, 0.1 M Potassium phosphate monobasic, 0.1 M MES monohydrate pH 6.5, 2.0 M Sodium chloride
F10	0.1 M MES monohydrate pH 6.5, 12% w/v Polyethylene glycol 20,000
F11	1.6 M Ammonium sulfate, 0.1 M MES monohydrate pH 6.5, 10% v/v 1,4-Dioxane
F12	0.05 M Cesium chloride, 0.1 M MES monohydrate pH 6.5, 30% v/v Jeffamine M-600
G1	0.01 M Cobalt(II) chloride hexahydrate, 0.1 M MES monohydrate pH 6.5, 1.8 M Ammonium sulfate
G2	0.2 M Ammonium sulfate, 0.1 M MES monohydrate pH 6.5, 30% w/v Polyethylene glycol monomethyl ether 5,000
G3	0.01 M Zinc sulfate heptahydrate, 0.1 M MES monohydrate pH 6.5, 25% v/v Polyethylene glycol monomethyl ether 550
G4	1.6 M Sodium citrate tribasic dihydrate pH 6.5
G5	0.5 M Ammonium sulfate, 0.1 M HEPES pH 7.5, 30% v/v (+/-)-2-Methyl-2,4-pentanediol
G6	0.1 M HEPES pH 7.5, 10% w/v Polyethylene glycol 6,000, 5% v/v (+/-)-2-Methyl-2,4-pentanediol
G7	0.1 M HEPES pH 7.5, 20% v/v Jeffamine M-600
G8	0.1 M Sodium chloride, 0.1 M HEPES pH 7.5, 1.6 M Ammonium sulfate
G9	0.1 M HEPES pH 7.5, 2.0 M Ammonium formate

G10	0.05 M Cadmium sulfate hydrate, 0.1 M HEPES pH 7.5, 1.0 M Sodium acetate trihydrate
G11	0.1 M HEPES pH 7.5, 70% v/v (+/-)-2-Methyl-2,4-pentanediol
G12	0.1 M HEPES pH 7.5, 4.3 M Sodium chloride
H1	0.1 M HEPES pH 7.5, 8% v/v Ethylene glycol, 10% w/v Polyethylene glycol 8,000
H2	0.1 M HEPES pH 7.5, 20% w/v Polyethylene glycol 10,000
H3	0.2 M Magnesium chloride hexahydrate, 0.1 M Tris pH 8.5, 3.4 M 1,6-Hexanediol
H4	0.1 M Tris pH 8.5, 25% v/v tert-Butanol
H5	0.01 M Nickel(II) chloride hexahydrate, 0.1 M Tris pH 8.5, 1.0 M Lithium sulfate monohydrate
H6	1.5 M Ammonium sulfate, 0.1 M Tris pH 8.5, 12% v/v Glycerol
H7	0.2 M Ammonium phosphate monobasic, 0.1 M Tris pH 8.5, 50% v/v (+/-)-2-Methyl-2,4-pentanediol
H8	0.1 M Tris pH 8.5, 20% v/v Ethanol
H9	0.01 M Nickel(II) chloride hexahydrate, 0.1 M Tris pH 8.5, 20% w/v Polyethylene glycol monomethyl ether 2,000
H10	0.1 M Sodium chloride, 0.1 M BICINE pH 9.0, 20% v/v Polyethylene glycol monomethyl ether 550
H11	0.1 M BICINE pH 9.0, 2.0 M Magnesium chloride hexahydrate
H12	0.1 M BICINE pH 9.0, 2% v/v 1,4-Dioxane, 10% w/v Polyethylene glycol 20,000

***Table 21: Hampton Research Crystal Screen HT Formulation***  
*(Hampton Research, 2021).*

## 9.4. Data Collection and Refinement Statistics

Data collection:	
Wavelength [Å]	0.9793
Resolution range [Å]	19.95-2.19 (2.27-2.19)
Space group	P 1
Unit cell (a, b, c) [Å] ( $\alpha$ , $\beta$ , $\gamma$ ) [°]	50.961, 58.402, 83.286 104.284, 98.494, 113.198
Total reflections	164051 (15510)
Unique reflections	40853 (3771)
Completeness [%]	96.08 (89.79)
I/ $\sigma$ (I)	6.73 (1.18)
CC <sub>1/2</sub>	0.99 (0.438)
Refinement:	
Resolution [Å]	2.19
Reflections used in refinement	40.587 (3771)
R <sub>work</sub>	0.1990 (0.2864)
R <sub>free</sub>	0.2394 (0.3374)
Number of non-hydrogen atoms	5837
Macromolecules	5419
Solvent	418
Protein residues	658
RMS(bonds)	0.002
RMS(angles)	0.50
Ramachandran favored (%)	97.82
Ramachandran allowed (%)	2.18
Ramachandran outliers (%)	0.00
Rotamer outliers (%)	0.00
Clashscore	5.76
Statistics for the highest-resolution shell are shown in parentheses.	

**Table 22: Data Collection and Refinement Statistics Sec3-PH/Sso2(aa1-270)**

Data collection and refinement statistics of the Sec3-PH/Sso2(aa1-270) complex crystal.

Data collection:	
Wavelength [Å]	0.6888
Resolution range [Å]	38.276-1.396 (1.446-1.396)
Space group	P 1
Unit cell (a, b, c) [Å] ( $\alpha$ , $\beta$ , $\gamma$ ) [°]	45.509, 45.972, 46.092 93.237, 91.53, 113.645
Total reflections	233255 (34015)
Unique reflections	65885 (10353)
Completeness [%]	97.13 (92.97)
I/ $\sigma$ (I)	8.68 (1.07)
CC <sub>1/2</sub>	0.997 (0.547)
Refinement:	
Resolution [Å]	1.40
Reflections used in refinement	65,863 (6,254)
R <sub>work</sub>	0.2091 (0.3747)
R <sub>free</sub>	0.2369 (0.3874)
Number of non-hydrogen atoms	3457
Macromolecules	2951
Solvent	506
Protein residues	355
RMS(bonds)	0.0066
RMS(angles)	0.96
Ramachandran favored (%)	95.99
Ramachandran allowed (%)	3.44
Ramachandran outliers (%)	0.57
Rotamer outliers (%)	0.30
Clashscore	6.29
Statistics for the highest-resolution shell are shown in parentheses.	

**Table 23: Data Collection and Refinement Statistics Sec3-PH/Sso1(aa1-224)**

Data collection and refinement statistics of the Sec3-PH/Sso1(aa1-224) complex crystal.